STRESSES IN PITCH-CAMBERED GLULAM BEAMS

by

WALTER K. THUT

Diploma Degree (Civil Engineering)

Swiss Institute of Technology, 1965

A THESIS SUBMITTED IN PARTIAL FULFILMENT OF

THE REQUIREMENTS FOR THE DEGREE OF

MASTER OF APPLIED SCIENCE

in the Department

of

CIVIL ENGINEERING

We accept this thesis as conforming

to the required standard

The University of British Columbia

In presenting this thesis in partial fulfilment of the requirements for an advanced degree at the University of British Columbia, I agree that the Library shall make it freely available for reference and study. I further agree that permission for extensive copying of this thesis for scholarly purposes may be granted by the Head of my Department or by his representatives. It is understood that copying or publication of this thesis for financial gain shall not be allowed without my written permission.

W. K. Thut

Department of Civil Engineering

The University of British Columbia
Vancouver 8, Canada
April 1970

ABSTRACT

The stress distribution near the centerline apex of pitch-cambered glulam beams is analysed. The analysis is done with an orthotropic trapezoidal finite element utilizing the stiffness approach. The element is tested with various grid sizes against known solutions and shown to give an overall accuracy to within five percent.

Radial tension stresses perpendicular to grain due to moment, were calculated for various geometries and plotted as a design aid. These stresses can be several times those found in a uniform curved beam.

The effect of changing the elastic moduli of the whole beam or individual laminations was investigated and found to be unimportant.

Radial stress due to shear forces was found to be unimportant.

Radial stress for one typical geometry due to moisture change was investigated in detail. This showed that ten pounds per square inch tensile stress was generated for a one percent change in moisture content.

Twenty two tests were performed on tension perpendicular to grain to indicate that the allowable stress would be near thirty five pounds per square inch.

A numerical example and design recommendations are included.

TABLE OF CONTENTS

LIST OF FIGURES AND TABLES

LIST OF MAJOR SYMBOLS

x , y	coordinates within the trapezoidal finite element.
u , v	displacement in x and y direction.
$\{\sigma\}^T = \{\sigma_x, \sigma_y, \tau\}$	stress vector.
$\{\varepsilon\}^T = \{\varepsilon_x, \varepsilon_y, \gamma\}$	strain vector.
σ_x	stress in x direction.
σ_y	stress in y direction.
τ	shear stress.
ε_x, ε_y, γ	similar for strains.
$\{\sigma\}_o$, $\{\varepsilon\}_o$	initial stress vector and initial strain vector.
σ_{x_o}, σ_{y_o}, τ_o	initial stresses.
ε_{x_o}, ε_{y_o}, γ_o	initial strains.

NOTE: x and y direction, in the finite element, correspond to the tangential and radial direction in the beam.

$\{\delta\}$	displacement vector containing the nodal displacements of the finite element.
$\{f\}$	force vector containing the nodal forces of the finite element.
$\{f\}_o$	force vector due to initial strain.
$[S]$	stress matrix.
$[k]$	stiffness matrix of the finite element.
$[\lambda]$	transformation matrix relating the polar coordinates to the xy coordinates.
$[k]', \{f\}', \{f\}_o', \{\delta\}'$	matrix and vectors of the finite element referring to polar coordinates.
$[K], \{F\}, \{F\}_o, \{\Delta\}$	similar matrix and vectors for the structure.
$\{B\}$	structure load vector.
$[D]$	elasticity matrix.
$E_1 = E_x/(1-\nu_{xy}\nu_{yx})$	in the tangential direction of the structure.
$E_2 = E_y/(1-\nu_{yx}\nu_{xy})$	in the radial direction of the structure.

$E_\nu = \nu_{xy} \cdot E_x = \nu_{yx} \cdot E_y$

E_x	modulus of elasticity in x direction (tangential).
E_y	modulus of elasticity in y direction (radial).
G	shear modulus.
ν_{xy}	Poisson's ratio (strain in y direction for stress in x direction).
ν_{yx}	similar to ν_{xy}.
M	bending moment.
V	shear force.
b	width of the beam.
d	depth of the beam.
R	radius of curvature of lower edge of the beam.
ΔR	distance in radial direction between two adjacent nodes of the finite element grid.
β	angle between two adjacent radii describing the finite element grid.
ϕ	reference angle of the radii.
α	slope angle of upper straigth edge of pitch-cambered beam w.r.t. a horizontal line.

σ_t	tangential stress.
σ_r	radial stress.
τ	shear stress.
C_{rM}, C_{tM}	stress coefficient for stresses in radial and in tangential direction due to moment loading.
C_{rV}, C_{tV}	similar due to shear loading.
C_{rp}, C_{tp}	similar due to uniform distributed pressure.
C_{rT}, C_{tT}	similar due to temperature gradient.
Δ	difference in % between finite element solution and known solution.
$\sigma_{r_{max}} = C_{RM} \cdot \frac{6M}{bd^2}$	maximum radial stress at centerline of a pitch-cambered beam due to pure bending.
$\sigma_{tens} = C_{TM} \cdot \frac{6M}{bd^2}$	maximum tangential tensile stress at centerline of a pitch-cambered beam due to pure bending.
$\sigma_{comp} = C_{CM} \cdot \frac{6M}{bd^2}$	maximum tangential compression stress at centerline of a pitch-cambered beam due to pure bending.
C_{RM}, C_{TM}, C_{CM}	stress coefficients for above maximum stresses.

ACKNOWLEDGEMENTS

The author wishes to thank his supervisor, Dr. R.F. Hooley, for his invaluable assistance and encouragement during the development of this work. Gratitude is also expressed to Le Conseil des Arts du Canada for financial support, and to the U.B.C. Computing Centre for the use of the facilities.

April 1970
Vancouver, B.C.

INTRODUCTION

Pitch-cambered glulam beams (fig.1) are used as roof beams in many buildings. However the stresses within these beams have not been determined in a rigorous manner. Since the abundance of recorded failures in North America have not been satisfactorily explained, it seems justified to investigate the problem deeper.

The pitch-cambered glulam beam is manufactured in a way that, at any cross section, the grain is parallel to the lower edge. The individual laminations are curved in the middle part of the span, but are usually straight towards the supports.

For rectangular cross sections, such a beam can be considered to be in a state of plane stress. In this two dimensional state, the axes of the elastic properties, parallel and perpendicular to the grain, coincide with polar coordinates. This is called polar anisotropy.

In these pitch-cambered beams, there exist tensile stresses perpendicular to the grain. These stresses are caused by the variation in depth of the cross sections and by the curvature of the gravity axes. Present design procedures estimate these stresses from the formula

$$\sigma_r = \frac{3}{2} \frac{M}{bd\ R_a}$$

where M is the applied moment, b the width of the beam,

d the depth of the beam and R_a the radius of curvature of the beam axis. This formula is for isotropic material of constant curvature, constant depth and constant moment, and so neglects many parameters of the problem.

Most failures show a crack parallel to the grain in the lower half of the cross section, close to the middle of the span. At these sections there are large moments and small shear forces, as pitch-cambered beams are almost invariable determinate and simply supported. This leads to the conclusion, that a moment applied on the special shaped middle part might cause high radial stresses which bring the beam to failure. Also, moisture change could create radial stresses additive to those generated by the moment.

The theory of elasticity gives solutions for curved beams of constant section and curvature. A solution for a curved beam of Douglas Fir, under pure bending, is shown by Norris (1). A general solution, given by Carrier (2), is discussed and applied by Foschi (3), for the case of curved Douglas Fir beams of constant cross sections under combined bending moments, axial and shear forces. For pitch-cambered curved beams with polar anisotropy, there are no exact solutions available. However, there is a publication of S.P. Fox (4) in preparation, which will treat this problem. Also, as far as it is known, the influence of moisture change on stresses in beams of this type has not yet been treated.

The finite element method enables us today to find the stress and strain distribution in any elastic continuum. In this powerful method the real contineous body, in this case a plane structure, is replaced by a number of finite

structural elements. These finite elements are interconnected by a discrete number of nodal points. The continuum is now replaced by a type of structure which can be treated by means of normal structural analyses, usually the stiffness method.

The analysis is completely routine work and can be done by digital computers. The relatively large number of finite elements required to represent realistically the continuum, results in a large number of linear equations. To solve these, the computer is an important tool.

For this specific problem an appropriate finite element was derived. Then a computer program was written to handle cylindrical anisotropic structures with ease. After testing the finite element, pitch-cambered glulam beams, under external loads and under moisture change, were studied. Finally recommendations are made to modify the existing design procedures.

In addition, some laboratory tests on tension perpendicular to the grain were made and compared with published data, to show that revision was necessary in this area as well.

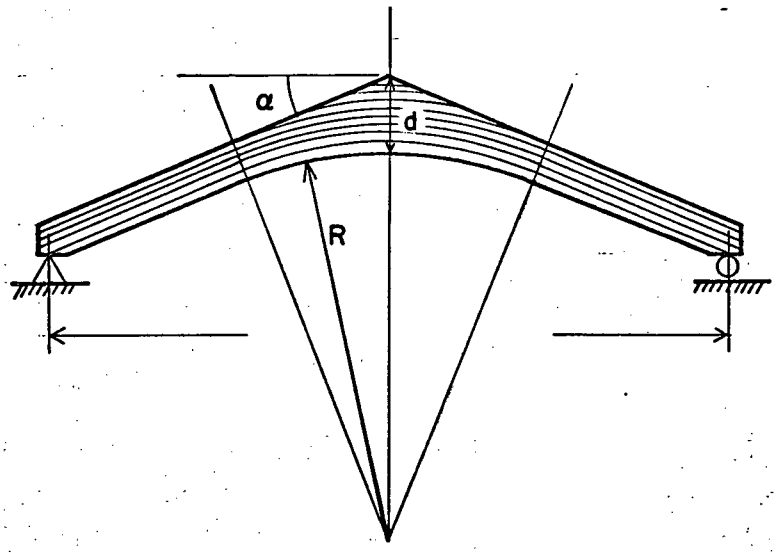

Fig.1. Pitch-cambered glulam beam.

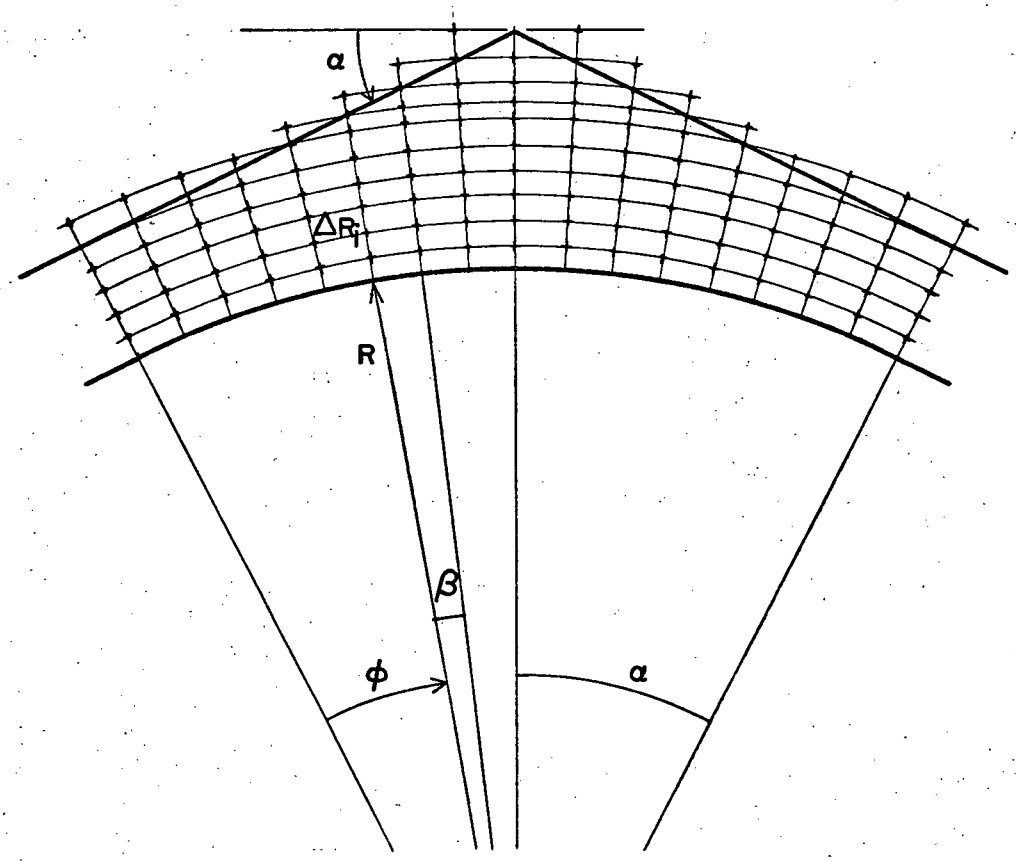

Fig.2. Arrangement of nodal points.

2. DERIVATION OF A TRAPEZOIDAL FINITE ELEMENT IN PLANE STRESS

2.1. GENERAL

Our interest is focused on plane stress problems in pitch-cambered glulam beams. The original plate is replaced by finite elements in an arrangement of nodal points on polar coordinates, as shown in fig.2. Herein, ΔR can vary with depth only and R and β can vary with ϕ. Trapezoidal elements are the most convenient for this arrangement of nodal points.

The original structure has cylindrical orthotropy but this will be approximated by rectangular orthotropy within the range of one element, as shown in fig.3. The smaller the angle β, the better will be this approximation.

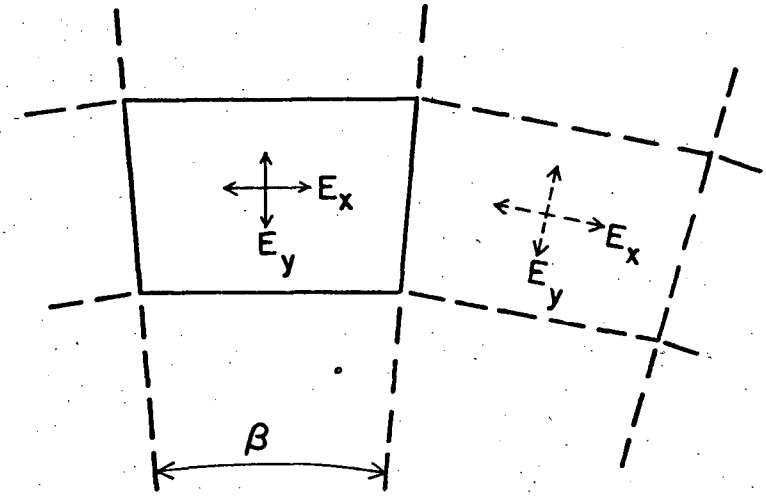

Fig.3. Trapezoidal finite element assumed with rectangular orthotropy.

The finite element must take into account initial strains due to change in moisture content and temperature. Initial strains occur if the single element is free to expand. If the element is constrained, then initial stresses occur under the action of a change in moisture content or temperature. Again these strains will be orthotropic on a rectangular system within an element, rather than on a polar system.

A practical and convenient way to idealize the elastic continuum is by means of displacement functions, as described in several papers (5,6). These displacement functions specify uniquely the state of strain within the element. If, the initial strains are included, together with the elastic properties, the stresses are also defined throughout the finite element, and, hence along the boundaries.

Expressing these stresses in terms of the nodal displacements will lead to the stress matrix. In matrix notation this is:

$$\{\sigma\} = [S]\cdot\{\delta\}+\{\sigma\}_o$$

$$\{\sigma\} = \begin{Bmatrix} \sigma_x \\ \sigma_y \\ \tau \end{Bmatrix} = \text{stress vector}$$

$$\{\sigma\}_o = \begin{Bmatrix} \sigma_{x_o} \\ \sigma_{y_o} \\ \tau_o \end{Bmatrix} = \text{initial stress vector}$$

$$[S]_{3x8} = \text{stress matrix}$$

$$\{\delta\} = \begin{Bmatrix} \delta_1 \\ \delta_2 \\ \delta_3 \\ \delta_4 \\ \delta_5 \\ \delta_6 \\ \delta_7 \\ \delta_8 \end{Bmatrix} = \text{displacement vector}$$

The boundary stresses are replaced by a set of generalized forces corresponding to the generalized nodal displacement. These nodal forces can be expressed in terms of the nodal displacements. This yields the stiffness matrix of the finite element or

$$\underline{\{f\} = [k]\cdot\{\delta\}+\{f\}_o} \qquad \{f\} = \begin{Bmatrix} f_1 \\ f_2 \\ f_3 \\ f_4 \\ f_5 \\ f_6 \\ f_7 \\ f_8 \end{Bmatrix} = \text{nodal forces}$$

$[k]_{8x8}$ = stiffness matrix of the finite element

$\{f\}_{o(8x1)}$ = nodal forces due to initial strain

2.2. DERIVATION OF THE FINITE ELEMENT

The variables used in the derivation are shown in fig.4. It indicates the element parameters, coordinate axes, nodal coordinates and the numbering of the nodal forces and displacements.

Following the standard procedure two displacement functions are assumed as

$$u = a_1 + a_2x + a_3y + a_4xy \qquad \{1\}$$

$$v = a_5 + a_6x + a_7y + a_8xy$$

This assumption seems reasonable, since the trapezoids have for small angles β, a shape close to a rectangle.

The nodal displacements $\{\delta\}$ in terms of the constants $a_1, a_2, \ldots\ldots\ldots a_8$ are obtained by placing the nodal coordinates into the displacement functions. This gives:

$$\{\delta\} = [T] \cdot \{a\} \qquad \{2a\}$$

where $\{a\}^T = \{a_1, a_2, a_3, a_4, a_5, a_6, a_7, a_8\}$

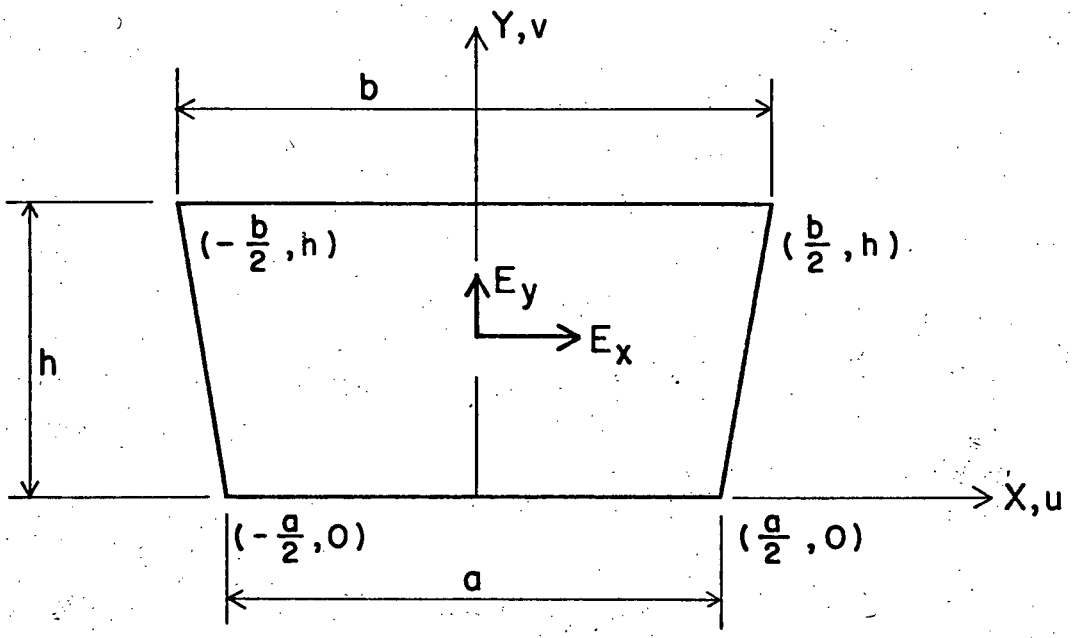

Fig.4a. Element parameters.

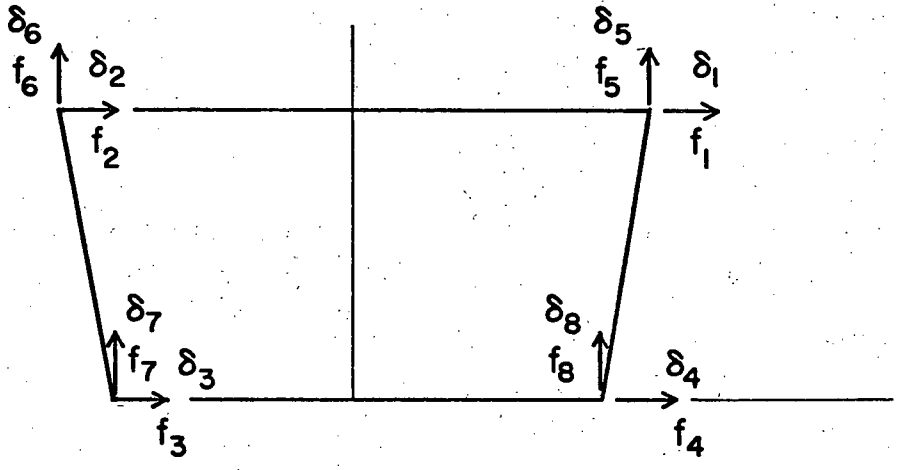

Fig.4b. Directions of positive nodal displacements and nodal forces.

and

$$[T] = \begin{bmatrix} 1 & \frac{b}{2} & h & \frac{bh}{2} & \cdot & \cdot & \cdot & \cdot \\ 1 & -\frac{b}{2} & h & -\frac{bh}{2} & \cdot & \cdot & \cdot & \cdot \\ 1 & -\frac{a}{2} & 0 & 0 & \cdot & \cdot & \cdot & \cdot \\ 1 & \frac{a}{2} & 0 & 0 & \cdot & \cdot & \cdot & \cdot \\ \cdot & \cdot & \cdot & \cdot & 1 & \frac{b}{2} & h & \frac{bh}{2} \\ \cdot & \cdot & \cdot & \cdot & 1 & -\frac{b}{2} & h & -\frac{bh}{2} \\ \cdot & \cdot & \cdot & \cdot & 1 & -\frac{a}{2} & 0 & 0 \\ \cdot & \cdot & \cdot & \cdot & 1 & \frac{a}{2} & 0 & 0 \end{bmatrix}$$

For later use, equation 2a has to be solved for {a} as

$$\{a\} = [T]^{-1}\{\delta\} \qquad \{2b\}$$

where $[T]^{-1} =$

$$\begin{bmatrix} 0 & 0 & \frac{1}{2} & \frac{1}{2} & \cdot & \cdot & \cdot & \cdot \\ 0 & 0 & -\frac{1}{a} & \frac{1}{a} & \cdot & \cdot & \cdot & \cdot \\ \frac{1}{2h} & \frac{1}{2h} & -\frac{1}{2h} & -\frac{1}{2h} & \cdot & \cdot & \cdot & \cdot \\ \frac{1}{bh} & -\frac{1}{bh} & \frac{1}{ah} & -\frac{1}{ah} & \cdot & \cdot & \cdot & \cdot \\ \cdot & \cdot & \cdot & \cdot & 0 & 0 & \frac{1}{2} & \frac{1}{2} \\ \cdot & \cdot & \cdot & \cdot & 0 & 0 & -\frac{1}{a} & \frac{1}{a} \\ \cdot & \cdot & \cdot & \cdot & \frac{1}{2h} & \frac{1}{2h} & -\frac{1}{2h} & -\frac{1}{2h} \\ \cdot & \cdot & \cdot & \cdot & \frac{1}{bh} & -\frac{1}{bh} & \frac{1}{ah} & -\frac{1}{ah} \end{bmatrix}$$

The total strains are found by appropriate differentiation of the displacement functions as:

$$\{\varepsilon\} = \begin{Bmatrix} \varepsilon_x \\ \varepsilon_y \\ \gamma \end{Bmatrix} = \begin{Bmatrix} \frac{\partial u}{\partial x} \\ \\ \frac{\partial v}{\partial y} \\ \\ \frac{\partial u}{\partial y} + \frac{\partial v}{\partial x} \end{Bmatrix} = [C]\{a\} \qquad \{3\}$$

where

$$[C] = \begin{bmatrix} 0 & 1 & 0 & y & 0 & 0 & 0 & 0 \\ 0 & 0 & 0 & 0 & 0 & 0 & 1 & x \\ 0 & 0 & 1 & x & 0 & 1 & 0 & y \end{bmatrix}$$

The initial strains, due to change in moisture content or temperature, are assumed independent of x and y within the element and are described by the initial strain vector.

$$\{\varepsilon\}_o = \begin{Bmatrix} \varepsilon_{xo} \\ \varepsilon_{yo} \\ \gamma_o \end{Bmatrix} \qquad \{4\}$$

Hookes law now gives

$$\{\sigma\} = \begin{Bmatrix} \sigma_x \\ \sigma_y \\ \tau \end{Bmatrix} = [D]\left\{\{\varepsilon\} - \{\varepsilon\}_o\right\} \qquad \{5\}$$

Herein [D] is called the elasticity matrix and is

$$[D] = \begin{bmatrix} E_1 & E_\nu & 0 \\ E_\nu & E_2 & 0 \\ 0 & 0 & G \end{bmatrix}$$

where $E_1 = E_x / (1 - \nu_{xy} \cdot \nu_{yx})$

$E_2 = E_y / (1 - \nu_{xy} \cdot \nu_{yx})$

$E_\nu = \nu_{xy} \cdot E_x = \nu_{yx} \cdot E_y$

and G is the shear modulus.

It should be noted that x and y correspond to tangential and radial direction so that E_x and E_y are $E_{tangential}$ and E_{radial} for the wood considered. The stresses and strains may be expressed now in terms of nodal displacements by substituting equation 2b into equation 3, and equations 2b and 3 into equation 5, to give

$$\{\varepsilon\} = [C]\,[T]^{-1}\{\delta\} \qquad \{6\}$$

$$\{\sigma\} = [D]\left([C][T]^{-1}\{\delta\}-\{\varepsilon\}_o\right) \qquad \{7a\}$$

Equation 7a can be written in the form

$$\{\sigma\} = [S]\{\delta\}+\{\sigma\}_o \qquad \{7b\}$$

where $[S] = [D][C][T]^{-1}$

is the stress matrix

and $\{\sigma\}_o = -[D]\{\varepsilon\}_o$

is the initial stress vector.

Once the nodal displacements have been determined by solving the structure stiffness equations, the stresses and strains at any point of the finite element can be found by the above relations. The stress matrix [S] obtained from the chosen displacement functions is explicitly:

$$[S]=[D]\begin{bmatrix} \frac{y}{bh} & -\frac{y}{bh} & -\frac{1}{a}+\frac{y}{ah} & \frac{1}{a}-\frac{y}{ah} & 0 & 0 & 0 & 0 \\ 0 & 0 & 0 & 0 & \frac{1}{2h}+\frac{x}{bh} & \frac{1}{2h}-\frac{x}{bh} & -\frac{1}{2h}+\frac{x}{ah} & -\frac{1}{2h}-\frac{x}{ah} \\ \frac{1}{2h}+\frac{x}{bh} & \frac{1}{2h}-\frac{x}{bh} & -\frac{1}{2h}+\frac{x}{ah} & -\frac{1}{2h}-\frac{x}{ah} & \frac{y}{bh} & -\frac{y}{bh} & -\frac{1}{ah}+\frac{y}{ah} & \frac{1}{a}-\frac{y}{ah} \end{bmatrix}$$

The principle of virtual displacements is now used to derive the element stiffness matrix [k] as shown below

$$d\{\delta\}^T\{f\} = \int_V d[\varepsilon]^T[\sigma]\, dV$$

where $d\{\delta\}$ is a virtual displacement of the nodes and $d\{\varepsilon\}$ is the corresponding change in the strains. Differentiation of equation 6 yields a link between $d\{\delta\}$ and $d\{\varepsilon\}$ so that

$$d\{\delta\}^T\{f\} = \int_V \left([C][T]^{-1}d\{\delta\}\right)^T[D]\left([C][T]^{-1}\{\delta\}-\{\varepsilon\}_o\right)dV$$

wherein $\{\sigma\}$ is expressed as in equation 7a. Expansion of this gives

$$d\{\delta\}^T\{f\} = d\{\delta\}^T[T]^{-1T}\left[\int_V [C]^T[D][C]dV[T]^{-1}\{\delta\}-[T]^{-T}\int_V [C]^T[D]\{\varepsilon\}_o dV\right].$$

Since $d\{\delta\}$ is arbitrary

$$\{f\} = [T]^{-1T}\int_V [C]^T[D][C]dV[T]^{-1}\{\delta\}-[T]^{-1T}\int_V [C]^T[D]\{\varepsilon\}_o dV \quad \{8a\}$$

This relation can be rewritten as

$$\{f\} = [k]\{\delta\} + \{f\}_o \qquad \{8b\}$$

where the stiffness matrix is

$$[k] = [T]^{-1T} \int_V [C]^T [D][C] dV [T]^{-1} \qquad \{9\}$$

and the nodal forces due to initial strain are

$$\{f\}_o = -[T]^{-1T} \int_V [C]^T [D]\{\varepsilon\}_o dV \qquad \{10\}$$

In a plane stress element with a constant thickness t the volume dV is t·dA or t·dx·dy. The stiffness matrix [k], established by the previous matrix operation, is symmetric due to the reciprocal theorem so that only the 36 terms of the lower half need to be stored. Because of element geometric symmetry, only twenty of these 36 need calculation as shown in fig.5.

$$[k] = t \times \begin{bmatrix} A & & & & & & & \\ B & A & & & & & & \\ C & D & I & & & & & \\ D & C & K & I & & & & \\ E & -F & L & -M & P & & & \\ F & -E & M & -L & Q & P & & \\ G & -H & N & -O & R & S & T & \\ H & -G & O & -N & S & R & U & T \end{bmatrix}$$

Fig.5. Stiffness matrix [k].

To reduce the lengthy expressions in [k] a set of abbrevations for the integrals over the range of the trapezoidal element is introduced as follows:

$$I_1 = \int 1 \, dxdy = \frac{h}{2}(a+b)$$

$$I_y = \int y \, dxdy = \frac{h^2}{6}(a+2b)$$

$$I_{xx} = \int x^2 dxdy = \frac{h}{36}(a^2+b^2)(a+b)$$

$$I_{yy} = \int y^2 dxdy = \frac{h^3}{12}(a+3b)$$

The integrals of $x \cdot dx \cdot dy$ and $xy \cdot dx \cdot dy$ disappear due to symmetry with respect to the Y-axis.

The twenty terms entering the stiffness matrix are given explicitely without presenting the intermediate calculations in table No.1.

The nodal forces due to initial strain, determined by equation 10, are given as follows:

$$\{f\}_o = \begin{Bmatrix} f_{10} \\ f_{20} \\ f_{30} \\ f_{40} \\ f_{50} \\ f_{60} \\ f_{70} \\ f_{80} \end{Bmatrix} = \begin{Bmatrix} \frac{ht}{6b}(a+2b)(E_1\varepsilon_{xo}+E_\nu\varepsilon_{yo}) + \frac{t}{4}(a+b)G\gamma_{xyo} \\ -\frac{ht}{6b}(a+2b)(E_1\varepsilon_{xo}+E_\nu\varepsilon_{yo}) + \frac{t}{4}(a+b)G\gamma_{xyo} \\ -\frac{ht}{6a}(2a+b)(E_1\varepsilon_{xo}+E_\nu\varepsilon_{yo}) - \frac{t}{4}(a+b)G\gamma_{xyo} \\ \frac{ht}{6a}(2a+b)(E_1\varepsilon_{xo}+E_\nu\varepsilon_{yo}) - \frac{t}{4}(a+b)G\gamma_{xyo} \\ \frac{t}{4}(a+b)(E_\nu\varepsilon_{xo}+E_2\varepsilon_{yo}) + \frac{ht}{6b}(a+2b)G\gamma_{xyo} \\ \frac{t}{4}(a+b)(E_\nu\varepsilon_{xo}+E_2\varepsilon_{yo}) - \frac{ht}{6b}(a+2b)G\gamma_{xyo} \\ -\frac{t}{4}(a+b)(E_\nu\varepsilon_{xo}+E_2\varepsilon_{yo}) - \frac{ht}{6a}(2a+b)G\gamma_{xyo} \\ -\frac{t}{4}(a+b)(E_\nu\varepsilon_{xo}+E_2\varepsilon_{yo}) + \frac{ht}{6a}(2a+b)G\gamma_{xyo} \end{Bmatrix}$$

	E_1			E_2		E_ν		G			
	I_1	I_y	I_{yy}	I_1	I_{xx}	I_1	I_y	I_1	I_y	I_{xx}	I_{yy}
A			$1/b^2h^2$					$1/4h^2$		$1/b^2h^2$	
B			$-1/b^2h^2$					$1/4h^2$		$-1/b^2h^2$	
C		$-1/abh$	$1/abh^2$					$-1/4h^2$		$1/abh^2$	
D		$1/abh$	$-1/abh^2$					$-1/4h^2$		$-1/abh^2$	
E							$1/2bh^2$		$1/2bh^2$		
F							$1/2bh^2$		$-1/2bh^2$		
G							$-1/2bh^2$	$-1/2ah$	$1/2ah^2$		
H							$-1/2bh^2$	$1/2ah$	$-1/2ah^2$		
I	$1/a^2$	$-2/a^2h$	$1/a^2h^2$					$1/4h^2$		$1/a^2h^2$	
K	$-1/a^2$	$2/a^2h$	$-1/a^2h^2$					$1/4h^2$		$-1/a^2h^2$	
L						$-1/2ah$	$1/2ah^2$		$-1/2bh^2$		
M						$-1/2ah$	$1/2ah^2$		$1/2bh^2$		
N						$1/2ah$	$-1/2ah^2$	$1/2ah$	$-1/2ah^2$		
O						$1/2ah$	$-1/2ah^2$	$-1/2ah$	$1/2ah^2$		
P				$1/4h^2$	$1/b^2h^2$						$1/b^2h^2$
Q				$1/4h^2$	$-1/b^2h^2$						$-1/b^2h^2$
R				$-1/4h^2$	$1/abh^2$				$-1/abh$		$1/abh^2$
S				$-1/4h^2$	$-1/abh^2$				$1/abh$		$-1/abh^2$
T				$1/4h^2$	$1/a^2h^2$			$1/a^2$	$-2/a^2h$		$1/a^2h^2$
U				$1/4h^2$	$-1/a^2h^2$			$-1/a^2$	$2/a^2h$		$-1/a^2h^2$

TABLE 1

2.3. TRANSFORMATION INTO POLAR COORDINATES

Before the member stiffness matrix [k] can be added to generate the structure stiffness matrix [K], the local coordinates must be transformed to a global polar system. The parameters determining the trapezoid are related to the polar coordinates by:

$$h = (R_2 - R_1) \cos \frac{\beta}{2}$$

$$a = 2R_1 \sin \frac{\beta}{2} \qquad \{11\}$$

$$b = 2R_2 \sin \frac{\beta}{2}$$

where R_1, R_2 and β are defined in fig.6.

After calculation of the stiffness matrix and the nodal forces due to initial strain is carried out in rectangular coordinates, it is desirable to convert the result into polar coordinates. The new set of axes, with the positive directions of the nodal forces and displacements chosen radially and tangentially, will be denoted with a prime (fig.7).

The direction cosines of the polar set referred to the rectangular set, written in a square array, constitute a transformation matrix $[\lambda]$ as:

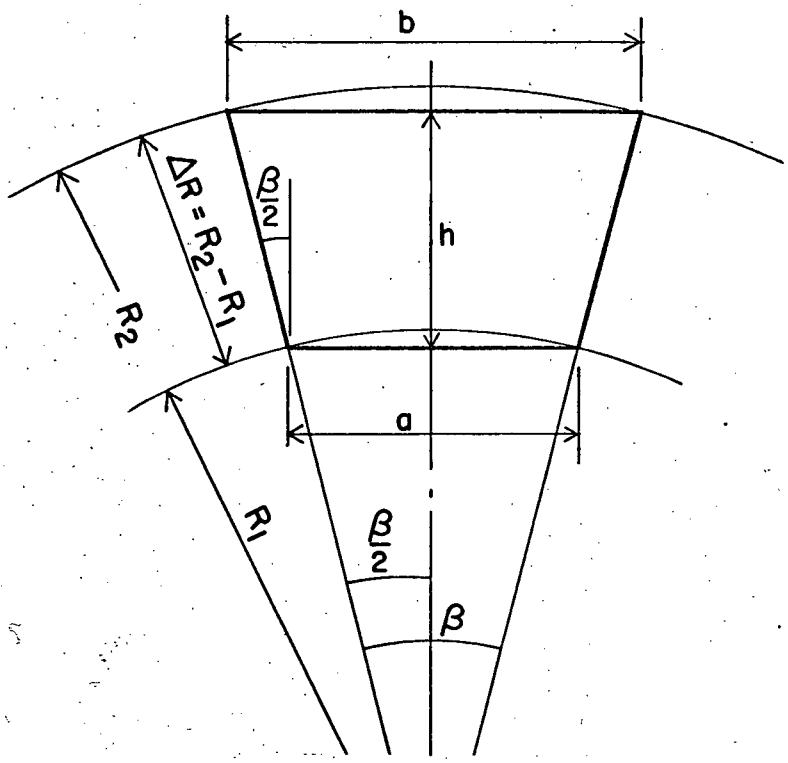

Fig.6. Parameters and coordinates determining the trapezoid.

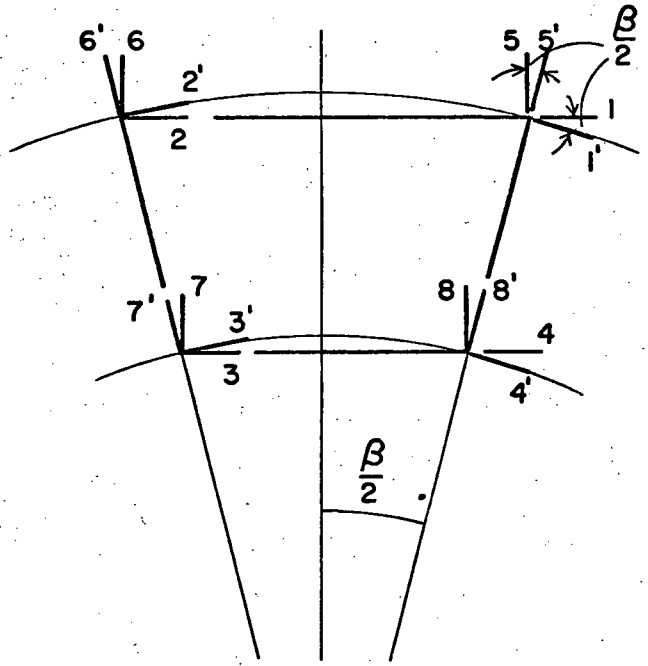

Fig.7. The two sets of nodal forces and displacements.

$$[\lambda] = \begin{bmatrix} \cos\frac{\beta}{2} & 0 & 0 & 0 & -\sin\frac{\beta}{2} & 0 & 0 & 0 \\ 0 & \cos\frac{\beta}{2} & 0 & 0 & 0 & \sin\frac{\beta}{2} & 0 & 0 \\ 0 & 0 & \cos\frac{\beta}{2} & 0 & 0 & 0 & \sin\frac{\beta}{2} & 0 \\ 0 & 0 & 0 & \cos\frac{\beta}{2} & 0 & 0 & 0 & -\sin\frac{\beta}{2} \\ \sin\frac{\beta}{2} & 0 & 0 & 0 & \cos\frac{\beta}{2} & 0 & 0 & 0 \\ 0 & -\sin\frac{\beta}{2} & 0 & 0 & 0 & \cos\frac{\beta}{2} & 0 & 0 \\ 0 & 0 & -\sin\frac{\beta}{2} & 0 & 0 & 0 & \cos\frac{\beta}{2} & 0 \\ 0 & 0 & 0 & \sin\frac{\beta}{2} & 0 & 0 & 0 & \cos\frac{\beta}{2} \end{bmatrix}$$

The components of the vectors $\{f\}'$ and $\{f\}'_o$ are related to the components referred to the rectangular axes by:

$$\{f\}' = [\lambda]\ \{f\}$$
$$\{f\}'_o = [\lambda]\ \{f\}_o \qquad \{12\}$$

and similarly for the components of the nodal displacements

$$\{\delta\}' = [\lambda]\ \{\delta\}$$

The member matrix in polar coordinates is then

$$[k]' = [\lambda]\ [k]\ [\lambda]^T \qquad \{13\}$$

so that

$$\{f\}' - \{f\}'_o = [k]'\ \{\delta\}' \qquad \{14\}$$

The matrix [k]' is easily obtained from [k] by replacing A by A', B by B' etc. in fig.5 where

$$\begin{Bmatrix} A' \\ B' \\ C' \\ D' \\ E' \\ F' \\ G' \\ H' \\ I' \\ K' \\ L' \\ M' \\ N' \\ O' \\ P' \\ Q' \\ R' \\ S' \\ T' \\ U' \end{Bmatrix} = \begin{bmatrix} A & -2E & P \\ B & 2F & -Q \\ C & G-L & -R \\ D & -H+M & S \\ E & A-P & -E \\ F & -B-Q & -F \\ G & -C-R & L \\ H & D-S & M \\ I & 2N & T \\ K & -2O & -U \\ L & C+R & G \\ M & -D+S & H \\ N & -I+T & -N \\ O & K+U & -O \\ P & 2E & A \\ Q & 2F & -B \\ R & G-L & -C \\ S & H-M & D \\ T & -2N & I \\ U & -2O & -K \end{bmatrix} \begin{Bmatrix} \cos^2 \frac{\beta}{2} \\ \cos \frac{\beta}{2} \cdot \sin \frac{\beta}{2} \\ \sin^2 \frac{\beta}{2} \end{Bmatrix}$$

3. COMPUTER SOLUTION PROCEDURE

3.1. BASIC STEPS IN THE PROCEDURE

The computer program developed is based on the displacement method using a structure stiffness matrix. The program, written for the IBM 7044, is given in the appendix. The setup is shown in the simplified flow diagram of (3.2).

The basic steps in the procedure are:

a) The pitch-cambered beam is subdivided by radial lines and many circular arcs. The area enclosed by the radial lines and the arcs, is approximated by equilateral trapezoids connected at the corners only. These trapezoidal elements retain the appropriate material and geometric properties of the structure.

An inclined, straight upper edge cannot be represented exactly in polar coordinates. Therefore it must be approximated by varying the boundary stepwise. The respective thickness given to these boundary elements is in proportion to the plate area they have to represent. The respective thickness of an element is taken as

$$t_{resp} = \frac{A_{structure}}{A_{element}} \; t_{structure}$$

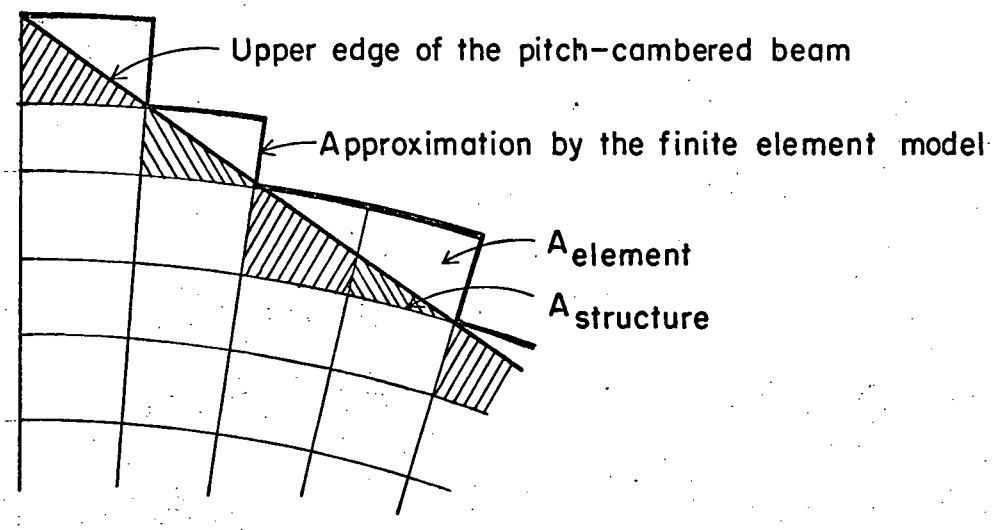

Fig.8. Approximation of the upper straight edge.

The area $A_{structure}$ is hatched in fig.8. $A_{element}$ is the area enclosed by the arcs and the radial lines. This stepwise approximation is checked in chapter four and shown to be sufficient for the limits of accuracy required herein.

b) The elements and the nodes are numbered.

c) The boundary conditions are simulated by locking or releasing the appropriate nodal displacements. The unlocked nodal displacements, i.e. the components of the structure displacement vector, are numbered.

d) The element stiffness matrix [k] is generated and transformed into polar coordinates [k]'.

e) The structure stiffness matrix [K] is generated from [k]' by using the code number technique. This tech-

nique automatically eliminates the rows and columns of the structure stiffness matrix, corresponding to the restrained joints.

f) The structure load vector {B} is generated.

The loads acting on the beam are applied to the model at the nodal points only. Therefore, the distributed external stresses have to be replaced by statically equivalent nodal forces to yield the terms of the structure force vector {F}.

The nodal forces due to initial strain are given by equation 10. The code number technique is used to place them into a structure force vector $\{F\}_o$, due to initial strain.

The structure load vector {B} is then

$$\{B\} = \{F\} - \{F\}_o$$

g) Cholesky's method is used to solve the system of simultaneous linear equations in the stiffness relation

$$\{B\} = [K]\{\Delta\}$$

h) Knowing the structure displacement vector {Δ}, the element displacement vector {δ}' is found by the code number technique and transformed into {δ}.

i) The stresses within the element are found by equation 7b. They are calculated at the center of the elements, since there the directions of the XY coordinates coincide with the polar coordinates.

3.2. SIMPLIFIED FLOW DIAGRAM

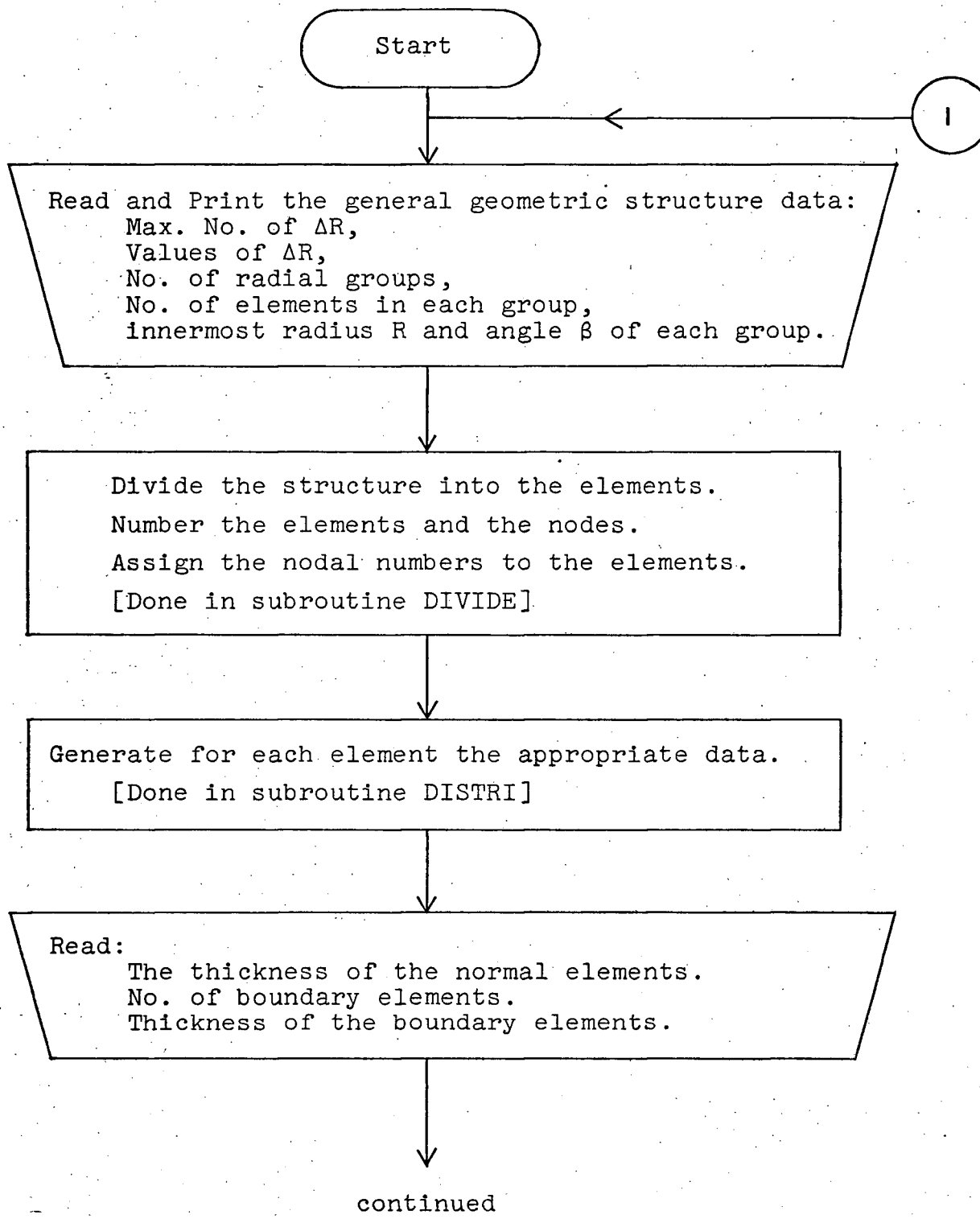

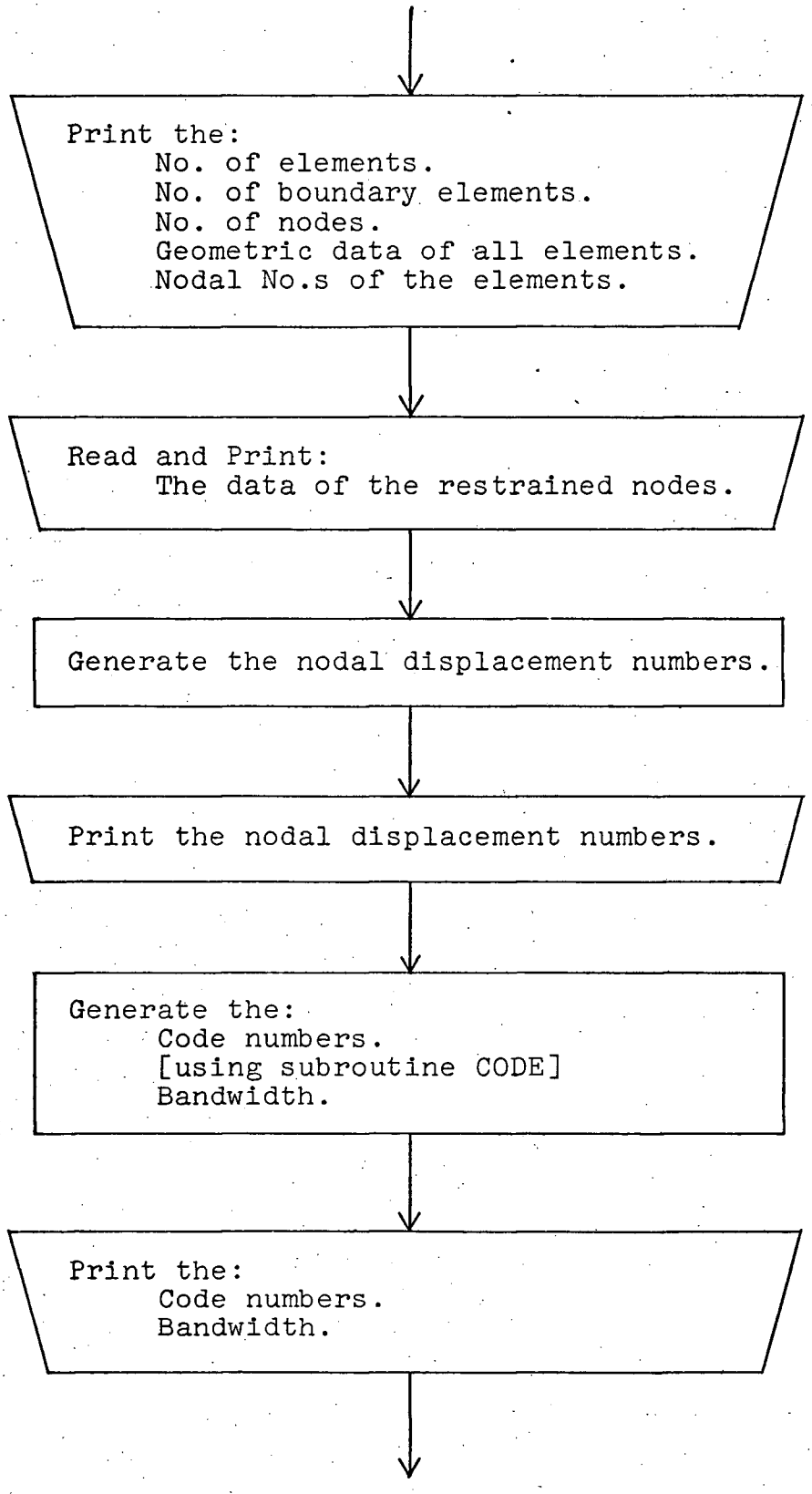
Print the:
No. of elements.
No. of boundary elements.
No. of nodes.
Geometric data of all elements.
Nodal No.s of the elements.
Read and Print:
The data of the restrained nodes.
Generate the nodal displacement numbers.
Print the nodal displacement numbers.
Generate the:
Code numbers.
[using subroutine CODE]
Bandwidth.
Print the:
Code numbers.
Bandwidth.

continued

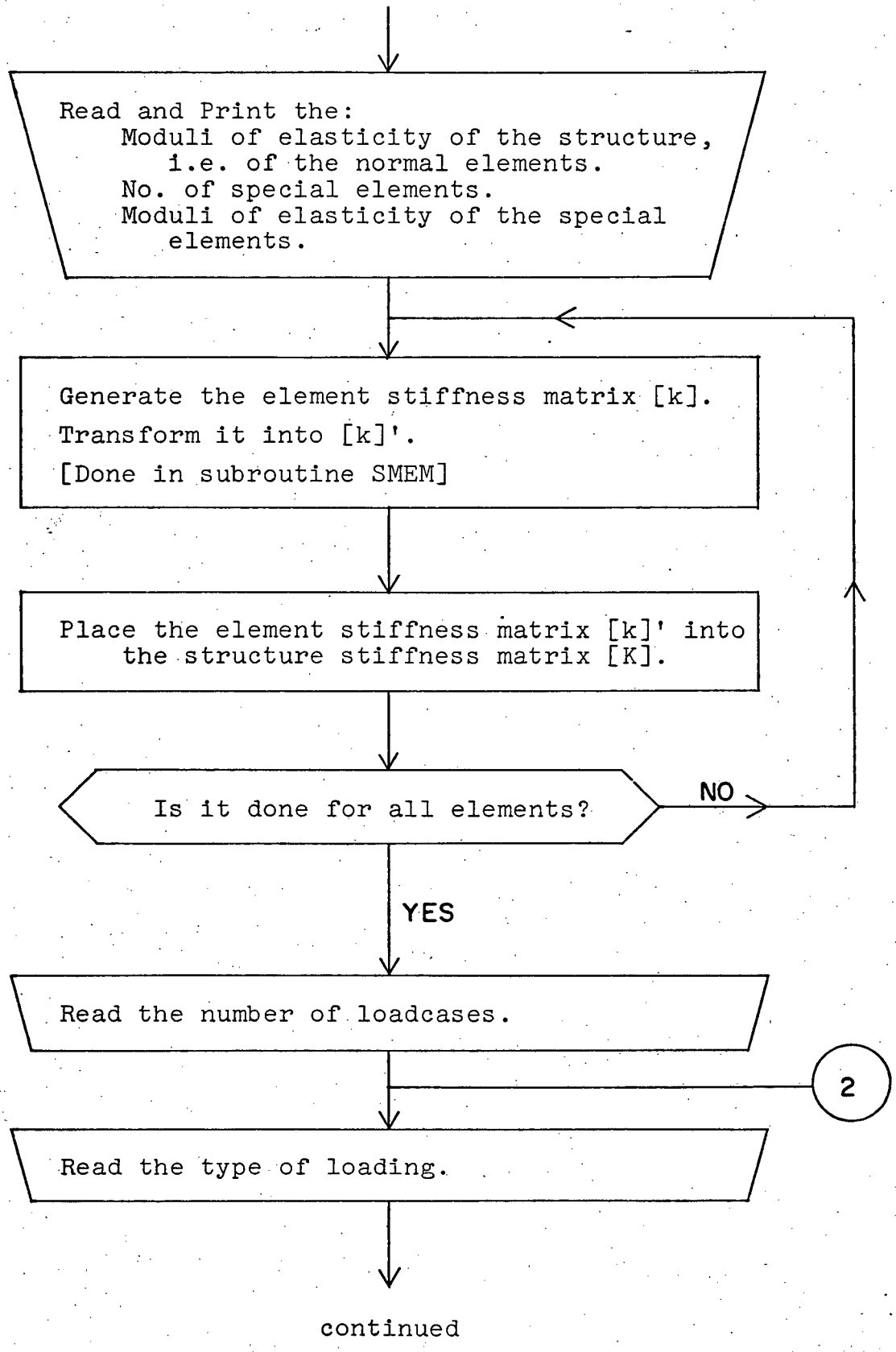
Read and Print the:
Moduli of elasticity of the structure, i.e. of the normal elements.
No. of special elements.
Moduli of elasticity of the special elements.
Generate the element stiffness matrix [k].
Transform it into [k]'.
[Done in subroutine SMEM]
Place the element stiffness matrix [k]' into the structure stiffness matrix [K].
Is it done for all elements?
NO
YES
Read the number of loadcases.
2
Read the type of loading.
continued

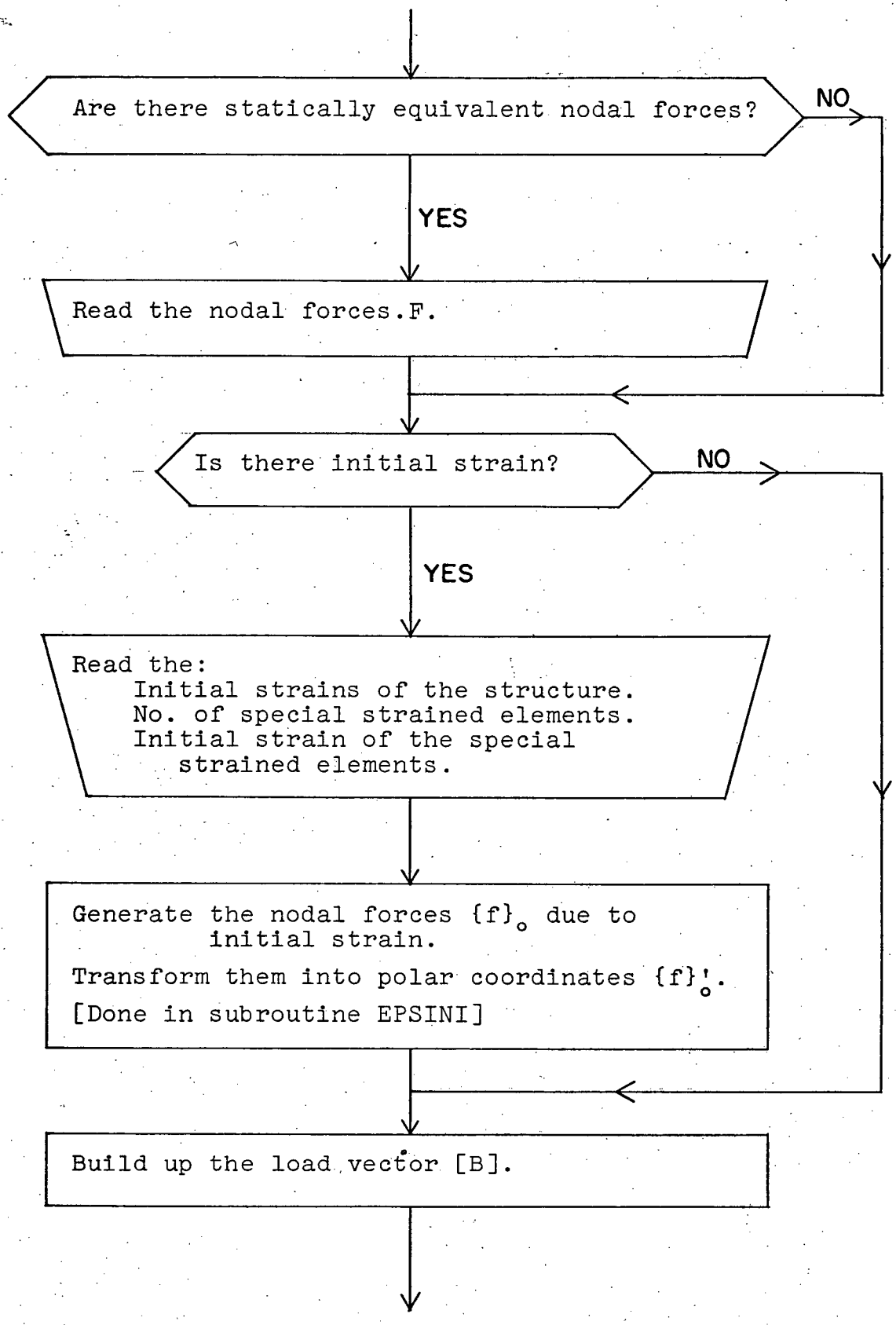
Are there statically equivalent nodal forces?
NO
YES
Read the nodal forces.F.
Is there initial strain?
NO
YES
Read the:
Initial strains of the structure.
No. of special strained elements.
Initial strain of the special strained elements.
Generate the nodal forces {f}o due to initial strain.
Transform them into polar coordinates {f}'o.
[Done in subroutine EPSINI]
Build up the load vector [B].

continued

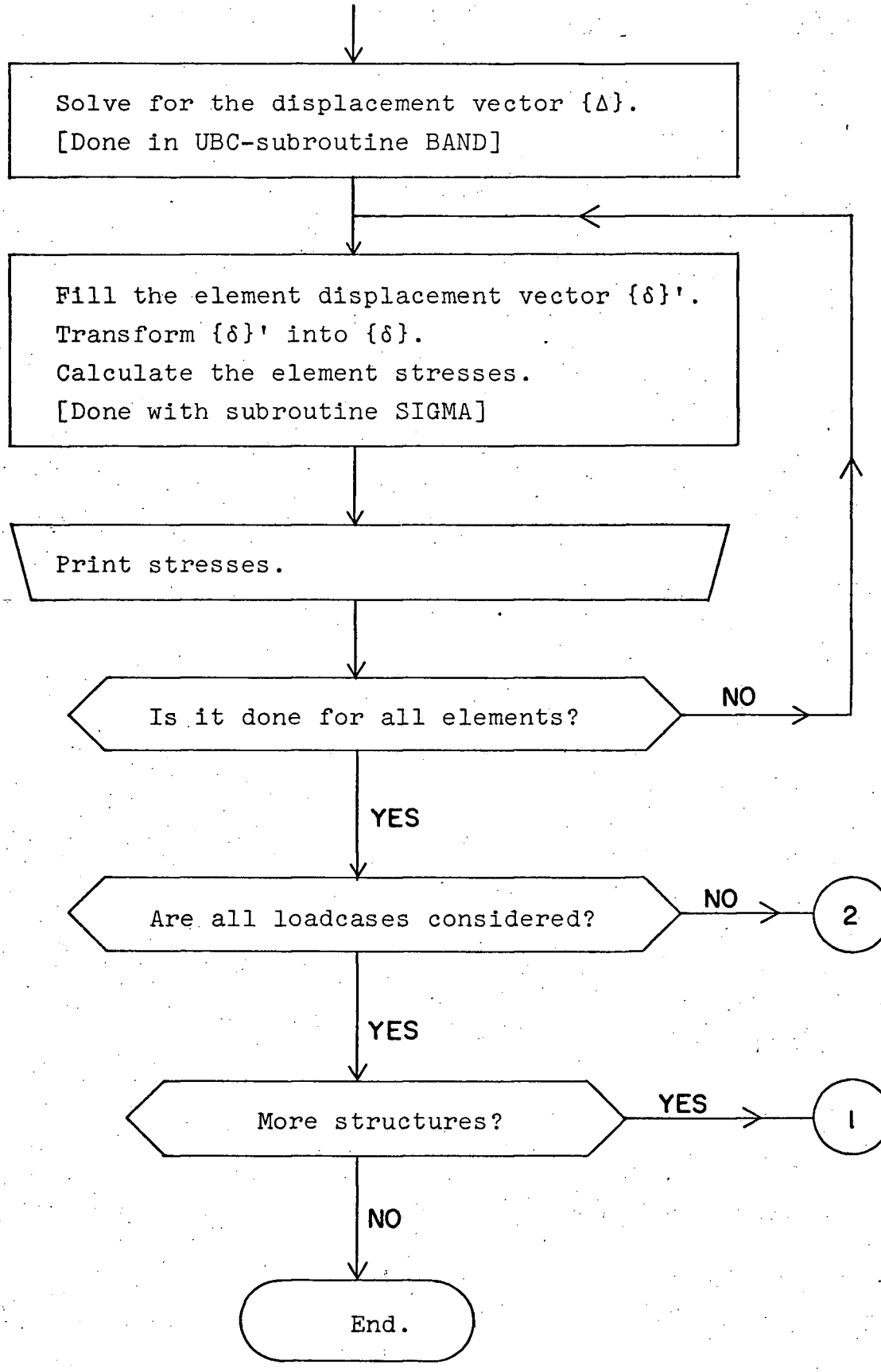
Solve for the displacement vector {Δ}.
[Done in UBC-subroutine BAND]
Fill the element displacement vector {δ}'.
Transform {δ}' into {δ}.
Calculate the element stresses.
[Done with subroutine SIGMA]
Print stresses.
Is it done for all elements?
NO
YES
Are all loadcases considered?
NO
2
YES
More structures?
YES
1
NO
End.

4. CHECKING OF THE FINITE ELEMENT WITH VARIOUS PROBLEMS

It is the object of this chapter to see if the finite element previously developed will predict, with sufficient accuracy, the stress distribution in pitch-cambered beams. To do this, finite element solutions are compared against elasticity solutions for various problems.

All percentage errors given in comparison with known solutions are calculated corresponding to the following relation based on absolute values

$$\Delta_{error}\% = \frac{|\text{calculated value}| - |\text{known value}|}{|\text{known value}|} \cdot 100$$

4.1. ISOTROPIC CIRCULAR BEAMS AND RINGS

The material in the finite element solution is determined by the [D]-matrix. To represent isotropic material [D] has to be the corresponding elasticity matrix, i.e.

$$[D] = \begin{bmatrix} E_1 & E_\nu & 0 \\ E_\nu & E_2 & 0 \\ 0 & 0 & G \end{bmatrix} = \frac{E}{1-\nu^2} \begin{bmatrix} 1 & \nu & 0 \\ \nu & 1 & 0 \\ 0 & 0 & \frac{1-\nu}{2} \end{bmatrix}$$

or $$E_1 = E_2 = \frac{E}{1-\nu^2}, \quad E_\nu = \frac{\nu E}{1-\nu^2} \quad \text{and} \quad G = \frac{E}{2(1+\nu)}$$

EXAMPLE 1

ISOTROPIC CIRCULAR BEAM, SHEAR LOADING

Fig.9a shows properties of a curved beam under shear loading for which the elasticity solution is given in Timoshenko (5) on page 73. Fig.9c gives a plot of the tangential stresses near the inside edge. Herein, two finite element solutions are shown: One for a constant distribution of shear load at $\phi = \pi/2$, and the other for the shear distribution according to the elasticity solution. In fig.9b are shown tangential and radial stresses at $\phi = \beta/2$. The two finite element solutions produced the same result at this section remote from the applied load. Even for this coarse grid size, the element predicts the stress distribution with sufficient accuracy.

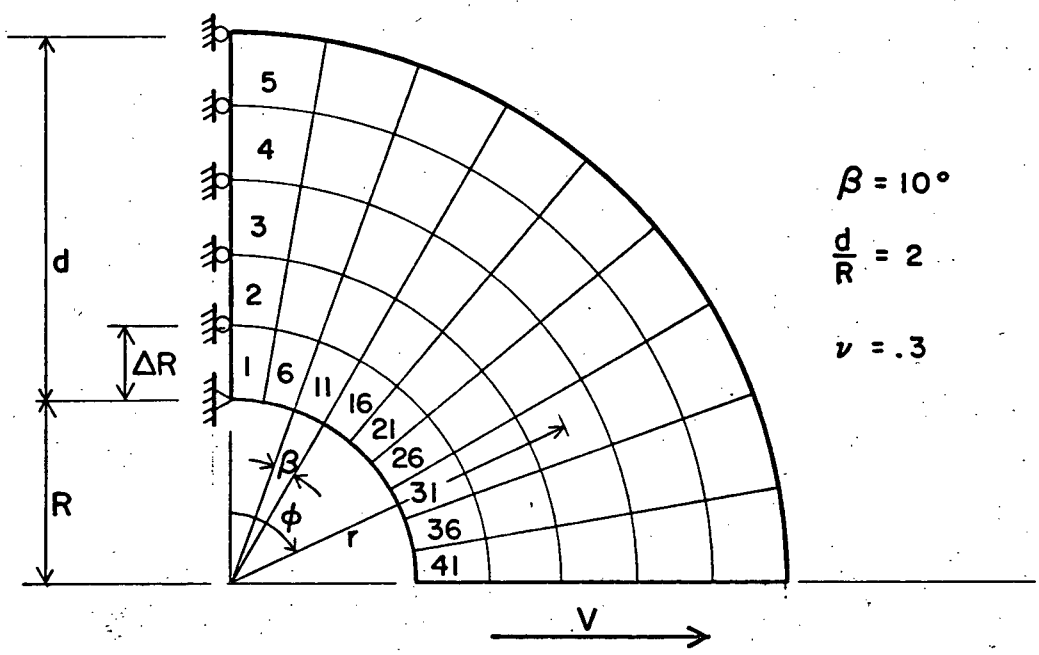

Fig.9a. Isotropic circular beam, shear loading.

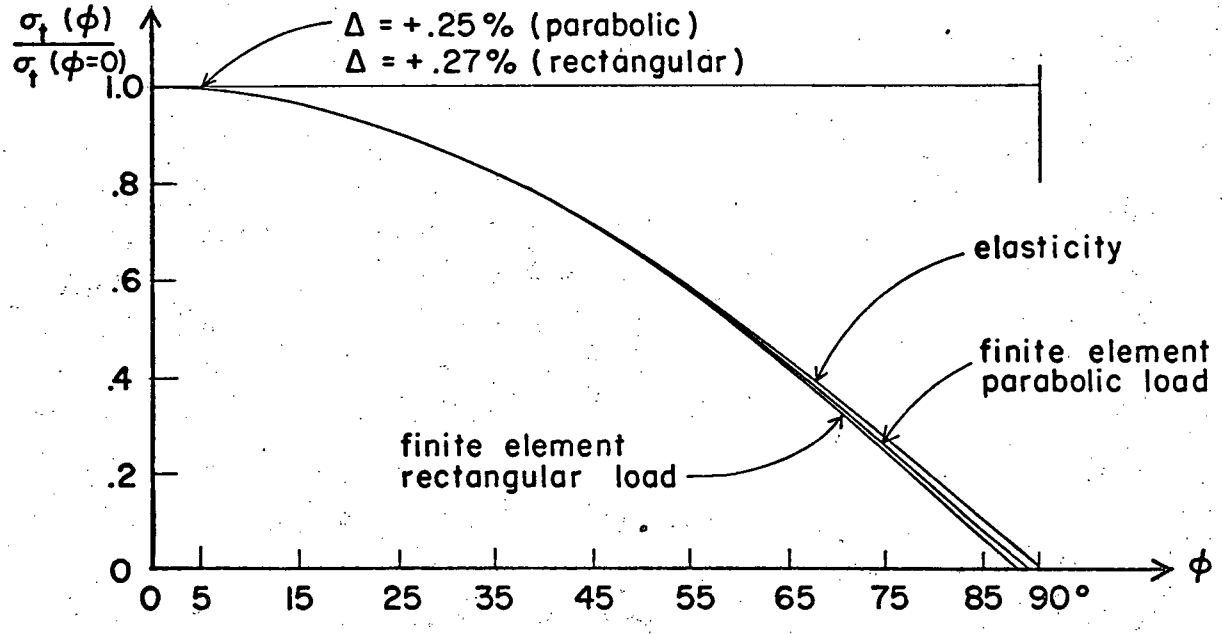

Fig.9c. Tangential stresses along $r = R + \frac{\Delta R}{2}$.

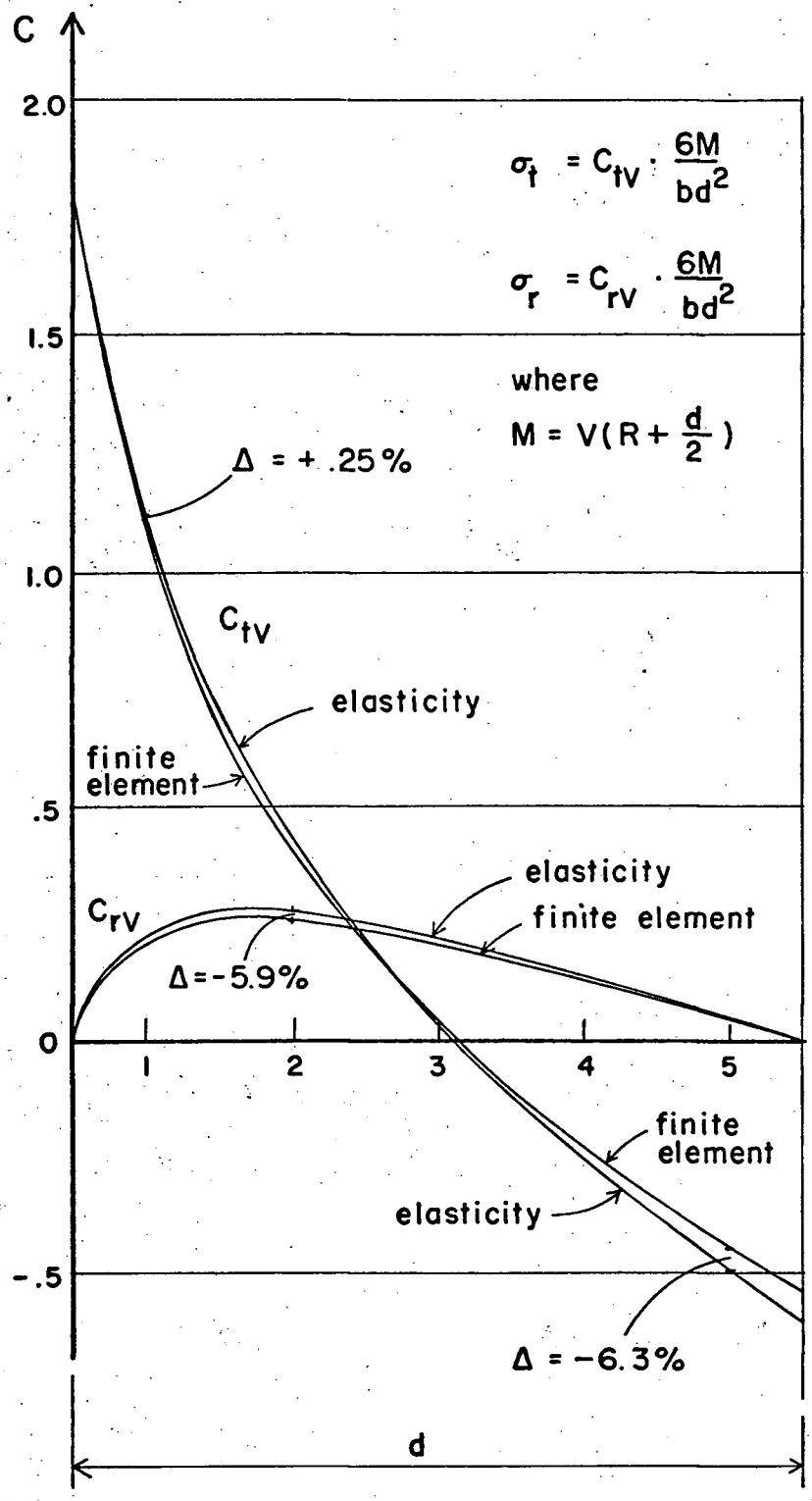

Fig.9b. Stresses at $\phi = \beta/2$.

EXAMPLE 2

ISOTROPIC CIRCULAR BEAM; MOMENT LOADING

Fig.10 shows the properties and stresses of a curved beam under pure bending for which the elasticity solution is given in Timoshenko (5) on page 61.

It is the same beam as in example 1, except that the load is pure moment. The nodal forces were distributed linearly at $\phi = \pi/2$ to represent the applied moment.

Again, the element predicts the stresses with sufficient accuracy.

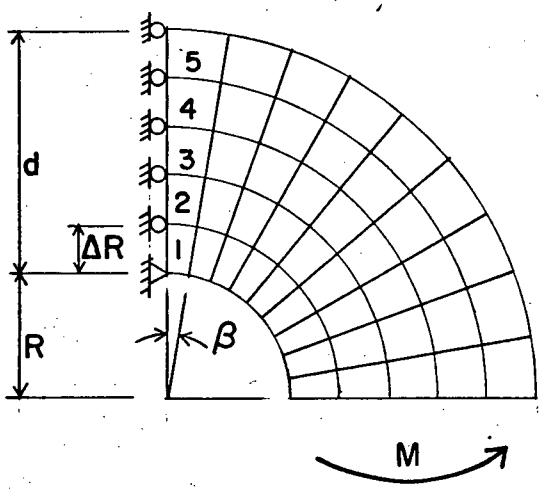

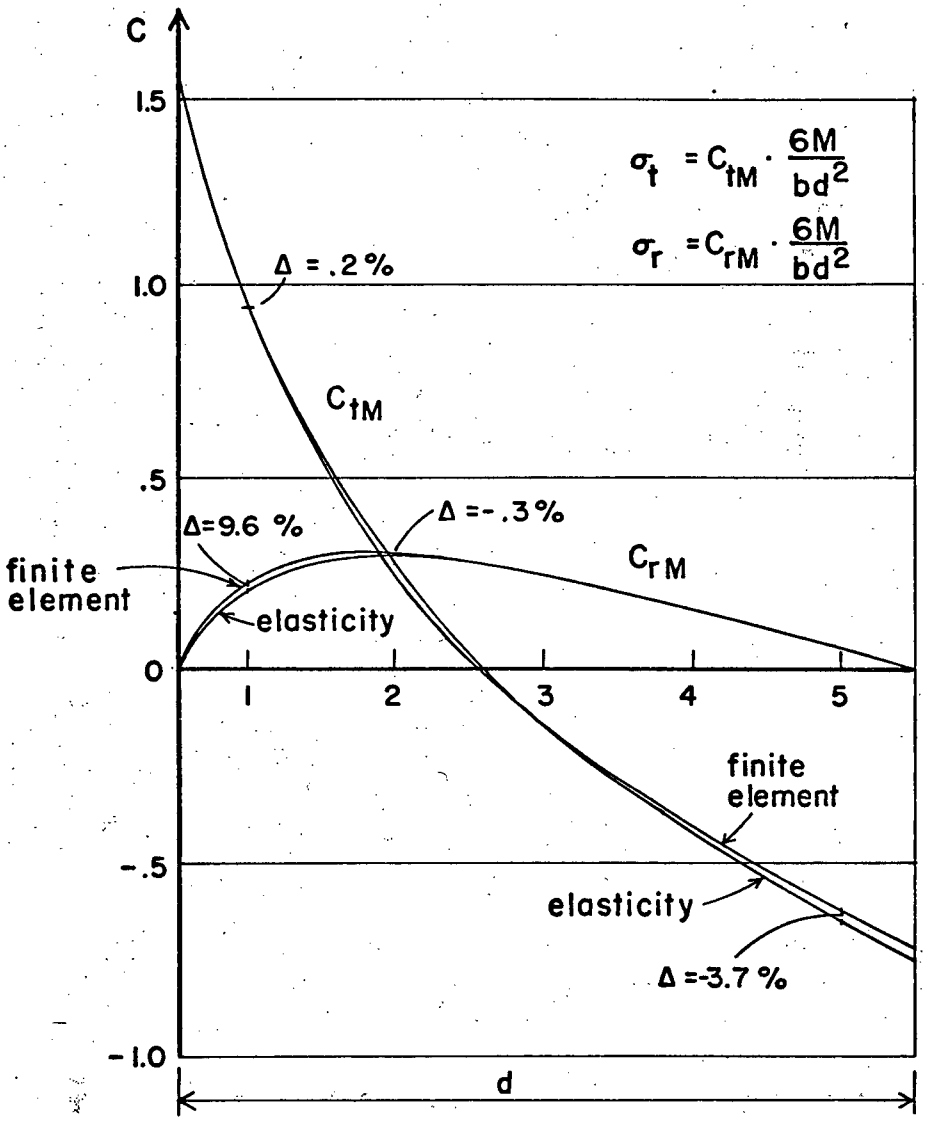

Fig.10. Isotropic circular beam, moment loading, stresses at $\phi = \beta/2$.

EXAMPLE 3

THICK ISOTROPIC CYLINDER UNDER UNIFORM EXTERNAL PRESSURE

The elasticity solution is given in Wang (6) on page 54.

Due to radial symmetry the problem is solved with one radial group (fig.11). However, to check the program, a quarter of the cylinder has been used too, with the same element size, and the same result was obtained.

The depth of the beam is divided into three elements and the group angle β is taken as 6°. The stresses are calculated for a ratio $\frac{d}{R} = .3$. The radial nodal forces, due to external pressure, are found by the formula

$$f_i = \frac{p \cdot (R + d) \cdot \beta}{2}$$

The remarkable accuracy found here with only three elements is due, of course, to the uniform stress set up within the element. However, previous examples have contained all modes of deformation and still showed good accuracy.

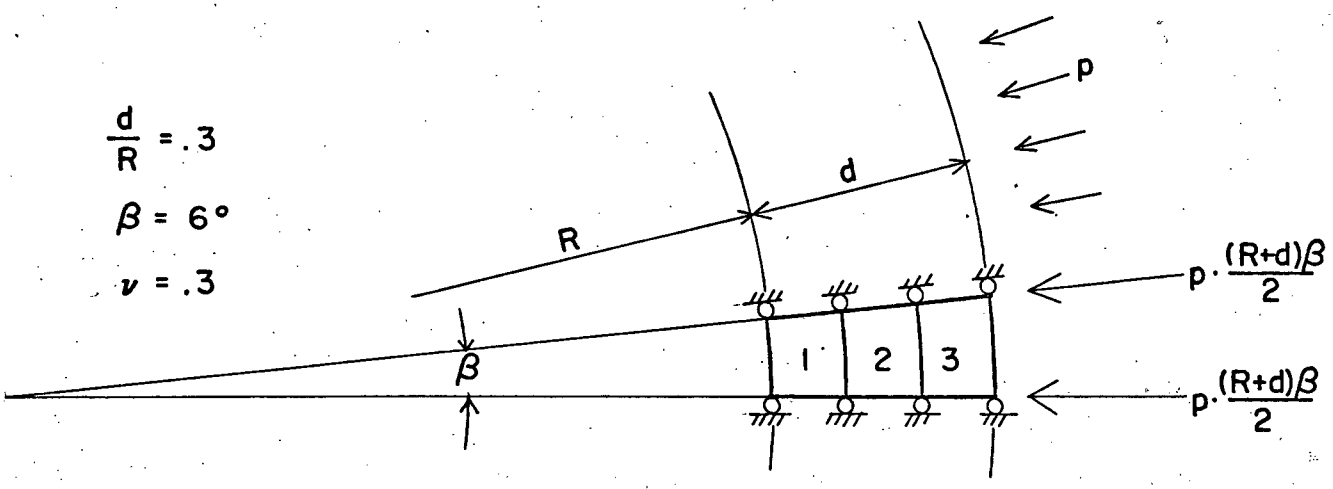

$\sigma_r = C_{rp} \cdot p$

$\sigma_t = C_{tp} \cdot p$

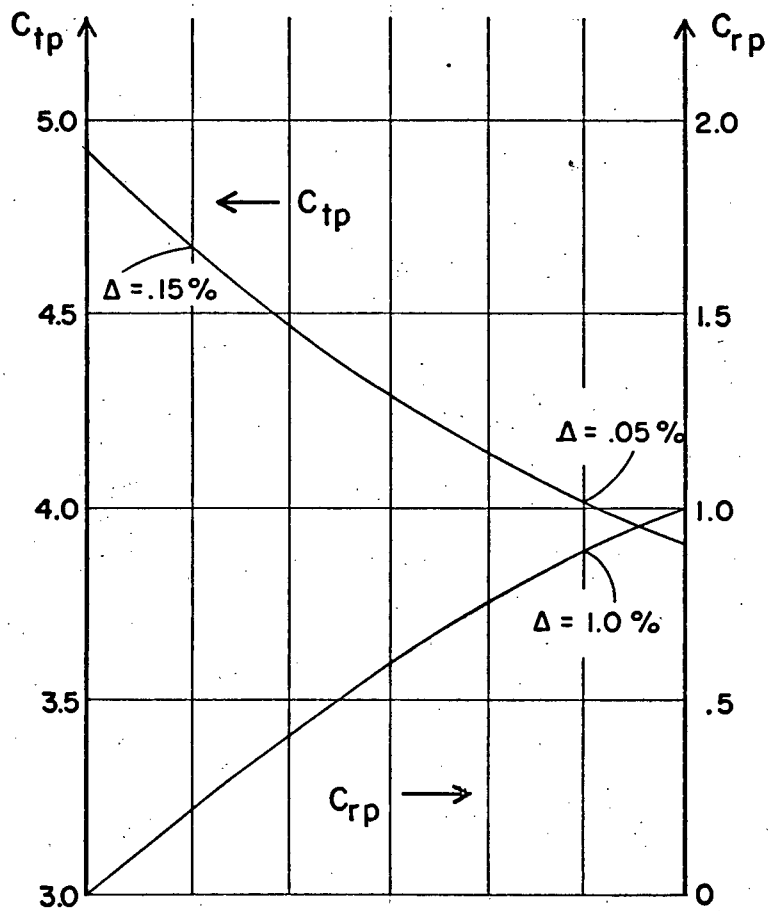

Fig.11. Thick isotropic cylinder under external pressure.

EXAMPLE 4

THICK ISOTROPIC CYLINDER UNDER UNIFORM TEMPERATURE GRADIENT

The elasticity solution is developed according to Timoshenko (5) on page 407.

By using the boundary conditions $\sigma_r = 0$ at $r = a$ (=R) and at $r = b$ (=R+d) and by introducing an assumed linear distribution of the temperature $T = T_o r$, the following elasticity solution for the stresses is obtained

$$\sigma_r = \frac{\alpha E T_o}{3r^2} \left[(r^2-a^2)\left(\frac{b^3-a^3}{b^2-a^2} \right) - (r^3-a^3) \right]$$

$$\sigma_t = \frac{\alpha E T_o}{3r^2} \left[(r^2+a^2)\left(\frac{b^3-a^3}{b^2-a^2} \right) - (2r^3+a^3) \right]$$

In the finite element solution, the respective initial strain is given by the formula

$$\{\varepsilon\}_o = \begin{Bmatrix} \alpha T_E \\ \alpha T_E \\ 0 \end{Bmatrix}$$

where T_E is the temperature in the center of the element as given by $T_E = T_o \left(R + \frac{d}{N}(n - 1/2)\right)$

N = total number of elements radially

n = element number from inside.

Again, due to radial symmetry, only one radial group is required to solve the problem. By taking five elements in the group, as shown in fig.12, the error in the maximum σ_r is 4.1%. With 10 elements in the group this is reduced to 1%.

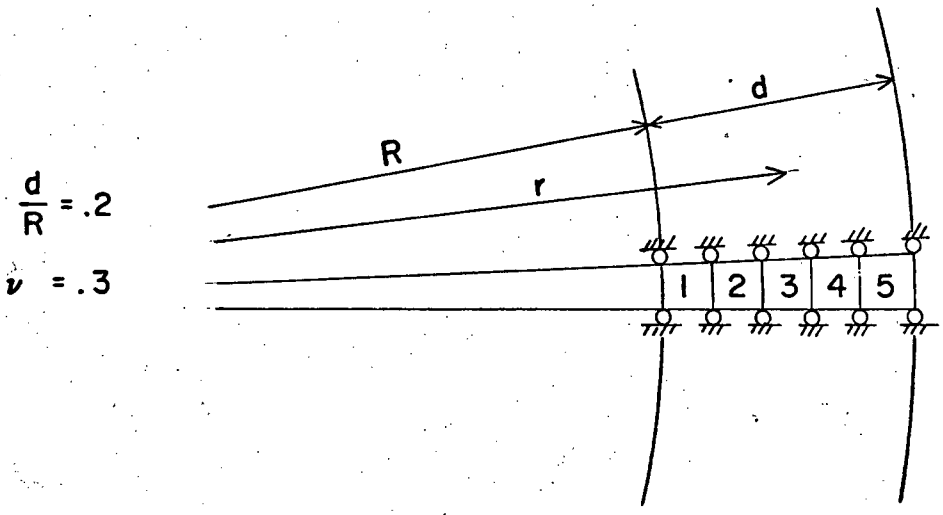

$\sigma_t = C_{tT} \cdot ET_o \frac{d}{2}$

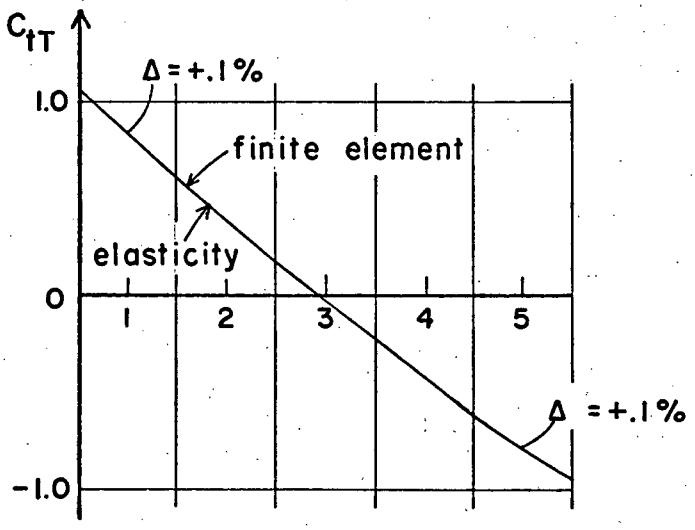

$\sigma_r = C_{rT} \cdot ET_o \frac{d}{2}$

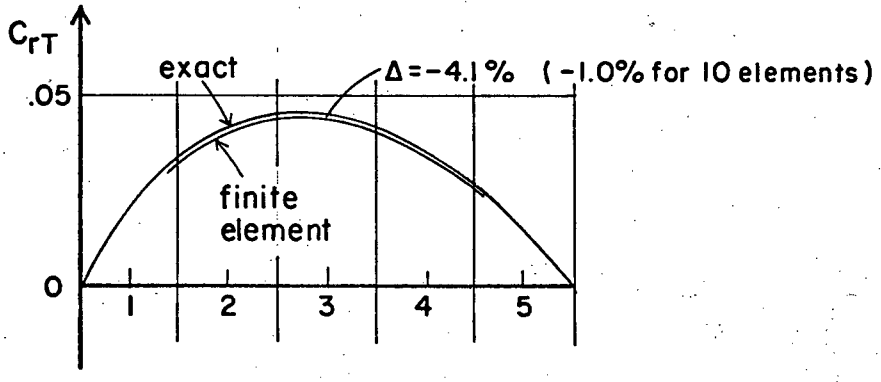

Fig.12. Thick isotropic cylinder, uniform temperature gradient.

4.2. ORTHOTROPIC CIRCULAR BEAMS

The remaining examples consider orthotropic material and the [D]-matrix is given with the example.

EXAMPLE 5

CIRCULAR ORTHOTROPIC BEAM UNDER PURE MOMENT

Fig. 13 shows properties of a curved orthotropic beam of Douglas Fir under pure moment for which the elasticity solution is given by Foschi (3). Foschi used the following elastic properties of Douglas Fir given by Hearmon (7).

$$E_x = 2.2765 \cdot 10^6 \text{ psi}$$
$$E_y = 0.1537 \cdot 10^6 \text{ psi}$$
$$\nu_{xy} = 0.290$$
$$\nu_{yx} = 0.020$$
$$G = 0.1276 \cdot 10^6 \text{ psi}$$

From these E_1, E_2, E_ν and G of the [D]-matrix are obtained as

$$E_1 = 2.29 \cdot 10^6 \text{ psi}$$
$$E_2 = 0.155 \cdot 10^6 \text{ psi}$$
$$E_\nu = 0.045 \cdot 10^6 \text{ psi}$$
$$G = 0.128 \cdot 10^6 \text{ psi}$$

To demonstrate the convergence trend by reducing the element size, the depth of the beam is divided once into three, once into five and once into ten elements, while β is kept constant. The nodal forces at the ends were distributed linearly to represent the applied moments. The result obtained with ten elements comes very close to the exact solution. Fig.13 shows the three finite element approximations and the exact solution at $\phi = \frac{\pi}{2}$. Also a part of the isotropic case is plotted for comparison.

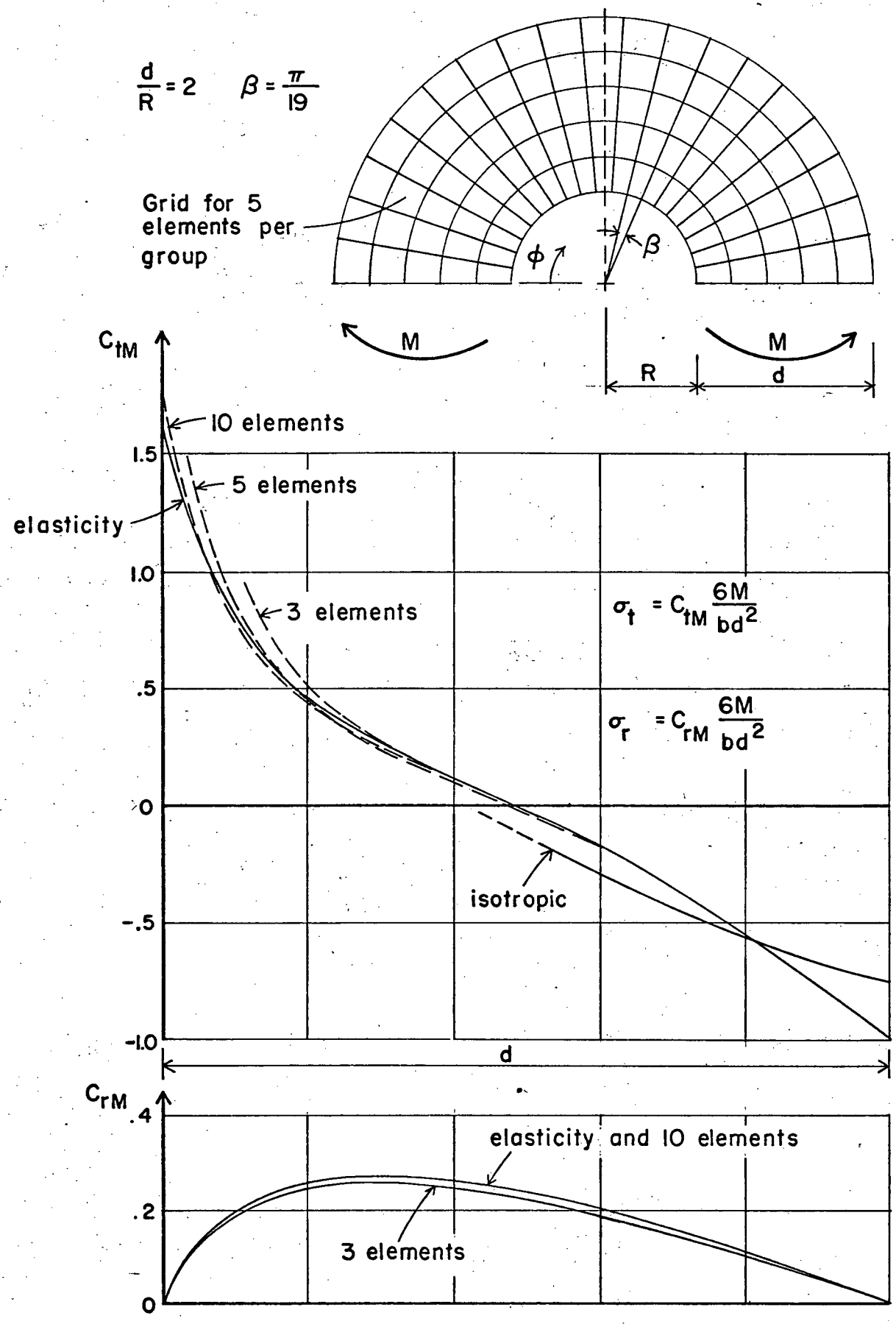

Fig.13. Circular orthotropic beam under pure moment.

EXAMPLE 6

CIRCULAR ORTHOTROPIC BEAM UNDER SHEAR LOAD

In this example shear loads, instead of moments, are applied on the same beam with the same [D]-matrix as in example 5. The applied shear load is represented by a set of equal nodal forces at the ends of the beam. In fig.14 the finite element approximation with ten elements over the depth is compared to Foschi's exact solution.

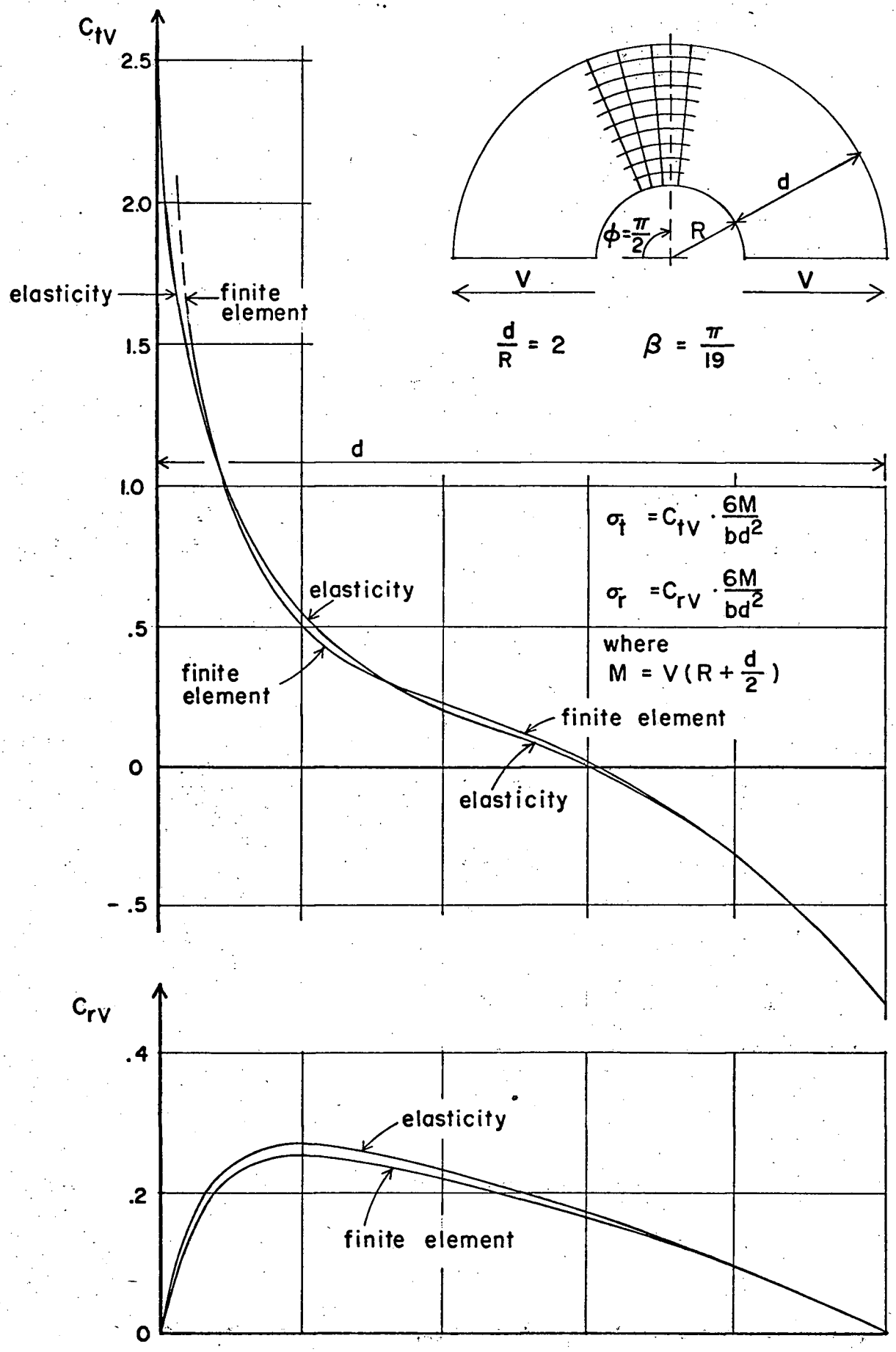

Fig.14. Circular orthotropic beam under shear load, stresses at $\phi = \pi/2$.

4.3. PITCH-CAMBERED ORTHOTROPIC BEAM

A favourable opportunity to check the finite element is offered by Fox. In his PROGRESS REPORT No.1 (4), on DOUBLE-TAPERED PITCHED BEAMS, a theoretical solution for the problem is obtained by using Fourier series and a point-matching method to satisfy the upper boundary conditions at several points. The other boundary conditions are satisfied everywhere. This theory has been verified by testing experimentally, a glued laminated beam with the geometric properties given in fig.15.

This test beam under pure moment is chosen as an example to compare the two theoretical solutions. The stress distribution given by S.P. Fox is based on the material properties

$$E_x = 2.45 \cdot 10^6 \text{ psi}$$
$$E_y = 0.169 \cdot 10^6 \text{ psi}$$
$$\nu_{xy} = 0.033$$
$$\nu_{yx} = 0.473$$
$$G = 0.137 \cdot 10^6 \text{ psi}$$

The equivalent [D]-matrix in the finite element solution has the terms

$$E_1 = 2.46 \cdot 10^6 \text{ psi}$$
$$E_2 = 0.169 \cdot 10^6 \text{ psi}$$
$$E = 0.0799 \cdot 10^6 \text{ psi}$$
$$G = 0.137 \cdot 10^6 \text{ psi}$$

The finite element grid, used to represent the beam, is shown in fig.16. The boundary elements are approximated as described in chapter 3.1. page 21. The stresses at centerline are obtained by quadratic interpolation and are plotted in fig.17, together with Fox's solution. The two solutions are close together. The difference in maximum tangential stress is 1.9%, in maximum radial stress 4.6% and in minimum tangential stress 3.0%.

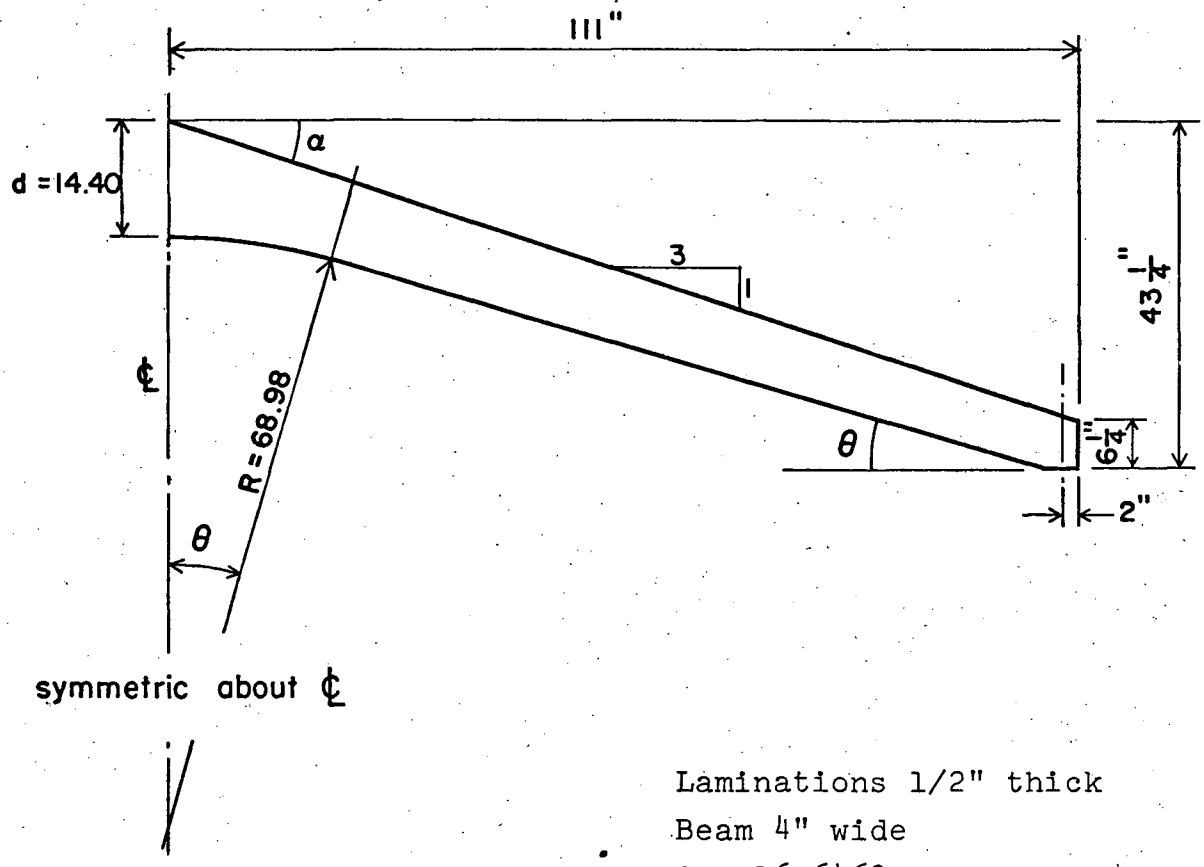

Laminations 1/2" thick
Beam 4" wide
$\theta = 16.646°$
$\alpha = 18.430°$ ($\tan\alpha = .333$)

Fig.15. Geometric dimension of the tested beam.

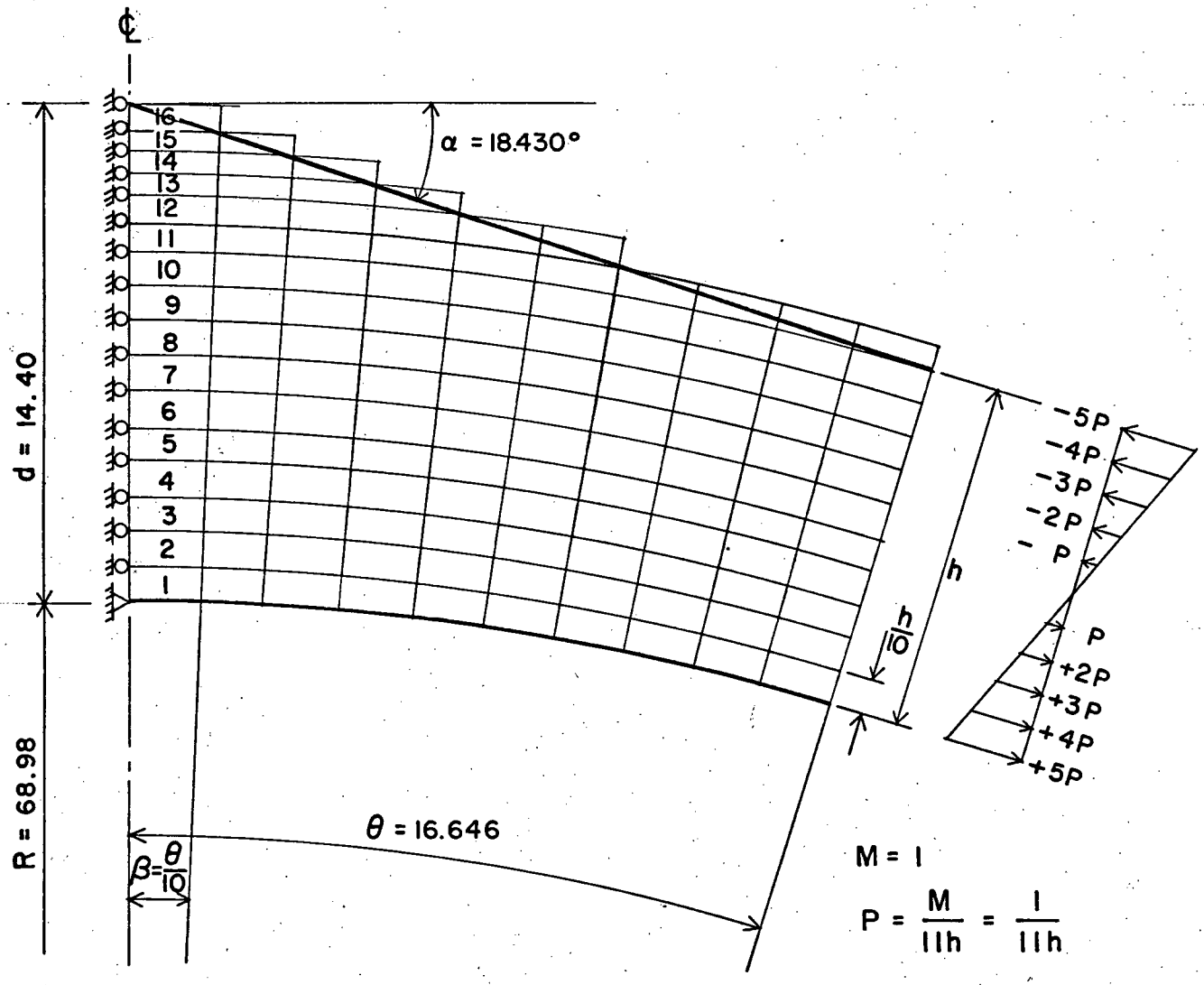

Fig.16. Finite element grid, loading condition moment.

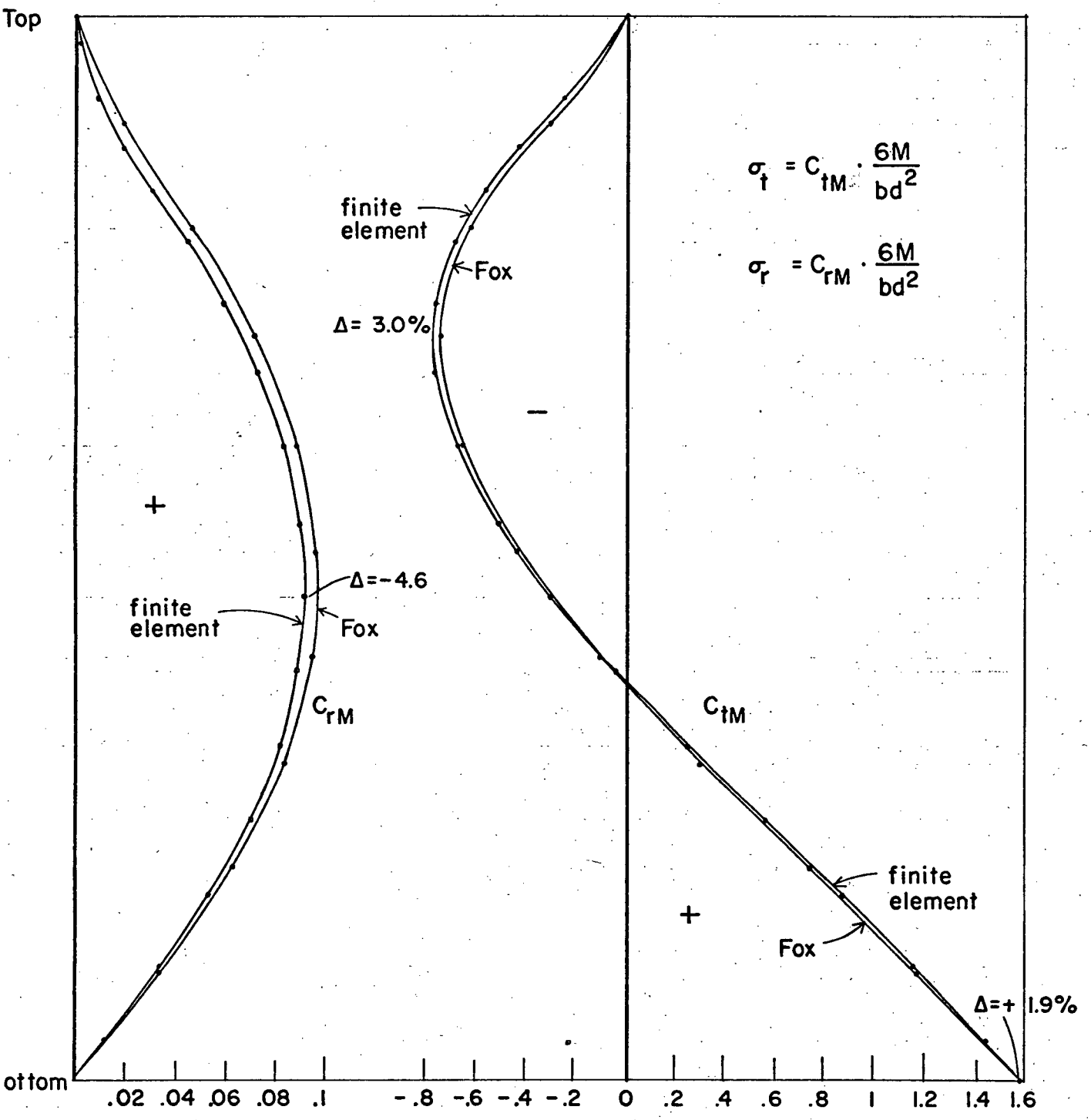

Fig.17. Stresses at centerline of the tested beam.

The chosen length $\theta \cdot R$ in the finite element approximation should be sufficient by St. Venant's principle to produce accurate results at the centerline. To check this, the beam under the same loading condition has been extended to a length of 1.5 θR. The change in maximum stresses at centerline was less than 1/2%, well within the desired accuracy.

In the extended case, where a part of the straight beam has to be used to get enough length, this straight part has to be simulated by a curved beam with a large radius $\bar{R} = 10\ R$, since the computer program is written for curved beams. A change from $\bar{R} = 10\ R$ to $\bar{R} = 20\ R$ varies the maximum stresses at centerline not more than .07%.

The last thing to be checked is the influence of the stepwise approximation of the upper boundary. To do this, stresses in this beam are calculated with upper boundary elements of zero thickness and also with full thickness. The maximum tangential stress changes by 8% between those two extremes, while the maximum radial stress changes by 5%. The approximation, using a thickness between the two extremes, can produce an error w.r.t. the original beam which is only a part of the total difference. Since this error has the same magnitude as in the examples 1 to 6 for curved beams, where no stepwise approximation is required, the desired accuracy is obtained. The actual accuracy is well within 5%, quite sufficient for the practical purpose herein.

The good results in the examples of this chapter, obtained by the finite element solution, justify the applications made in the next chapter. There the parameters d, R and α in the pitch-cambered beam are varied to cover the practical range.

5. STRESSES IN PITCH-CAMBERED BEAMS

PREAMBLE

In the following are shown stresses due to moments, shear loads, change in moisture content and change in elastic properties, in an attempt to evaluate the factors which might create high stresses.

The beams have been divided into 10 or more radial groups, with about 15 elements at centerline, to provide good results. The results are presented in terms of the parameters d/R and tanα. Fig.18 shows the parameters and the grid of an example which is used several times in this chapter to demonstrate various effects.

If not mentioned specifically, the following elasticity constants are used

$$E_x = E_{tan}$$
$$E_y = E_{tan} / 20$$
$$G = E_{tan} / 15$$
$$\nu_{xy} = .0185$$
$$\nu_{yx} = .370$$

This gives

$$[D] = \begin{bmatrix} E_1 & E_\nu & 0 \\ E_\nu & E_2 & 0 \\ 0 & 0 & G \end{bmatrix} = \begin{bmatrix} 1 & E/E_1 & 0 \\ E/E_1 & E_2/E_1 & 0 \\ 0 & 0 & G \end{bmatrix} E_1 = \begin{bmatrix} 1 & .0185 & 0 \\ .0185 & .0500 & 0 \\ 0 & 0 & .6621 \end{bmatrix} E_1$$

where $E_1 = E_x / (1-\nu_{xy} \cdot \nu_{yx})$ can have any value, as this constant factor does not effect the distribution or magnitude of the stresses, except in the case of moisture change where E_1 is taken as 1810. ksi.

This is reasonable for Douglas Fir. The effect of ratio changes in this [D]-matrix is checked in section 5.4. It should be noted that x and y correspond with the tangential and radial direction of the beam, that is with the grain and perpendicular to the grain direction of the wood.

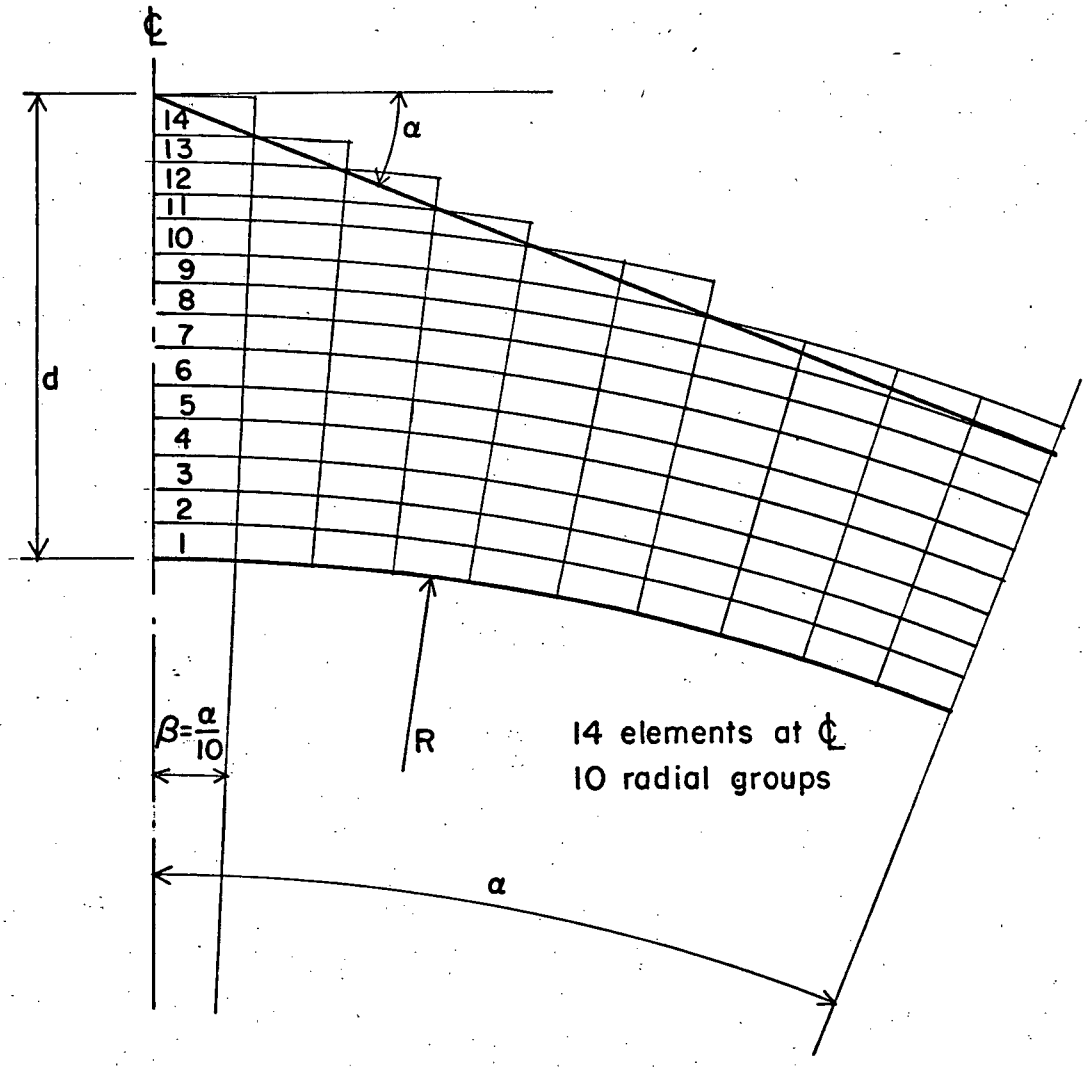

Fig.18. Arrangement for d/R = .2 and tan α = .4.

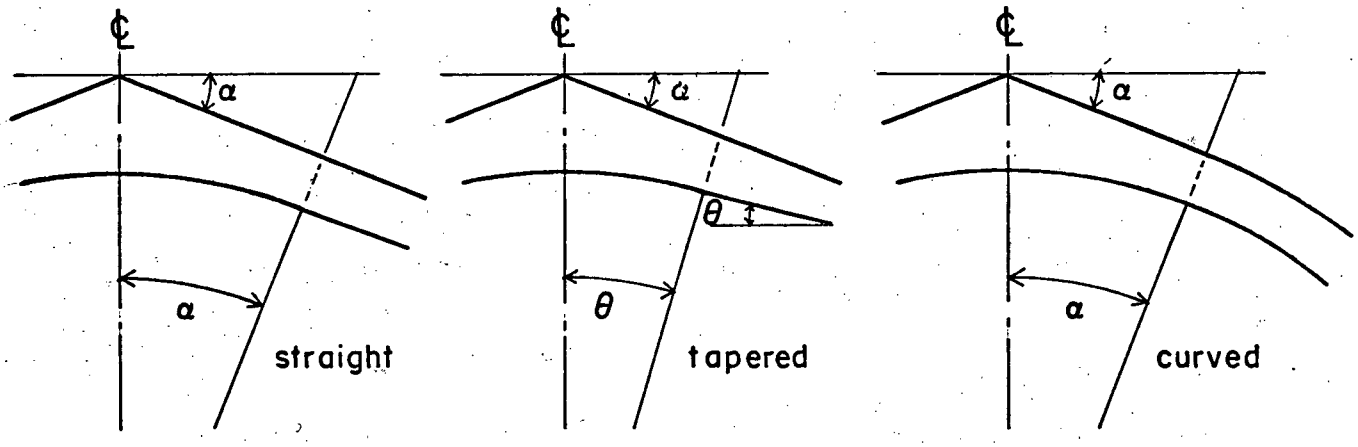

Fig.19. Three possible cases of pitch-cambered beams.

5.1. STRESSES FROM MOMENTS

The peak at midspan of the pitch-cambered beam induces a stress concentration. This stress concentration is local by St. Venant's principle. At some distance from the centerline where the beam is straight, uniform tapered or curved (see fig.19), the existing formulas are valid.

The stress concentration at centerline in beams under pure bending moments, is investigated in this section. To cover the practical range a group of 26 beams, with d/R varying from .01 to .8 and tanα from .1 to .6, has been chosen for the finite element solution. A sketch of four beams in the upper and lower parameter range is given in fig.20 to aid in visualising the parameters.

All beams showed at centerline the characteristic stress distribution sketched in fig.21 with zero radial and tangential stress at the top of the beam. For cross sections adjacent to the centerline the stresses at the top edge are different from zero. The stress concentration produces a local maximum in the radial stresses.

The maximum and minimum stresses at centerline, as indicated in fig.21, are related to the value

$$\frac{M}{Z_{centerline}} = \frac{6\,M}{bd^2}$$

by the dimensionless coefficients C_{RM}, C_{TM} and C_{CM} as follows:

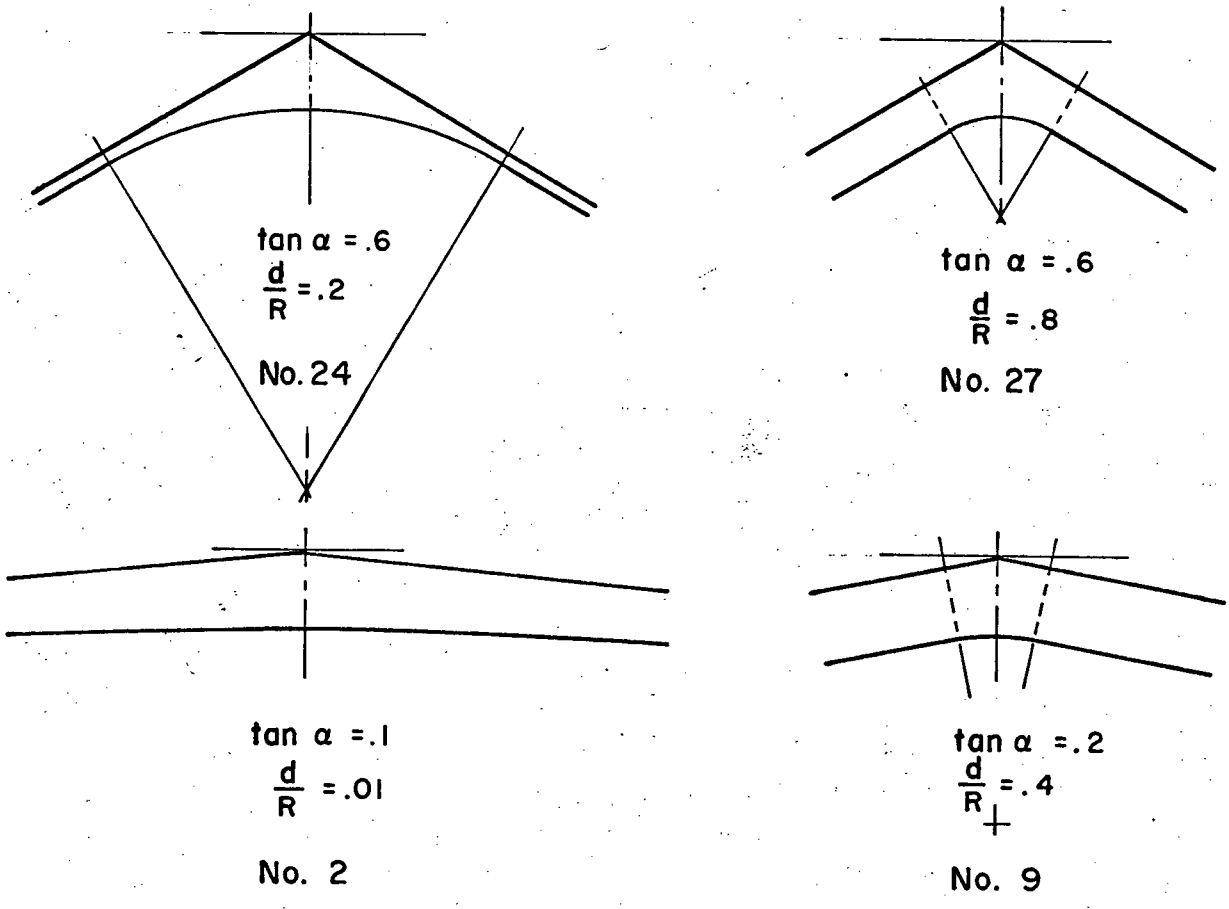

Fig.20. Beams No. 2, 9, 24 and 27.

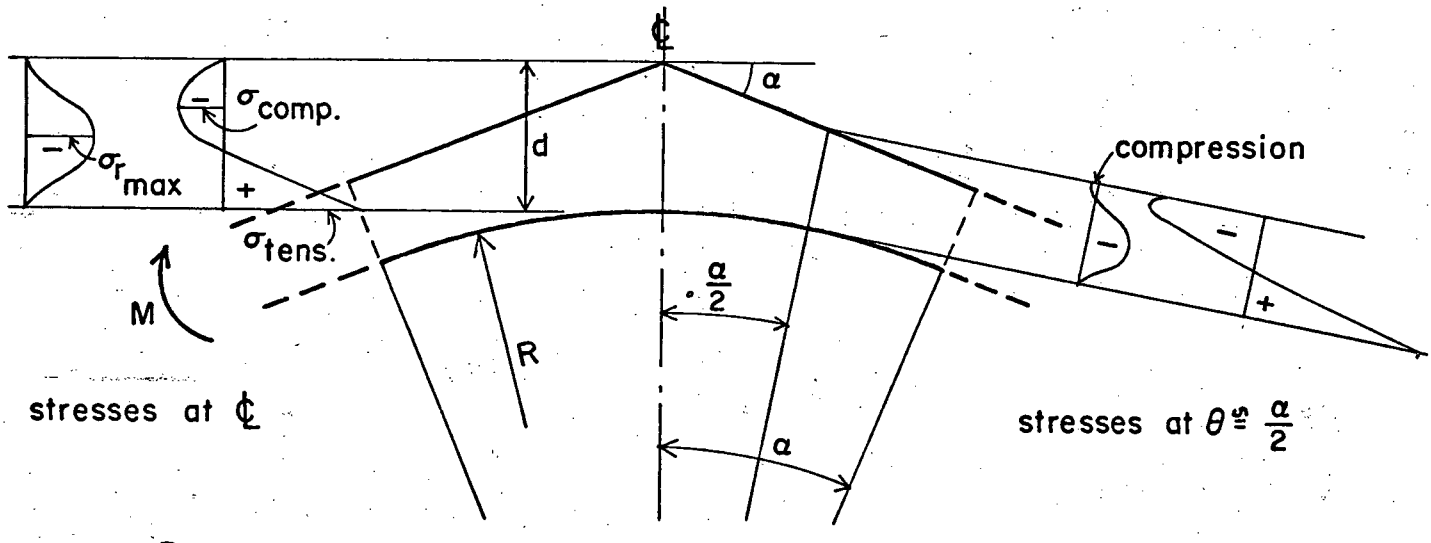

Fig.21. Characteristic stress distribution for pure bending moment.

maximum radial stress $\sigma_{r_{max}} = C_{RM} \frac{6\,M}{bd^2}$

maximum tangential tensile stress $\sigma_{tens} = C_{TM} \frac{6\,M}{bd^2}$

maximum tangential compression stress $\sigma_{comp} = C_{CM} \frac{6\,M}{bd^2}$

Due to symmetry, only one half of the beam had to be solved by finite elements and a quadratic interpolation had to be used to get the values at centerline, since the computer program produces stresses at the centers of the elements.

Table 2 shows for each considered beam the parameters d/R and tanα, the number of elements NE at centerline, the number of radial groups NG and the stress coefficients C_{RM}, C_{TM} and C_{CM}.

A graphical presentation of the radial stress coefficients C_{RM} is given in fig.22. The coefficients are plotted against (d/R). A set of curves is obtained by connecting the points of constant tanα. The coefficients C_{RM} of radial stresses can readily be taken out of this graph for any parameters.

The values for radial stresses obtained by the classical formula for curved beams

$$\sigma_r = \frac{3}{2} \frac{M}{bd(R+d/2)} = \frac{1}{4} \cdot \frac{d}{(R+d/2)} \frac{6\,M}{bd^2}$$

are plotted by a dashed line. From the comparison it can be seen that the whole practical range produces up to 4 times

TABLE 2

Parameters and stress coefficients
of the considered beams

No	tanα	d/R	NG	NE	C_{TM}	C_{CM}	C_{RM}
1	0.0	.5	9	10	1.067	-1.323	.0599
2	0.1	.01	12	22	1.151	-0.710	.0243
3	0.1	.05	15	16	1.124	-0.751	.0253
4	0.1	.1	16	19	1.127	-0.763	.0302
5	0.2	.01	11	23	1.371	-0.687	.0455
6	0.2	.05	10	15	1.324	-0.7025	.0463
7	0.2	.1	10	16	1.2826	-0.7165	.0487
8	0.2	.2	13	15	1.2743	-0.7320	.0601
9	0.2	.4	14	14	1.3869	-0.7281	.0825
10	0.3	.1	10	15	1.5538	-0.7341	.0731
11	0.3	.2	10	15	1.4881	-0.7434	.0817
12	0.3	.4	10	13	1.5241	-0.7281	.1059
13	0.3	.6	12	13	1.6343	-0.7182	.1252
14	0.4	.01	16	20	2.042	-0.818	.0946
15	0.4	.1	10	11	1.9174	-0.7775	.1000
16	0.4	.2	10	14	1.7805	-0.7937	.1076
17	0.4	.4	16	15	1.7244	-0.7794	.1312
18	0.4	.6	11	16	1.8015	-0.7672	.1550
19	0.5	.2	15	13	2.2418	-0.8964	.1438
20	0.5	.4	13	14	2.0202	-0.8569	.1608
21	0.5	.6	15	15	2.0202	-0.8271	.1851
22	0.5	.8	14	15	2.1001	-0.7999	.2071
23	0.6	.01	16	20	3.016	-1.066	.1600
24	0.6	.2	15	15	2.6702	-0.9870	.1788
25	0.6	.4	13	13	2.4215	-0.9502	.1975
26	0.6	.6	13	13	2.3208	-0.9030	.2189
27	0.6	.8	14	12	2.3561	-0.8764	.2431

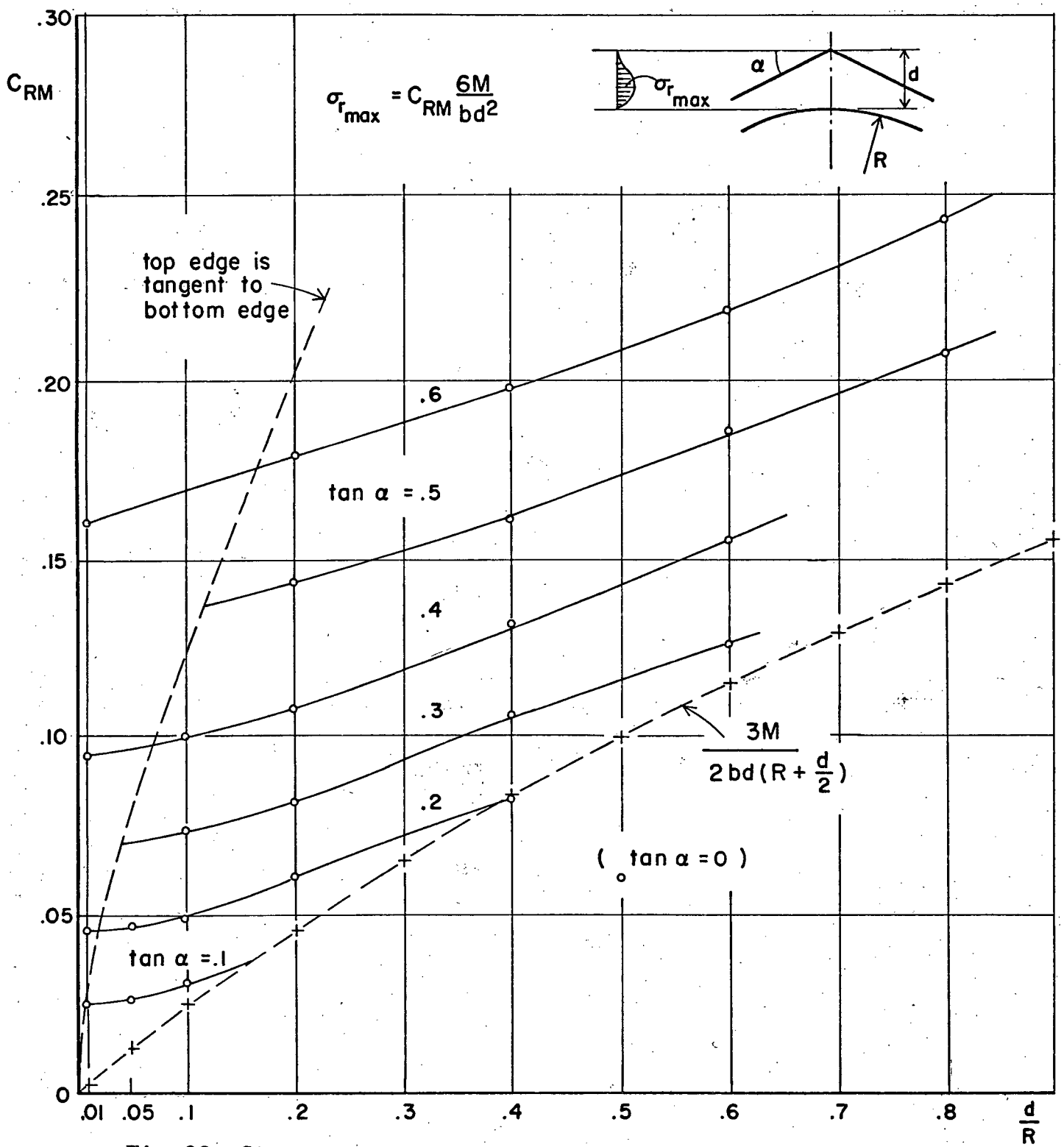

Fig. 22. Stress coefficient C_{RM} for maximum radial stress at centerline due to pure bending.

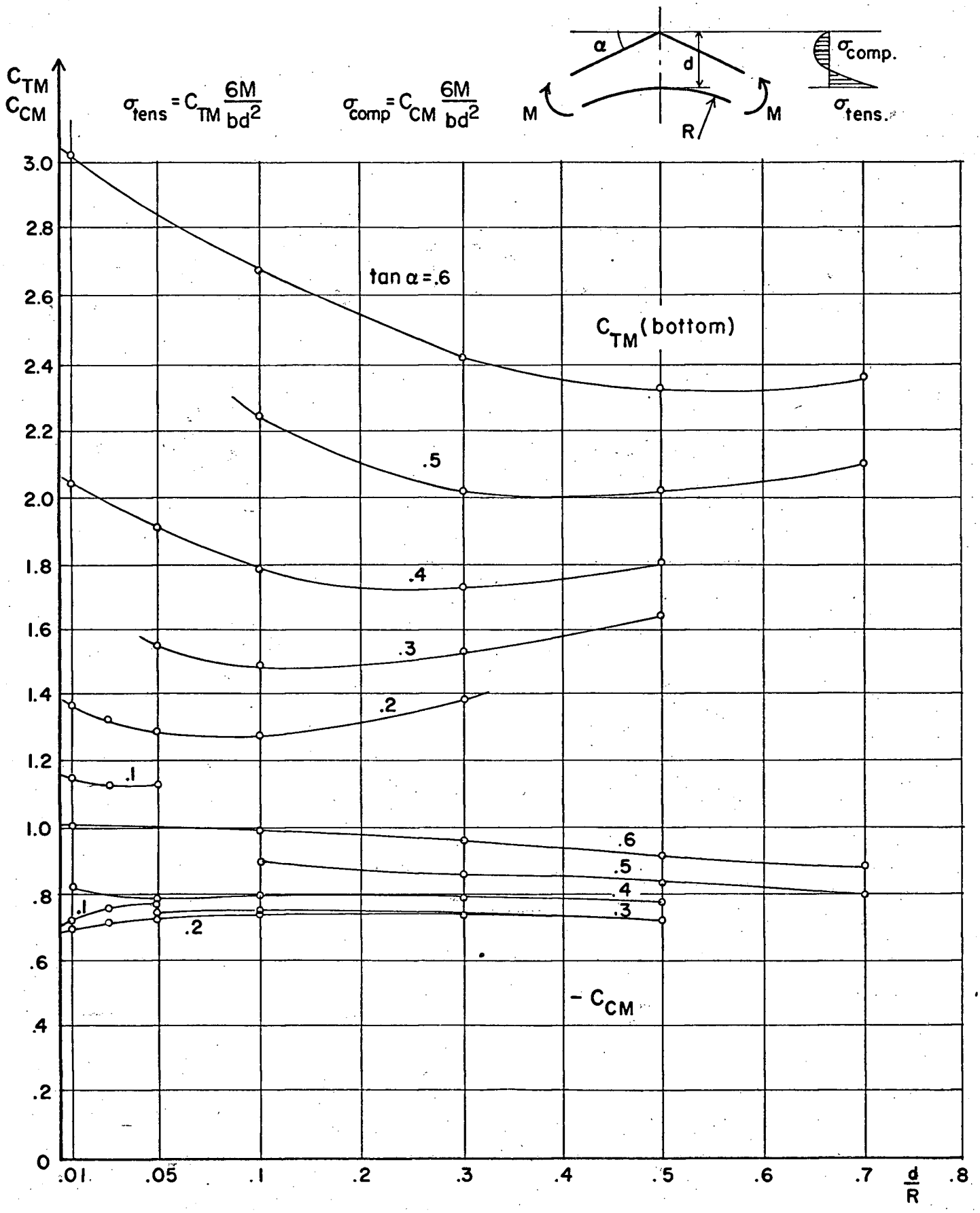

Fig.23. Stress coefficients C_{TM} and C_{CM} for tangential stresses at centerline due to pure bending.

higher stresses than given by this classical formula. Even if the depth at the point of tangency is used in the formula, the stresses obtained by finite elements are still remarkably higher for small d/R's.

The calculated stress coefficients for the tangential stresses are plotted in fig.23. The points are connected by hand, to produce curves from which the stress coefficients for tangential stresses can be obtained for any parameter. For the considered beams with deepest cross sections at centerline, the significant tangential stresses for design do not occur at centerline cross sections. From an inspection of the stresses in each element in the computer output, it was observed that the tangential bottom fibre stress, due to pure bending, was the smallest at the centerline. Even though C_{TM} is greater than 1, the extra depth at center keeps the tangential stress smaller than in adjacent cross sections.

5.2. STRESSES FROM SHEAR LOAD

A pure shear load at centerline is produced by the loading conditions shown in fig.24.

Due to antimetry, there is, at centerline, no tangential stress (σ_t) and also there is no radial strain (ε_r). Introducing $\sigma_t = \varepsilon_r = 0$ into Hooke's law

$$\sigma_t = E_1 \varepsilon_t + E_\nu \varepsilon_r$$

$$\sigma_r = E_\nu \varepsilon_t + E_2 \varepsilon_r$$

it can be seen that the radial stress must be zero.

To check the magnitude of the centerline shear stresses, the beam with $\tan\alpha = .4$ and $d/R = .2$ of fig.18 is investigated. Fig.25 shows the shear stress distribution at centerline. The maximum shear stress at centerline is:

$$\tau_{max} = 1.4 \left(\frac{3}{2} \frac{V}{bd} \right)$$

Even though the maximum shear stress at centerline is 40% more than normal, this will not govern design since the depth here is larger than at the supports and the maximum shear force is about one quarter the support shear.

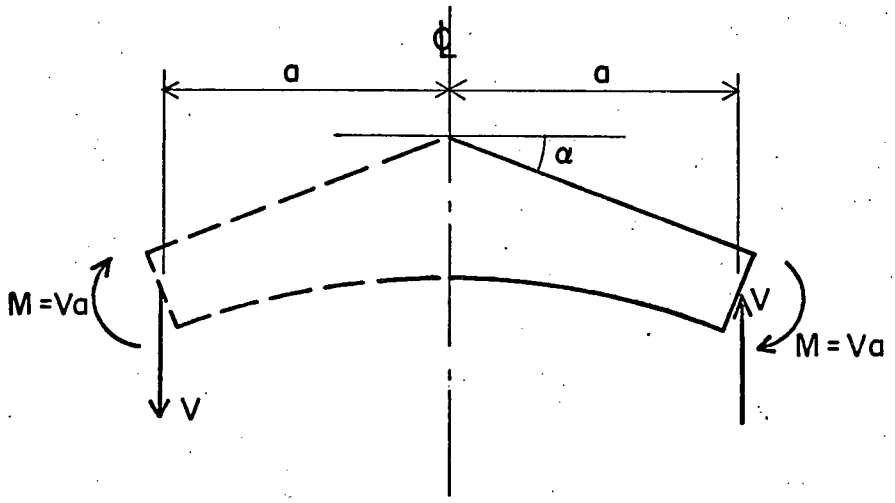

Fig.24. Antimetric loadcase for a pure shear load at centerline.

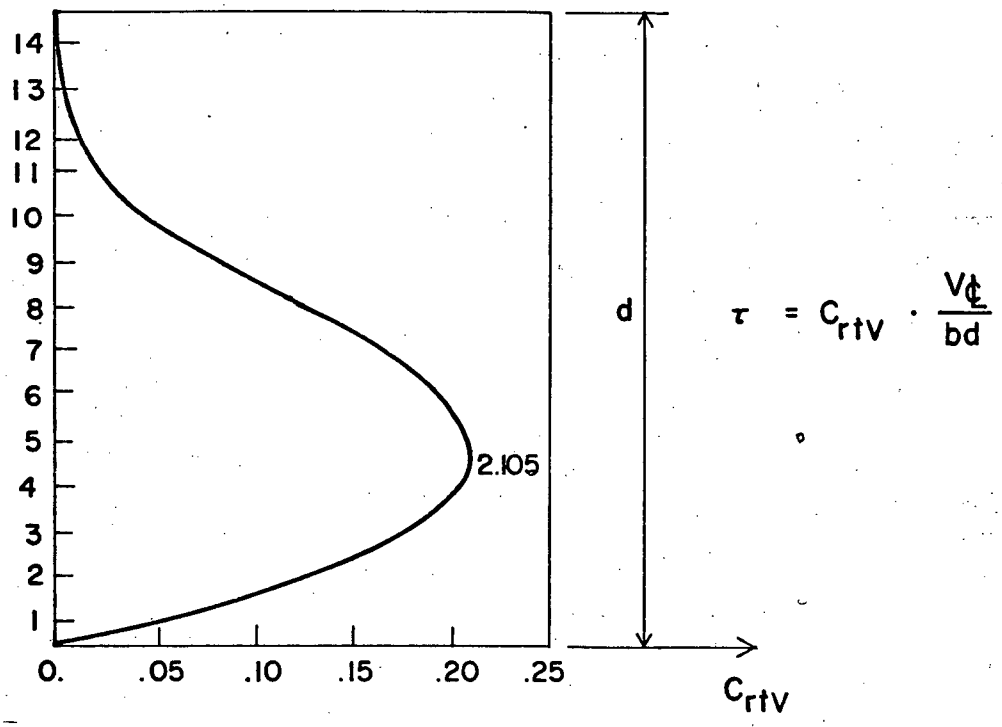

Fig.25. Shear stresses at centerline from pure shear load.

5.3. STRESSES DUE TO CHANGE IN MOISTURE CONTENT

Change in moisture content causes the initial strains ε_{ro} and ε_{to}, i.e.

$$\{\varepsilon\}_o = \begin{Bmatrix} \varepsilon_{r_o} \\ \varepsilon_{t_o} \\ 0 \end{Bmatrix}$$

If the distribution of strains $\{\varepsilon\}_o$ satisfies the compatibility equation

$$\frac{\partial^2 \varepsilon_t}{\partial r^2} + \frac{1}{r}\frac{\partial}{\partial r}\{2\varepsilon_t - \varepsilon_r\} + \frac{1}{r^2}\frac{\partial^2 \varepsilon_r}{\partial \theta^2} = \frac{1}{r^2}\frac{\partial \gamma_{rt}}{\partial \theta} + \frac{1}{r}\frac{\partial \gamma_{rt}}{\partial r \partial \theta}$$

then no stresses are produced, if the structure is supported in a determinate way. With $\{\varepsilon\} = \{\varepsilon\}_o$ the equation is

$$\frac{\partial^2 \varepsilon_{to}}{\partial r^2} + \frac{1}{r}\frac{\partial}{\partial r}\{2\varepsilon_{to} - \varepsilon_{ro}\} + \frac{1}{r^2}\frac{\partial^2 \varepsilon_{ro}}{\partial \theta^2} = 0$$

This equation is satisfied if ε_{ro} and ε_{to} are independent of r and θ, or if $\varepsilon_{to} = 1/2\varepsilon_{ro}$ and varies linearly with r and θ. The latter case is unlikely. The first case shows that a uniform moisture change causes no stresses, but nonuniform moisture change will induce stresses.

Since in a pitch-cambered beam it is not obvious what strain distribution $\{\varepsilon\}_o$ causes maximum stresses, a closer look into a representative example is indicated. The beam with $\tan\alpha = .4$ and $d/R = .2$ shown in fig.18 is investigated. As shown in the figure, the elements 1 to 8 are spaced equally while the depth of the elements 9 to 14 are fixed by the approximation of the upper edge. A total of 14 pairs of load cases were run. For each pair one group of elements of constant radius were given

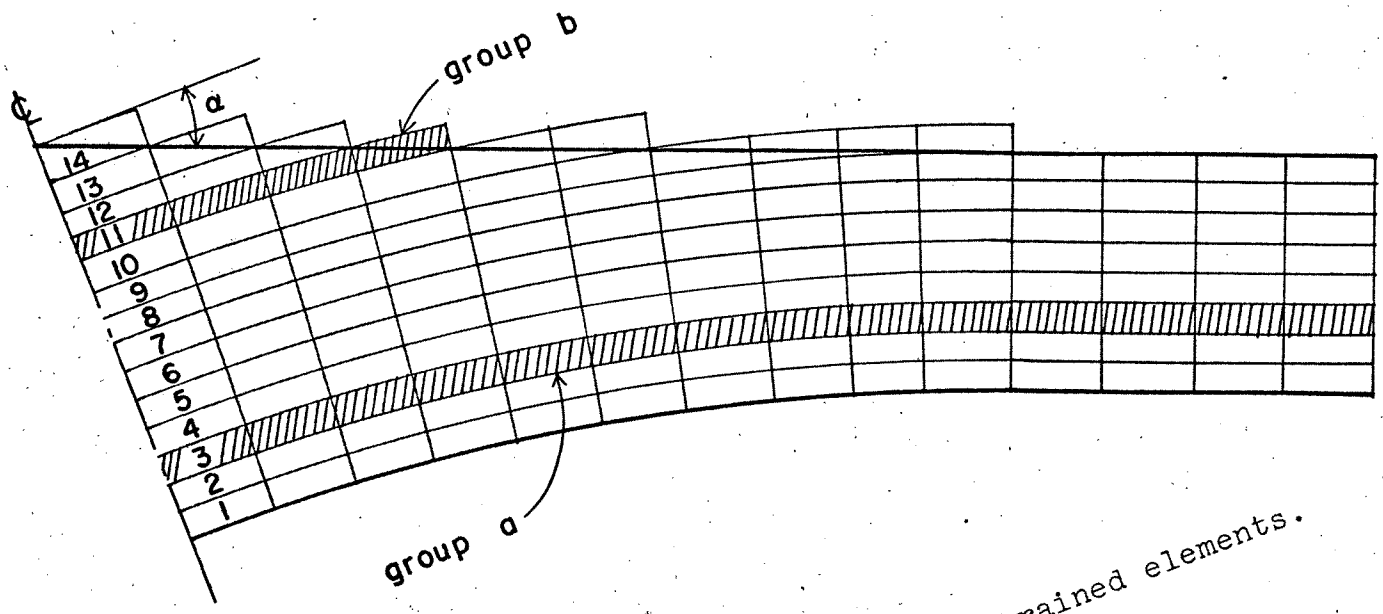

Fig.26. Two cases of a group of strained elements.

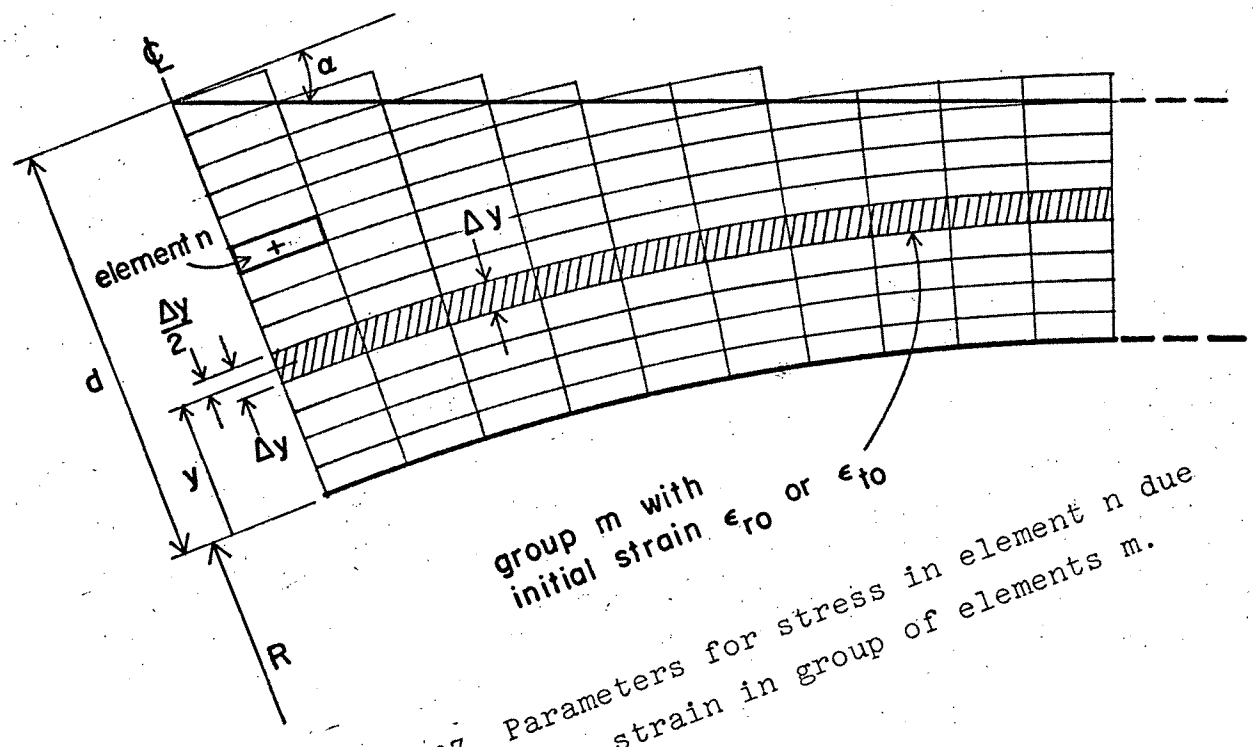

Fig.27. Parameters for stress in element n due to strain in group of elements m.

first	$\varepsilon_{ro} = .01$	$\varepsilon_{to} = 0$
and then	$\varepsilon_{ro} = 0$	$\varepsilon_{to} = .01$

In fig.26 two different cases of a group of strained elements are shown. Group a has elements along the whole beam, while group b reaches the top edge before the support.

The stresses of all these load cases can be combined to represent other states of initial strain by superposition. Similarly influence lines can be obtained. The latter was done for radial stresses.

As the radial stresses at centerline are the largest, influence lines are of interest there. The stresses $\Delta\sigma_r$ at the center of an element n adjacent to the centerline, due to strain change in one group of elements at level y, is a function of seven parameters.

$$\Delta\sigma_r = f[\Delta y,\ y,\ d,\ R,\ \alpha\ ,\ \varepsilon_o,\ E]$$

The parameters are shown in fig.27. A dimensionless representation is in the form

$$\frac{\Delta\sigma_r}{E} = f[\ \frac{\Delta y}{d}\ ,\ \frac{y}{d}\ ,\ \frac{d}{R}\ ,\ \varepsilon_o,\ \alpha\ ]$$

which requires only five parameters. Here $\frac{d}{R}$ and $\tan\alpha$ are set at .2 and .4 by the chosen geometry of the example; the modulus E is fixed as given on page 50; the radial or tangential strain ε_o is taken as .01. Since there exists a linear system, the stress varies directly with ε_o so that results for other strain magnitudes are in direct ratio to the one chosen. The stresses can now be written as

$$\Delta\sigma_r = f[\ \frac{\Delta y}{d}\ ,\ \frac{y}{d}\ ]$$

since the other three parameters are now constant.

Because $\frac{\Delta y}{d}$ is small, it can be assumed that $\Delta\sigma_r$ varies linearly with Δy so that

$$\frac{\Delta\sigma_r d}{\Delta y} = g\left(\frac{y}{d}\right)$$

and

$$\sigma_r = \int_0^d g\left(\frac{y}{d}\right)\frac{\Delta y}{d} = \int_0^1 g\left(\frac{y}{d}\right)\Delta\left(\frac{y}{d}\right)$$

For an influence line at one point, due to initial strain in the element groups 1 to 14, the stresses at this point are required from all load cases. The sum of the stresses of all load cases is zero, since it represents uniform strain over the whole beam. From these stresses the values g are calculated and plotted at the corresponding level (y/d) of the strained group. Now the total area, enclosed by an influence line, corresponding to uniform strain over the whole beam, is zero. Influence lines were calculated for the centers of all 14 elements at centerline. A few of them are shown in fig.28 and fig.29.

It should be noted that these plots are for radial or tangential strain $\varepsilon_o = .01$, so that results for other strains can be obtained by direct ratio. As well they are calculated using the modulus E_1 = 1810 ksi of page 51 so that results for other E_1 are obtained by direct ratio again.

The influence lines for radial stress show that the largest possible stress, due to pure radial or tangential strain, is obtained at the center of element 9, however, with a different strain distribution for each. The two influence lines for this point are shown in figures 30a and 30b together with the two strain loads providing maximum σ_r. From the figure it can be seen, that each strain load produces a considerable stress only in one influence line, while the other influence line does not contribute.

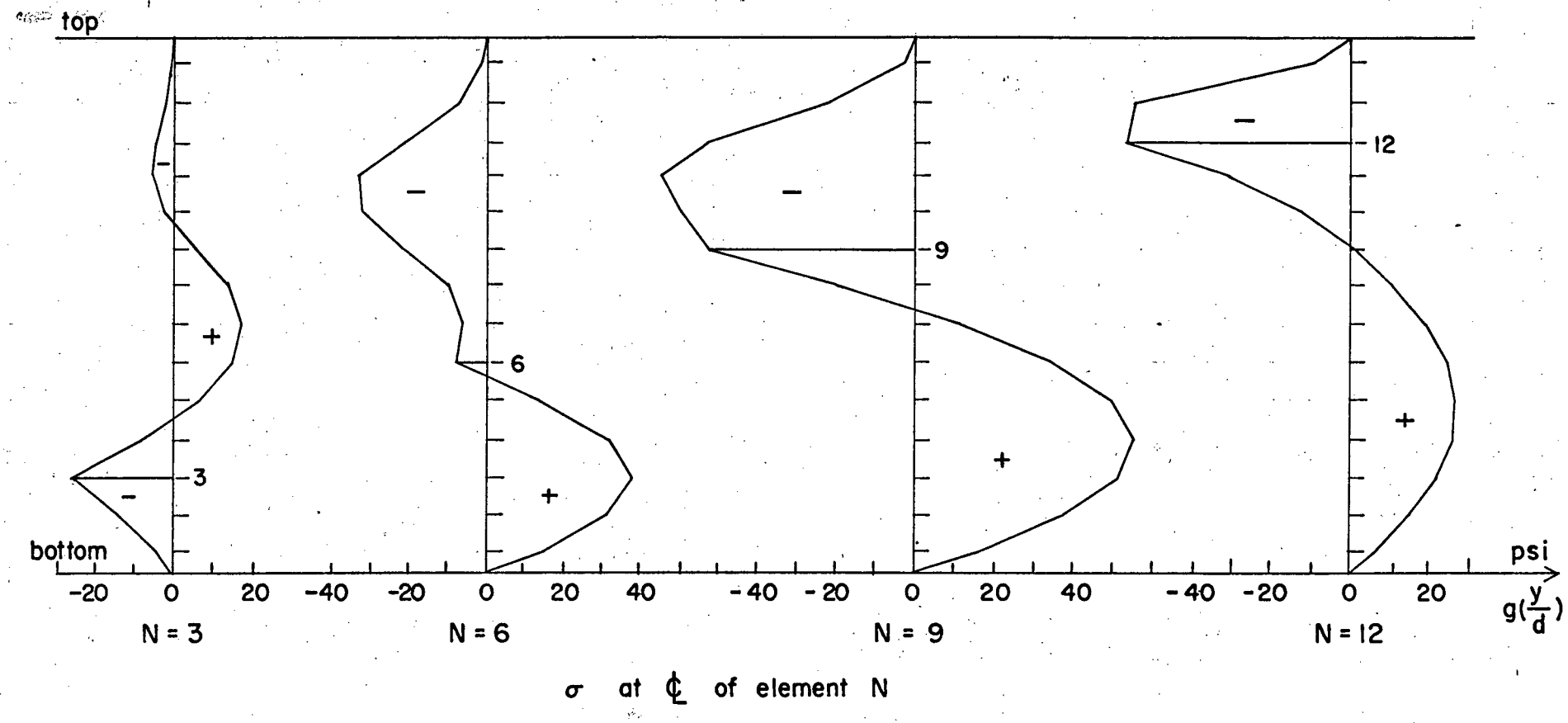

Fig.28. Influence lines for radial stresses due to initial radial strain of 1%.

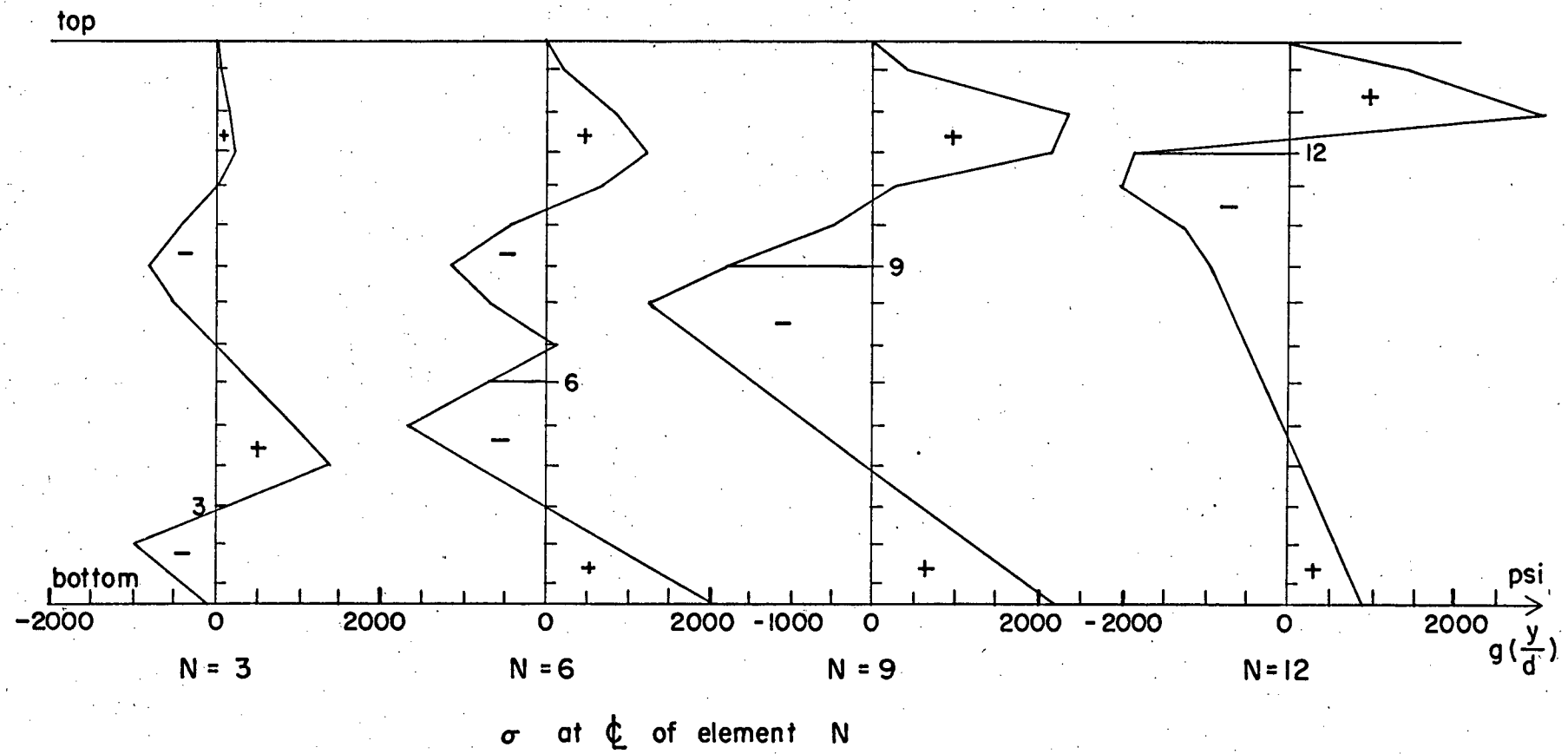

Fig.29. Influence lines for radial stresses due to initial tangential strain of 1%.

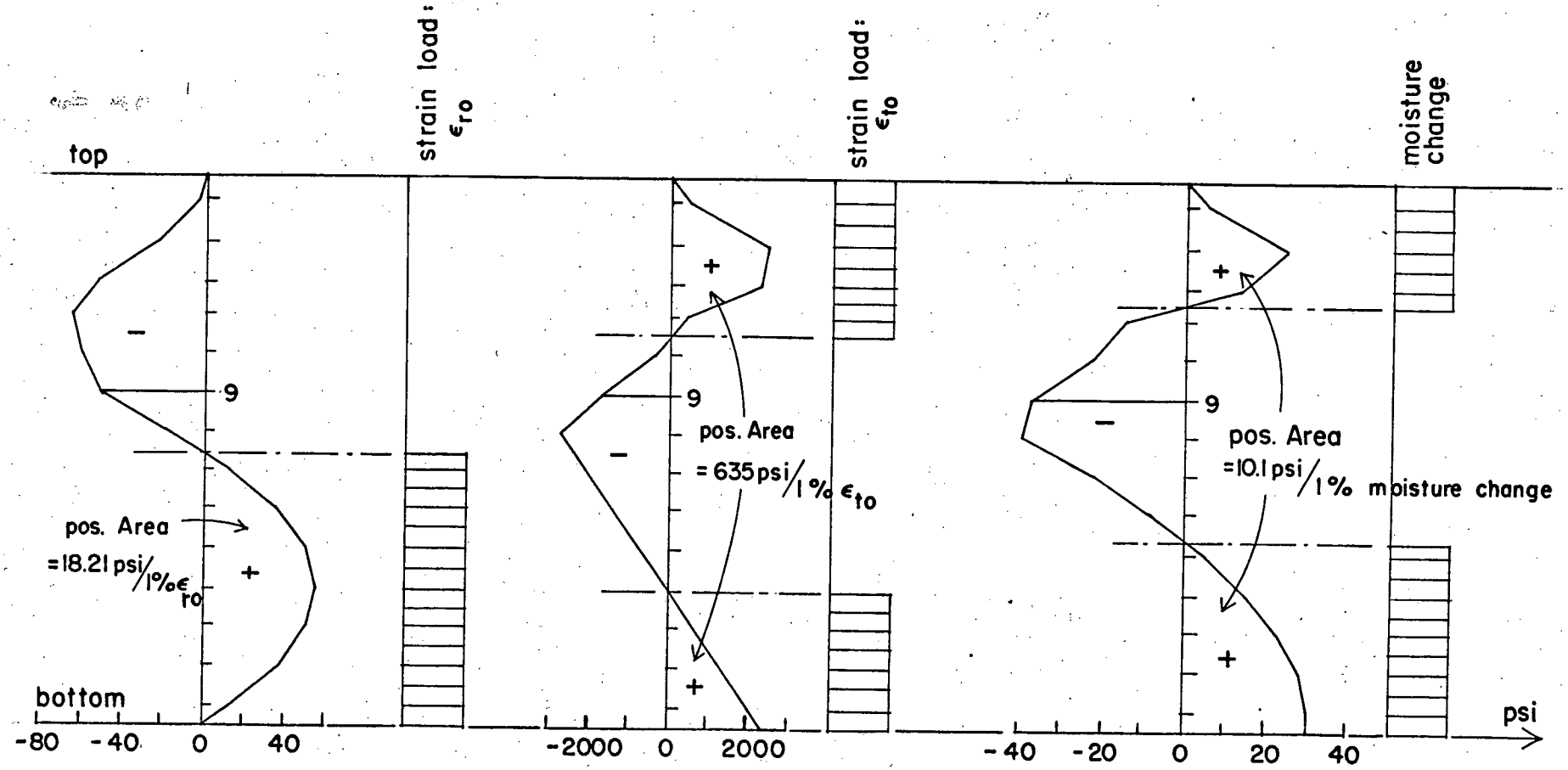

Fig.30. Influence lines for radial stress at centerline of element 9.

These two influence lines for radial stress due to initial strain can be combined to one for radial stress due to moisture change if the relation between moisture content and shrinkage of the wood is known.

Wood shrinks most in the direction of the annual growth rings (tangentially to the tree), somewhat less across these rings (radially), and very little along the grain (longitudinally). The Wood Handbook (8), fig.71 on page 319, gives for Douglas Fir a flat grain (tangential) shrinkage of about 1.5% when the moisture changes from 10% to 15%. F. Kollmann in TECHNOLOGIE DES HOLZES (9) gives the longitudinal strain due to moisture change as approximately 1/23 of the flat grain shrinkage.

Herewith, the following initial strains, corresponding to 1% moisture change are assumed to be reasonable

$\varepsilon_{ro} = (1.5\%)/5 = .3\%$ for a 1% moisture change

$\varepsilon_{to} = (\varepsilon_{ro})/23 = (.3\%)/23 = .013\%$ for a 1% moisture change.

With these relations, the influence line, due to moisture change, as shown in fig.30c, is obtained by superposition of the adjusted influence lines due to strain change from figures 30a and 30b.

With the maximum area of 10.1 psi/% m.c. under the influence line, a moisture change of 5%, distributed as shown in fig.30b, produces the following maximum stress

$$\sigma_r = 5 \cdot 10.1 = 50.5 \text{ psi}$$

This will be tension perpendicular to grain when the moisture in the central region decreases.

However, it has to be noted that these influence lines represent moisture or strain distributions, as shown in fig.26, which means the moisture contents within the groups of elements are constant. This occurs, for example, if a different amount of moisture content is present in the laminations at the time of glueing, and subsequent drying shrinkage produces stresses.

The influence lines cannot be used for a moisture distribution as shown in fig.31, since the moisture content there varies along one group of elements. Influence lines could be made by an analogous procedure to treat this type of strain distributions. Instead the case was solved by applying to all elements the corresponding initial strain as shown in fig.31. The maximum radial stress σ_r at centerline was then

$$\sigma_r = 46.8 \text{ psi tension}$$

For the increase in moisture content the radial initial strain ε_{ro} contributes the most, namely 45.5 psi, while ε_{to} with 1.3 psi produces almost no radial stress in this case.

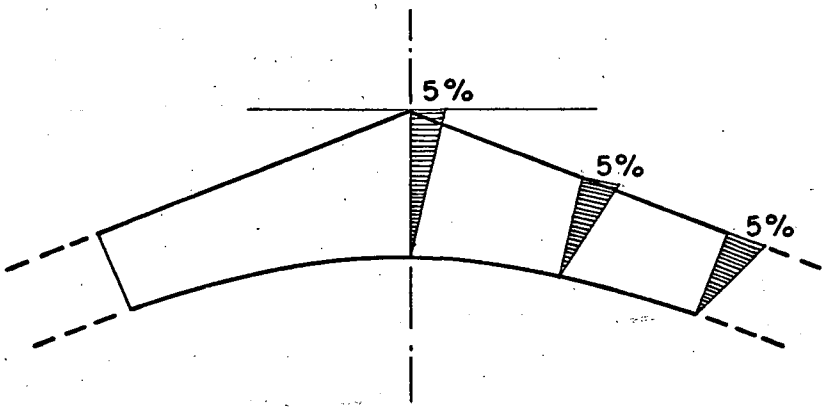

Fig.31. Assumed linear change of moisture content.

5.4. VARIATION IN ELASTIC PROPERTIES

Up to here, the [D]-matrix given on page 50, has been used as the 'basic'matrix for the investigations.

Table 3 shows how the stresses due to pure moment are affected by changes in the moduli of elasticity.

TABLE 3

Effect of variation in elastic properties of the whole beam.

D-matrix	E_2/E_{2basic}	$E_\nu/E_{\nu basic}$	G/G_{basic}	$\Delta\sigma$ in %		
				tangential		radial
				tens.	comp.	
basic	1	1	1	-	-	-
E_2 varied	2	1	1	- 2.4	- 1.6	+ 4.9
E_ν varied	1	2	1	- 0.9	- 1.3	+ 1.1
G varied	1	1	1/2	+10.1	+13.0	-11.7

A doubling of E_2 or E_ν has a small effect, but the stresses are somewhat sensitive to a change of G. However, the amount of change is still tolerable.

More likely the elastic properties may vary from lam to lam. This influence has been checked for bending moment, by assuming a variation in one modulus of elasticity in one lam at a time. Table 4 shows the changes in maximum radial stress, due to changes in the elastic properties of the bottom layer of elements with high tangential

tensile stresses (see fig.26); of the seventh layer with high radial stresses; of the tenth layer with high tangential compressive stress.

TABLE 4

Effect of variation in elastic properties in one lam.

Change of modulus in one lam to	$\Delta\sigma_r$ in %		
	Var. in layer 1	Var. in layer 7	Var. in layer 10
$E_1 \rightarrow 2E_1$	- 8.82	- 4.58	- 2.14
$E_2 \rightarrow 2E_2$	0.00	+ 0.72	+ 0.84
$E_\nu \rightarrow 2E_\nu$	+ 0.16	+ 0.61	0.00
$G \rightarrow 1/2G$	- 0.22	+ 1.03	- 1.86

As before, the effect of these changes is tolerable.

SUMMARY

This chapter has shown, that the maximum radial stresses at centerline due to shear and variation in elastic properties are negligible, but that the stresses due to moment and moisture change are important.

The pointed peak induces concentrations of radial stresses from moments at the centerline, and these stresses must be calculated by the graphs of fig.22. At other points on the beam, one or two depths away from this stress riser, the regular curved or tapered beam formulas may be used for stress calculations.

This pointed peak also generates stresses due to non uniform moisture change, whether the beam is loaded or not. It is difficult to set the magnitude, as field testing is necessary to establish some realistic moisture gradients. In the meantime, however, it might be advisable to add 20 psi radial tension to any calculated stress from moments at the peak. This 20 psi is about half the absolute magnitude determined herein for one geometry.

6. EXPERIMENTAL TESTS ON STRESS PERPENDICULAR TO GRAIN

Average strength values of Douglas Fir are listed in the publication STRENGTH AND RELATED PROPERTIES OF WOODS GROWN IN CANADA by the Forest Products Research Branch of the Department of Forestry, Canada (10).

For air-dry condition the ultimate tensile stress perpendicular to grain is given there as 440. psi. This value results from short time tests. To compare it with the allowable working stress under long time loading, it may be multiplied by the factor 9/16. For Douglas Fir, the maximum tensile strength perpendicular to grain under long time loading, now becomes 9/16 x 440. = 248. psi.

The CSA-Code 086 (11) specifies, on table 8, the allowable working tensile stress perpendicular to grain for glulam Douglas Fir 24 f strength grade in dry conditions as 65 psi, or 1/3.8 times the long term ultimate.

The calculated radial stresses in section 5.1., are about twice the values given by the curved beam theory. But with the ultimate strength of 3.8 times the allowable stress, a factor of two does not explain failure, especially when many failures occured under little more than dead load. Other influences must be significant. It could be that the allowable stress perpendicular to grain, given in the code, is too high. Therefore a series of tests were done to check the allowable stress.

Samples from two different glulam plants in the Vancouver area were tested. The test pieces, of the shape given in fig.32, had a cross section of 4.5"x4.5" or 20.2 in^2.

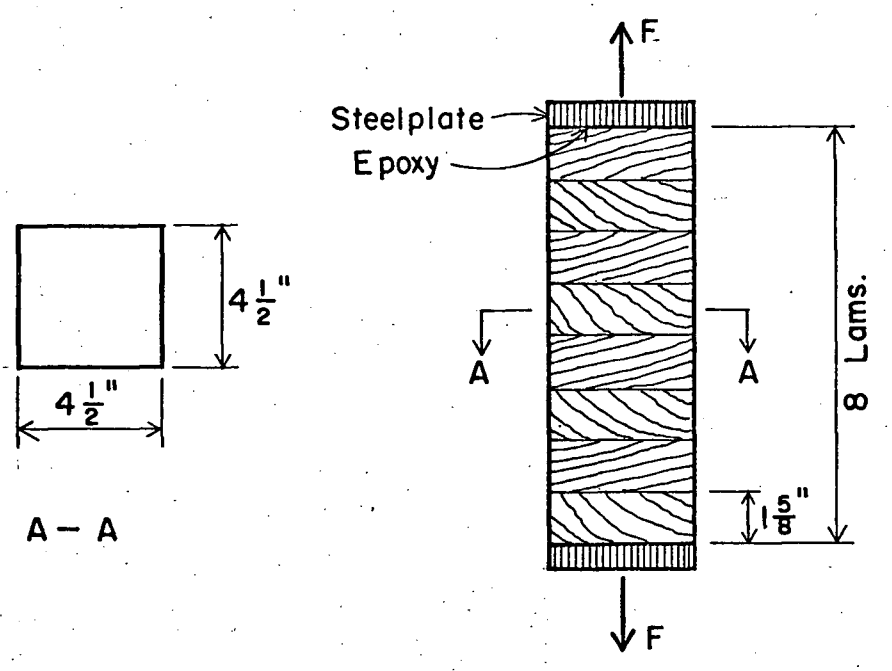

Fig.32. Example of Testmember

Two steel plates, with concentric threaded holes, were glued on with Epoxy for application of the tensile forces.

Twenty two members have been tested with the result shown in table 5. The average value is

$$\sigma_{failure} = 128. \text{ psi}$$

This value is less than 1/3 of the advertised ultimate and it must be recognized that beams designed, with the classical formula, under pure bending only, might be already in the critical range.

Although the number of tests is small, the tendency is clear and the conclusion must be drawn, that the ultimate radial stresses must be further investigated. Such investigations should not use clear samples and the study should include size effects and drying cracks.

TABLE 5

RESULTS OF TESTS ON TENSION PERPENDICULAR TO GRAIN

Loading time about 5 minutes; moisture content about 10%.

Test member	Ult. load lb.	Ult. stress psi	v	vv
1	2890	143	- 15	225
2	1685	83	+ 45	2025
3	2415	119	+ 9	81
4	2000	99	+ 29	841
5	1740	86	+ 42	1764
6	1940	96	+ 32	1024
7	2130	105	+ 23	529
8	2120	105	+ 23	529
9	2300	114	+ 14	196
10	2020	100	+ 28	784
11	2310	114	+ 14	196
12	2090	103	+ 25	625
13	3300	163	- 35	1225
14	1955	97	+ 31	961
15	4290	212	- 84	7056
16	2340	116	+ 12	144
17	3100	153	- 25	625
18	2375	117	+ 11	121
19	2235	110	+ 18	324
20	4625	228	-100	10000
21	2725	135	- 7	49
22	4350	215	- 87	7569
	Sum =	2813	+356	36893
	Average =	128	-353	

Standard deviation $\sqrt{\frac{36893}{22}}$ = ± 41. psi

Coefficient of variation $\frac{41}{128}$ = 32 %.

This difference of three between the ultimate stress of Douglas Fir in radial tension and the values found herein are probably due to drying cracks which appeared in many of the 22 samples. If a clear, straight grained sample is used, drying will not induce nearly as many cracks as if 'real' wood is used. Those cracks normal to the direction of radial tension induce exceedingly large stress concentration factors which reduce the ultimate strength.

The long term ultimate stress taken as 9/16 of the short term gives 72 psi. A safety factor of 2 gives an allowable stress of 36 psi. Since this is 60% of the allowable now used, and the peak about doubles the actual stress calculated by the classical curved beam formula, it is not surprising that failures occur.

7. NUMERICAL EXAMPLE

The geometry of a roof beam for use in wet conditions is shown in fig.33. The beam spans 40 feet with a spacing of 16 feet. The laminations of the size 1 5/8" x 7" are out of Douglas Fir 24 f strength grade. The centerline cross section of 39 inches requires 24 lams.

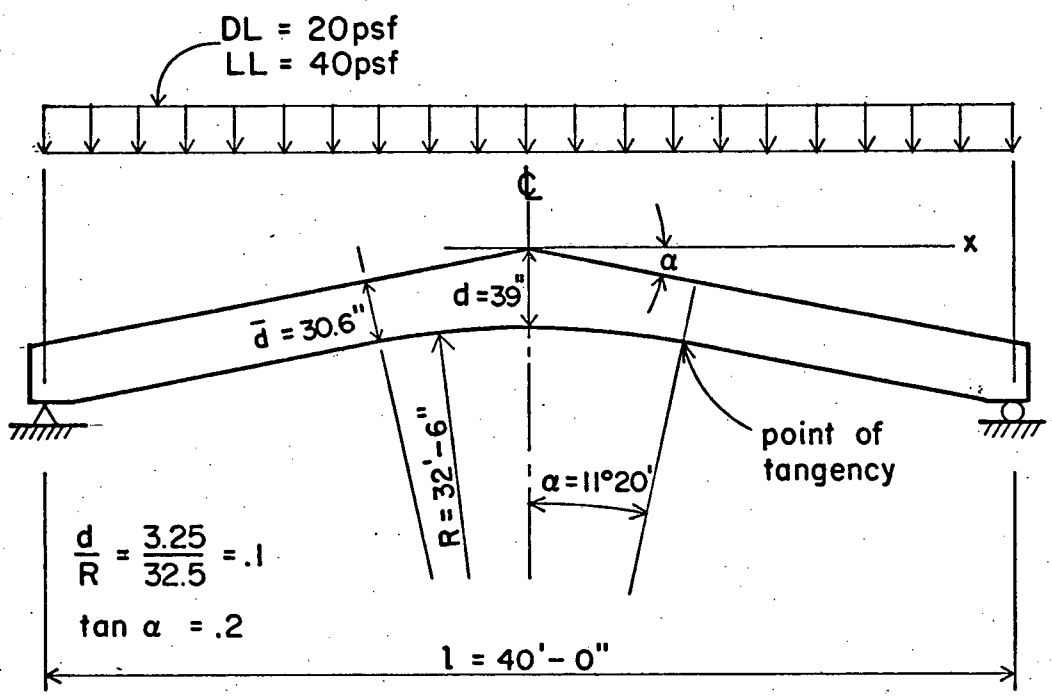

Fig.33. Roof beam.

The dead load (normal duration of load) is 20 psf and the live load (2 months duration of load, i.e. snow duration) is 40 psf. Herewith, the beam has to be designed for a total uniformly distributed load of

$$(20. + 40.) \times 16 = 960. \text{ lb/ft}$$
$$= 0.96 \text{ k/ft.}$$

The allowable working stresses for glulamed Douglas Fir 24 f strength grade for wet conditions are given in table 8 of the CSA-code 086 (11) to

1900 psi for bending

145 psi for shear and

55 psi for tension perpendicular to grain.

These values are for normal duration of loads. Since the governing stresses for the considered beam occur over a two months duration, the allowable stresses may be increased by the factor 1.15 to

$$\sigma_{t_{all}} = 1900. \times 1.15 = 2185. \text{ psi}$$

$$\sigma_{r_{all}} = 55. \times 1.15 = 63. \text{ psi}$$

$$\tau_{all} = 145. \times 1.15 = 167. \text{ psi}$$

The design is made by checking the tangential and radial stresses at centerline of the beam and at the point of tangency and by checking the shear stress at the support.

The stresses at centerline are calculated for comparison by the proposed as well as by the existing formulas. The parameters $d/R = .1$ and $\tan \alpha = .2$ give the stress coefficients (see table 2 or figures 22 and 23)

$$C_{RM} = 0.0487$$

$$C_{TM} = 1.283$$

$$C_{CM} = -0.717$$

The moment at centerline is

$$M = \frac{ql^2}{8} = \frac{.96 \times 40^2}{8} = 192.0 \text{ kft}$$

The maximum bending stresses obtained by the formula M/Z are

$$\sigma = \frac{6\,M}{bd^2} = \frac{192 \times 12000 \times 6}{7 \times 39 \times 39} = 1298. \text{ psi}$$

Better design practice uses the smaller cross section at the point of tangency

$$\sigma = \frac{6\,M}{bd^2} = \frac{192 \times 12000 \times 6}{7 \times 30.6 \times 30.6} = 2109. \text{ psi} < \sigma_{all} = 2185. \text{ psi}$$

The proposed formula gives the bending stresses

$$\sigma_{comp} = C_{CM} \times \frac{6\,M}{bd^2} = -0.717 \times 1298 = -931. \text{ psi}$$

$$\sigma_{tens} = C_{TM} \times \frac{6\,M}{bd^2} = 1.283 \times 1298 = 1665. \text{ psi}$$

It can be seen that the stresses obtained by the present design method give very little information about the actual tangential stresses, although the stresses are on the safe side, if the cross section at the point of tangency is used.

The radial tensile stresses by the curved beam formula are

$$\sigma_{r_{max}} = \frac{3M}{2bd\ (R+d/2)} = \frac{3 \times 192 \times 12000}{2 \times 7 \times 39 \times (390 + 19.5)} = 30.9 \text{ psi}$$

Here, too, better design practice would use the depth at the point of tangency to give

$$\sigma_{r_{max}} = \frac{3M}{2b\bar{d}\ (R+\bar{d}/2)} = \frac{3 \times 192 \times 12000}{2 \times 7 \times 30.6 \times (390+15.3)} = 39.8 \text{ psi}$$

The proposed formula gives

$$\sigma_{r_{max}} = C_{RM} \times \frac{6\ M}{bd^2} = .0487 \times 1298 = 63.2 \text{ psi}$$

The curved beam formula underestimates the maximum radial stress considerably. The actual stress is about twice as much as given by the curved beam formula. It even exceeds the present allowable stress slightly. If 20 psi are added for coverage of stresses due to change in moisture content, the present allowable stress is exceeded by an intolerable amount.

For the stresses at point of tangency existing formulas can be used. The bending moment there, at a distance x = 6.63 ft from centerline, is

$$M = q\left(\frac{l^2}{8} - \frac{x^2}{2}\right) = .96\left(\frac{40^2}{8} - \frac{6.63^2}{2}\right) = .96(200-22) = 170.9 \text{ kft.}$$

Herewith, the tangential stress is

$$\sigma = \frac{6\,M}{b\bar{d}^2} = \frac{170.9 \times 12000 \times 6}{7 \times 30.6 \times 30.6} = \frac{170.9 \times 12000}{1092.7} = 1873.\ \text{psi}$$

The maximum radial stress is

$$\sigma_{r_{max}} = \frac{3M}{2b\bar{d}\,(R+\bar{d}/2)} = \frac{3 \times 170.9 \times 12000}{2 \times 7 \times 30.6 \times (390+15.3)} = 35.4\ \text{psi}$$

Both stresses are smaller than the allowable ones.

The shear stresses are checked at the support, where the maximum shear force occurs. The vertical reaction at the support is

$$F = \frac{ql}{2} = \frac{.96 \times 40}{2} = 19.2\ \text{k}$$

Herewith, the maximum shear stress is obtained as

$$\tau_{max} = \frac{3}{2}\frac{V}{b\bar{d}} = \frac{3}{2}\frac{F\cos\alpha}{b\bar{d}}$$

$$= \frac{3}{2}\frac{19.2 \times 1000 \times \cos(11°20')}{7 \times 30.6} = 132.3\ \text{psi}$$

This example shows that the present design method gives the significant stresses in tangential direction but does not satisfy for radial stresses. For a safe design the actual stresses have to be known at centerline. They are readily obtained by the proposed method using the stress coefficients C_{CM}, C_{TM} and C_{RM} as shown in fig. 22 and fig. 23.

8. CONCLUSIONS

The trapezoidal element proposed does predict a stress distribution close enough for all practical purposes on these problems. Also, it allows stress determinations from changes in moisture content and elastic properties.

The peak at the centerline of pitch-cambered beams induces a stress concentration so that curved beam formulas are invalid near the top. Therefore coefficients from fig.22 and fig.23 should be used to calculate the maximum radial and tangential stresses, due to bending moment.

Radial stresses induced by shear and variation in elastic properties are not significant, but those created by change in moisture content are in the order of magnitude of 20 psi and should be considered.

The allowable stresses, used at present, should be reduced to about half their value, but testing needs to be done to find a more realistic reduction.

With the increased calculated radial stresses and the reduced allowable radial stresses, it will be difficult to produce an economic design in some cases. When such occurs, the designer could consider reinforcing the beam with steel dowells. These dowells from 3/8" to say 3/4" diameter are placed in slightly oversized holes,

drilled almost the full depth of the beam, and partially filled with an adhesive such as 'Epoxy'. Such dowells serve the same purpose as reinforcing steel in concrete. It is also possible to carry the total force arising from the radial stresses by two vertical steel plates fastened with glulam rivets to either side of the beam at its centerline.

REFERENCES

1. NORRIS, C.B. 1963. Stresses within curved laminated beams of Douglas Fir. FPL -020. Forest Prod. Lab., U.S. Dep. Agri. Madison, Wisc.

2. CARRIER, G.F. 1943. Stress distribution in cylindrically aelotropic plates. J. Appl. Mech. Vol. 10, Trans, ASME Vol.65. A - 117 - 122.

3. FOSCHI, R.O. 1968. Plane Stress problem in a body with cylindrical anisotropy, with special reference to curved Douglas Fir beams. Department of Forestry and Rural Development, Departmental Publication No. 1244, Ottawa, Ont.

4. FOX, S.P. 1968. Stresses in glued-laminated timbers: double-tapered pitched beams. Forest Prod. Lab, Dept. Forest. Rural Develop. Vancouver, Canada.

5. TIMOSHENKO, S. and GOODIER, J. Theory of Elasticity, McGraw-Hill. 1957.

6. WANG, Chi-Teh, Applied Elasticity, McGraw-Hill. 1953.

7. HEARMON, R.F.S. 1948. The elasticity of wood and plywood. Forest Prod. Res. Spec. Rep. No.7. London, England.

8. WOOD HANDBOOK, Handbook No. 72, U.S. Department of Agriculture, 1955.

9. KOLLMANN, F. Dr. Ing., Technologie des Holzes und der Werkstoffe, Volume I, Springer Berlin 1951.

10. KENNEDY, E.I. 1965. Strength and related Properties of Woods grown in Canada, Department of Forestry, Forest Products, Research Branch, Dep. of Forest. Publication No. 1104, Ottawa, Ont.

11. CANADIAN STANDARDS ASSOCIATION, Ottawa, 086 - 1959, Engineering Design in Timber. Revised reprint - August 1963.

APPENDIX

Listing of the computer program
described in chapter 3.

```
      DIMENSION RG(30),MEG(30),JO(200,4),DELR(20),BETAG(30),BETAM(200),
     1R1(200),R2(200),THM(200),ND(250,2),NCODE(200,8),FI(8),EPSIJ(3)
      DIMENSION SMM(36),S(12950),B( 500),DP(8),EPSIM(200,2),E(200,4)
      DOUBLE PRECISION START,WORD
      MAXMEM=200
      MAXJO=250
C     MAXMEM AND MAXJO ARE USED TO DEFINE THE DIMENSIONS IN THE SUBROUTINES
      DATA START /5HSTART/
100   PRINT 20
      READ 10
      PRINT 10
      PRINT 20
10    FORMAT (72H
     1                    )
20    FORMAT (//132H ************************************************************
     1************************************ ************************************
     2**************//)
      READ 2, MXDELR,MASTR,MATEL,NPS
2     FORMAT(18I4)
      PRINT 101, MXDELR
101   FORMAT (1H /25H NUMBER OF DELTA RADIUS =,I4/12H    I      DELR)
      READ 102, (DELR(I),I=1,MXDELR)
102   FORMAT (F10.6)
      PRINT 103, (I,DELR(I),I=1,MXDELR)
103   FORMAT (I4,F12.6)
      READ 2,NRG
      PRINT 201, NRG
201   FORMAT (//26H NUMBER OF RADIAL GROUPS =,I4/25H IRG  MEG     RG
     1BETAG)
      READ 202, (MEG(IRG),RG(IRG),BETAG(IRG),IRG=1,NRG)
202   FORMAT (I4,F10.3,F10.6)
      PRINT 203, (IRG,MEG(IRG),RG(IRG),BETAG(IRG),IRG=1,NRG)
203   FORMAT (2I4,F10.3,F10.6)
      CALL DIVIDE (MAXMEM,NRG,RG,MEG,JO,ME,NJ)
      CALL DISTRI (NRG,RG,MEG,DELR,BETAG,BETAM,ME,R1,R2)
      READ 204, TH,NSM
204   FORMAT (F12.6,I4)
      DO 208 I=1,ME
208   THM(I)=TH
      PRINT 210,ME,NSM,NJ
210   FORMAT (//20H NUMBER OF MEMBERS =,I4/20H N OF SPEC.MEMBERS =,I4/20
     1H NUMBER OF JOINTS  =,I4)
      IF (NSM.EQ.0) GO TO 222
      PRINT 212
212   FORMAT (//16H SPECIAL MEMBERS/12H    I      THM)
      DO 220 I=1,NSM
      READ 214,ISM,THM(ISM)
214   FORMAT (I4,F10.6)
      PRINT 216,ISM,THM(ISM)
216   FORMAT (I4,2X,F10.6)
220   CONTINUE
222   PRINT 224
224   FORMAT (//22H MEMBER SPECIFICATIONS/59H    I      JOINTNRS(I,J)
     1 R1          R2        BETAM       THM)
      PRINT 226, (I,JO(I,1),JO(I,2),JO(I,3),JO(I,4),R1(I),R2(I),BETAM(I)
```

```
     1,THM(I),I=1,ME)
226   FORMAT (I4,2X,4I4,2F10.3,2F10.6)
300   MS=8
      NCO=4
      MST=MS/NCO
      READ 2, NRJ
      PRINT 305, NRJ
305   FORMAT (//30H NUMBER OF RESTRAINED JOINTS =,I4/12H  JR ND1 ND2)
      DO 310 I=1,NJ
      DO 311 K=1,MST
      ND(I,K)=1
311   CONTINUE
310   CONTINUE
      DO 312 I=1,NRJ
      READ 2, JR,ND(JR,1),ND(JR,2)
      PRINT 2,JR,ND(JR,1),ND(JR,2)
312   CONTINUE
      NUM=0
      DO313 I=1,NJ
      DO 314 K=1,MST
      IF (ND(I,K).EQ.0)GO TO 314
      NUM=NUM+1
      ND(I,K)=NUM
314   CONTINUE
313   CONTINUE
      PRINT 320
320   FORMAT (//19H JOINT CODE NUMBERS)
      PRINT 321, (I,(ND(I,J),J=1,MST),I=1,NJ)
321   FORMAT (5(3I4,2X))
      DO 316 I=1,ME
      DO 317 J=1,MS
      CALL CODE (MAXMEM,MAXJC,JO,ND,I,J,ICOM)
      NCODE(I,J)=ICOM
317   CONTINUE
316   CONTINUE
      PRINT 325
325   FORMAT (//21H ELEMENT CODE NUMBERS/24H   I     NCODE(I,1TO8)  )
      PRINT 326, (I,(NCODE(I,J),J=1,MS),I=1,ME)
326   FORMAT (I4,2X,8I4)
      NU=NUM
      NB=1
      DO 350 I=1,ME
      MSM=MS-1
      DO 351 J=1,MSM
      ICDJ=NCODE(I,J)
      IF(ICDJ) 353,351,353
353   JP=J+1
      DO 352 K=JP,MS
      ICDK=NCODE(I,K)
      IF (ICDK) 354,352,354
354   NBT=IABS((IABS(ICDK)-IABS(ICDJ)))+1
      IF (NBT-NB) 352,352,355
355   NB=NBT
352   CONTINUE
351   CONTINUE
```

```
  350   CONTINUE
        READ 362, E1,E2,EMU,G,NESP
  362   FORMAT (4X,4F16.8,I4)
        PRINT 360, E1,E2,EMU,G,NESP
  360   FORMAT (//5H E1 =,F12.4/5H E2 =,F12.4/5H EMU=,F12.4/5H G  =,F12.4/
       1/42H NUMBER OF MEMBERS WITH SPECIAL E-MODULI =,I4)
        DO 370 I=1,ME
        E(I,1)=E1
        E(I,2)=E2
        E(I,3)=EMU
  370   E(I,4)=G
        IF (NESP .EQ. 0) GOTO 380
        DO 376 I=1,NESP
        READ 372,  IESP,E(IESP,1),E(IESP,2),E(IESP,3),E(IESP,4)
        PRINT 373, IESP,E(IESP,1),E(IESP,2),E(IESP,3),E(IESP,4)
  372   FORMAT (I4,4F16.8)
  373   FORMAT (I4,4E16.8)
  376   CONTINUE
  380   CONTINUE
        IF (MATEL) 400,401,400
  400   PRINT 402
  402   FORMAT (1H1, 25H ELEMENT STIFFNESS MATRIX//)
        GO TO 404
  401   PRINT 403
  403   FORMAT (//37H ELEMENT STIFFNESS MATRIX NOT PRINTED)
  404   CONTINUE
        NS = NU*NB
        DO 405 I=1,NS
  405   S(I)=0.0
        NB1=NB-1
        DO 407 L=1,ME
        DO 408 I=1,36
  408   SMM(I)=0.0
        R1L=R1(L)
        R2L=R2(L)
        BETAL=BETAM(L)
        THL=THM(L)
        E1L=E(L,1)
        E2L=E(L,2)
        EMUL=E(L,3)
        GL=E(L,4)
        CALL SMEM (R1L,R2L,BETAL,THL,E1L,E2L,EMUL,GL,SMM)
        IF (MATEL .EQ. 0) GO TO 422
        PRINT 420, L
  420   FORMAT (/I4)
        PRINT 421, SMM(1)
        PRINT 421, SMM(2),SMM(9)
        PRINT 421, SMM(3),SMM(10),SMM(16)
        PRINT 421, SMM(4),SMM(11),SMM(17),SMM(22)
        PRINT 421, SMM(5),SMM(12),SMM(18),SMM(23),SMM(27)
        PRINT 421, SMM(6),SMM(13),SMM(19),SMM(24),SMM(28),SMM(31)
        PRINT 421, SMM(7),SMM(14),SMM(20),SMM(25),SMM(29),SMM(32),SMM(34)
        PRINT 421, SMM(8),SMM(15),SMM(21),SMM(26),SMM(30),SMM(33),SMM(35),
       1SMM(36)
  421   FORMAT (1X,8G16.6)
```

```
  422   CONTINUE
        DO 409 J=1,8
        IF (NCODE(L,J)) 409,409,412
  412   J1=(J-1)*(16-J)/2
        DO 410 I=J,8
        IF (NCODE(L,I)) 410,410,406
  406   IF(NCODE(L,J)-NCODE(L,I)) 413,450,414
  450   IF(I-J) 451,413,451
  451   K=(NCODE(L,I)-1)*NB1+NCODE(L,J)
        N=J1+I
        S(K)=S(K)+(2.0*SMM(N))
        GO TO  410
  413   K=(NCODE(L,J)-1)*NB1+NCODE(L,I)
        GO TO 415
  414   K=(NCODE(L,I)-1)*NB1+NCODE(L,J)
  415   N=J1+I
        S(K)=S(K)+SMM(N)
  410   CONTINUE
  409   CONTINUE
  407   CONTINUE
        IF (MASTR .EQ. 0) GOTO 460
        PRINT 1000
 1000   FORMAT (1H1)
  460   CONTINUE
        PRINT 462, NU,NB
  462   FORMAT (//22H NUMBER OF UNKNOWNS  =,I4///22H BANDWIDTH          =
       1,I4)
        IF (MASTR ) 464,466,464
  464   PRINT 465
  465   FORMAT (////27H STRUCTURE STIFFMESS MATRIX/)
        PRINT 425, (S(K),K=1,NS)
  425   FORMAT (1X,8G16.6)
        GO TO 500
  466   PRINT 467
  467   FORMAT (//39H STRUCTURE STIFFNESS MATRIX NOT PRINTED)
  500   READ 2,NLC
        PRINT 501, NLC
  501   FORMAT (////22H NUMBER OF LOADCASES =,I4)
        DO 590 L=1,NLC
        DO 502 I=1,NU
  502   B(I)=0.0
        READ 2, NBL,NEI
        PRINT 503, L
  503   FORMAT (1H1,9H LOADCASE,I4)
        IF (NBL .EQ. 0) GO TO 700
        PRINT 506, NBL
  506   FORMAT (//24H NUMBER OF LOADS GIVEN =,I4/12H   K     B(K))
        DO 504 I=1,NBL
        READ 505, K,B(K)
  504   PRINT 505, K,B(K)
  505   FORMAT  (I4,F10.3)
  700   IF (NEI) 701,722,701
  701   READ 702, EPSI1,EPSI2,EPSI3,NSSM
  702   FORMAT (3F10.6,I4)
        PRINT 704, EPSI1,EPSI2,EPSI3,NSSM
```

```
  704   FORMAT (//23H INITIAL STRAIN ETANG. =,F10.6/23H                ERAD
       1  =,F10.6/23H                ESHEAR=,F10.6//37H NUMBER OF SPECIAL
       2STRAINED MEMBERS =,I4)
        DO 706 J=1,ME
        EPSIM(J,1)=EPSI1
  706   EPSIM(J,2)=EPSI2
        IF (NSSM .EQ. 0) GO TO 709
        DO 708 I=1,NSSM
        READ 710, ISSM,EPSIM(ISSM,1),EPSIM(ISSM,2)
  710   FORMAT (I4,2F10.6)
        PRINT 711, ISSM,EPSIM(ISSM,1),EPSIM(ISSM,2),EPSI3
  711   FORMAT (I4,3(2X,F10.6))
  708   CONTINUE
  709   DO 720 J=1,ME
        R1J=R1(J)
        R2J=R2(J)
        BETAJ=BETAM(J)
        THJ=THM(J)
        EPSIJ(1)=EPSIM(J,1)
        EPSIJ(2)=EPSIM(J,2)
        EPSIJ(3)=EPSI3
        E1J=E(J,1)
        E2J=E(J,2)
        EMUJ=E(J,3)
        GJ=E(J,4)
        CALL EPSINI (R1J,R2J,BETAJ,THJ,E1J,E2J,EMUJ,GJ,EPSIJ,FI)
        DO 714 NC=1,8
        IF (NCODE(J,NC)) 712,714,712
  712   NCM=NCODE(J,NC)
        B(NCM)=B(NCM)+FI(NC)
  714   CONTINUE
  720   CONTINUE
        GO TO 750
  722   DO 724 I=1,ME
        DO 724 J=1,2
  724   EPSIM(I,J)=0.
        EPSI3=0.
  750   CONTINUE
        PRINT 507
  507   FORMAT (//11H LOADVECTOR)
        PRINT 513, (B(I),I=1,NU)
        DET=1.E-8
        CALL BAND (S,B,NU,NB,L,DET)
        IF(DET) 508,509,510
  508   PRINT 511,DET
  511   FORMAT (34HOMATRIX A IS NOT POSITIVE-DEFINITE/7HODET = ,E15.7)
        GO TO 590
  509   PRINT 512,DET
  512   FORMAT (20HODETERMINANT IS ZERO/7HODET = ,E15.7)
        GO TO 590
  510   PRINT 514
  514   FORMAT (//19H DISPLACEMENTVECTOR)
        PRINT 513,(B(I),I=1,NU)
  513   FORMAT (1X,8G16.6)
        PRINT 555
```

```
  555   FORMAT (/////9H STRESSES/51H   J            RADIAL            TANGEN
       1T          TAU)
  550   DO 560 J=1,ME
        R1J=R1(J)
        R2J=R2(J)
        BETAJ=BETAM(J)
        DO 554 NC=1,8
        IF (NCODE(J,NC)) 553,552,553
  552   DP(NC)=0.0
        GO TO 554
  553   NCM=NCODE(J,NC)
        DP(NC)=B(NCM)
  554   CONTINUE
        EPSIJ(1)=EPSIM(J,1)
        EPSIJ(2)=EPSIM(J,2)
        EPSIJ(3)=EPSI3
        E1J=E(J,1)
        E2J=E(J,2)
        EMUJ=E(J,3)
        GJ=E(J,4)
        CALL SIGM (R1J,R2J,BETAJ,E1J,E2J,EMUJ,GJ,DP,EPSIJ,STH,SRAD,SRTH)
  556   PRINT 558, J,SRAD,STH,SRTH
  558   FORMAT (I4,3X,3(1X,F15.6))
        IF (J.GT.NPS) GO TO 560
        WRITE (7,558) J,SRAD,STH,SRTH
  560   CONTINUE
  590   CONTINUE
        READ 610, WORD
  610   FORMAT (A5)
        IF (WORD .NE. START) GO TO 620
        PRINT 1000
        GO TO 100
  620   CONTINUE
        STOP
        END
```

```
      SUBROUTINE DIVIDE (MAXMEM,NRG,RG,MEG,JO,IMUS,NJ)
      DIMENSION RG(1), MEG(1),JO(MAXMEM,4)
      IBAS=0
      IMUS=0
      DO 10 IRG=1,NRG
      IF (IRG.EQ.1) GO TO 11
      IF(MEG(IRG-1)-MEG(IRG)) 11,11,12
11     MM=MEG(IRG)
      DO 13 JRG=1,MM
      I=IMUS+JRG
      JO(I,1)=IBAS+JRG+MEG(IRG)+2
      JO(I,2)=IBAS+JRG+1
      JO(I,3)=IBAS+JRG
      JO(I,4)=IBAS+JRG+MEG(IRG)+1
13    CONTINUE
      IBAS=IBAS+MEG(IRG)+1
      IMUS=IMUS+MEG(IRG)
      GO TO 10
12    MM=MEG(IRG)
      DO 14 JRG=1,MM
      I=IMUS+JRG
      JO(I,1)=IBAS+JRG+MEG(IRG-1)+2
      JO(I,2)=IBAS+JRG+1
      JO(I,3)=IBAS +JRG
      JO(I,4)=IBAS+JRG+MEG(IRG-1)+1
14    CONTINUE
      IBAS=IBAS+MEG(IRG-1)+1
      IMUS=IMUS+MEG(IRG)
10    CONTINUE
      NJ=IBAS+MEG(NRG)+1
      RETURN
      END
```

```
      SUBROUTINE DISTRI (NRG,RG,MEG,DELR,BETAG,BETAM,IMUS,R1,R2)
      DIMENSION RG(1),MEG(1),DELR(1),BETAG(1),BETAM(1),R1(1),R2(1)
      IMUS=0
      DO 20 IRG=1,NRG
      R1M=RG(IRG)
      MM=MEG(IRG)
      DO 21 JRG=1,MM
      I=IMUS+JRG
      R1(I)=R1M
      R2(I)=R1M+DELR(JRG)
      R1M=R2(I)
      BETAM(I)=BETAG(IRG)
   21 CONTINUE
      IMUS=IMUS+MEG(IRG)
   20 CONTINUE
      RETURN
      END
```

```
      SUBROUTINE CODE(MAXMEM,MAXJO,JO,ICD,I,J,ICDM)
      DIMENSION JO(MAXMEM,4),ICD(MAXJO,2)
      GO TO (1,2,3,4,5,6,7,8),J
1     JNU=1
      GO TO 10
2     JNU=2
      GO TO 10
3     JNU=3
      GO TO 10
4     JNU=4
10    JD=1
      GO TO 20
5     JNU=1
      GO TO 11
6     JNU=2
      GO TO 11
7     JNU=3
      GO TO 11
8     JNU=4
11    JD=2
20    II=JO(I,JNU)
      ICDM=ICD(II,JD)
      RETURN
      END
```

```
      SUBROUTINE SMEM (R1,R2,BETA,TH,E1,E2,EMU,G,S)
C     TRAPEZOIDAL ELEMENT TRANSFORMED INTO POLARCOORDINATES
      DIMENSION SK(36),S(36)
      H=(R2-R1)*COS(BETA/2.)
      A=2.*R1*SIN(BETA/2.)
      B=2.*R2*SIN(BETA/2.)
      F1 =(A+B)*H/2.
      FY =(A+2.*B)*H*H/6.
      FXX=((A*A+B*B)*(A+B))*H/36.
      FYY=(A+3.*B)*H*H*H/12.
      SA1=1./(A*A)
      SA2=1./(A*H)
      SA3=1./(A*A*H)
      SA4=1./(A*A*H*H)
      SA5=1./(A*H*H)
      SA6=1./(A*B*H)
      SA7=1./(A*B*H*H)
      SB1=1./(H*H)
      SB2=1./H
      SB3=1./(B*H*H)
      SB4=1./(B*B*H*H)
      SC1=1./(4.*H*H)*(F1*G)
      SC2=(FYY*E1)+(FXX*G)
      SD1=FY*G
      SD2=FY*E1
      SD3=FY*EMU
      SE1=F1*G
      SE2=F1*E1
      SE3=F1*EMU
      SF1=1./(4.*H*H)*(F1*E2)
      SF2=(FXX*E2)+(FYY*G)
      SK(1) = SC1+SB4*SC2
      SK(2) = SC1-SB4*SC2
      SK(3) =-SC1-SA6*SD2+SA7*SC2
      SK(4) =-SC1+SA6*SD2-SA7*SC2
      SK(5) = SB3/2.*(SD1+SD3)
      SK(6) = SB3/2.*(-SD1+SD3)
      SK(7) =-SA2/2.*SE1+(SA5/2.*SD1)-(SB3/2.*SD3)
      SK(8) = (SA2/2.*SE1)-(SA5/2.*SD1)-(SB3/2.*SD3)
      SK(16)= (SA1*SE2)-(SA3*2.*SD2)+(SA4*SC2)+SC1
      SK(17)=-(SA1*SE2)+(SA3*2.*SD2)-(SA4*SC2)+SC1
      SK(18)=-(SA2/2.*SE3)+(SA5/2.*SD3)-(SB3/2.*SD1)
      SK(19)=-(SA2/2.*SE3)+(SA5/2.*SD3)+(SB3/2.*SD1)
      SK(20)= (SA2/2.*SE3)+(SA2/2.*SE1)-(SA5/2.*SD3)-(SA5/2.*SD1)
      SK(21)= (SA2/2.*SE3)-(SA2/2.*SE1)-(SA5/2.*SD3)+(SA5/2.*SD1)
      SK(27)= SF1+(SB4*SF2)
      SK(28)= SF1-(SB4*SF2)
      SK(29)=-SF1+(SA7*SF2)-(SA6*SD1)
      SK(30)=-SF1-(SA7*SF2)+(SA6*SD1)
      SK(34)= SF1+(SA1*SE1)-(SA3*2.*SD1)+(SA4*SF2)
      SK(35)= SF1-(SA1*SE1)+(SA3*2.*SD1)-(SA4*SF2)
      CC=COS(BETA/2.)*COS(BETA/2.)
      CS=COS(BETA/2.)*SIN(BETA/2.)
      SS=SIN(BETA/2.)*SIN(BETA/2.)
      S(1) = CC*SK(1)-CS*2.*SK(5)+SS*SK(27)
```

```
      S(2) = CC*SK(2)+CS*2.*SK(6)-SS*SK(28)
      S(3) = CC*SK(3)+CS*(SK(7)-SK(18))-SS*SK(29)
      S(4) = CC*SK(4)+CS*(-SK(8)+SK(19))+SS*SK(30)
      S(5) = CC*SK(5)+CS*(SK(1)-SK(27))-SS*SK(5)
      S(6) = CC*SK(6)+CS*(-SK(2)-SK(28))-SS*SK(6)
      S(7) = CC*SK(7)+CS*(-SK(3)-SK(29))+SS*SK(18)
      S(8) = CC*SK(8)+CS*(SK(4)-SK(30))+SS*SK(19)
      S(9) = S(1)
      S(10)= S(4)
      S(11)= S(3)
      S(12)=-S(6)
      S(13)=-S(5)
      S(14)=-S(8)
      S(15)=-S(7)
      S(16)= CC*SK(16)+CS*2.*SK(20)+SS*SK(34)
      S(17)= CC*SK(17)-CS*2.* SK(21)-SS*SK(35)
      S(18)= CC*SK(18)+CS*(SK(3)+SK(29))+SS*SK(7)
      S(19)= CC*SK(19)+CS*(-SK(4)+SK(30))+SS*SK(8)
      S(20)= CC*SK(20)+CS*(-SK(16)+SK(34))-SS*SK(20)
      S(21)= CC*SK(21)+CS*(SK(17)+SK(35))-SS*SK(21)
      S(22)= S(16)
      S(23)=-S(19)
      S(24)=-S(18)
      S(25)=-S(21)
      S(26)=-S(20)
      S(27)= CC*SK(27)+CS*2.*SK(5)+SS*SK(1)
      S(28)= CC*SK(28)+CS*2.*SK(6)-SS*SK(2)
      S(29)= CC*SK(29)+CS*(SK(7)-SK(18))-SS*SK(3)
      S(30)= CC*SK(30)+CS*(SK(8)-SK(19))+SS*SK(4)
      S(31)= S(27)
      S(32)= S(30)
      S(33)= S(29)
      S(34)= CC*SK(34)-CS*2.* SK(20)+SS*SK(16)
      S(35)= CC*SK(35)-CS*2.* SK(21)-SS*SK(17)
      S(36)= S(34)
      DO 10 I=1,36
   10 S(I)=S(I)*TH
      RETURN
      END
```

```
      SUBROUTINE EPSINI (R1,R2,BETA,TH,E1,E2,EMU,G,EPSI,FI)
      DIMENSION FT(8),FI(1),EPSI(1)
      C=COS(BETA/2.)
      S=SIN(BETA/2.)
      H=C*(R2-R1)
      A=2.*R1*S
      B=2.*R2*S
      AA= TH*(A+B)/4.
      AB= TH*H*(2.*A+B)/(6.*A)
      AC= TH*H*(A+2.*B)/(6.*B)
      AE=E1*EPSI(1)+EMU*EPSI(2)
      AF=EMU*EPSI(1)+E2*EPSI(2)
      AG=G*EPSI(3)
      FT(1)= AC*AE +AA*AG
      FT(2)=-AC*AE +AA*AG
      FT(3)=-AB*AE -AA*AG
      FT(4)= AB*AE -AA*AG
      FT(5)= AA*AF +AC*AG
      FT(6)= AA*AF -AC*AG
      FT(7)=-AA*AF -AB*AG
      FT(8)=-AA*AF +AB*AG
      FI(1)= C*FT(1)-S*FT(5)
      FI(2)= C*FT(2)+S*FT(6)
      FI(3)= C*FT(3)+S*FT(7)
      FI(4)= C*FT(4)-S*FT(8)
      FI(5)= C*FT(5)+S*FT(1)
      FI(6)= C*FT(6)-S*FT(2)
      FI(7)= C*FT(7)-S*FT(3)
      FI(8)= C*FT(8)+S*FT(4)
      RETURN
      END
```

```
      SUBROUTINE SIGM (R1,R2,BETA,E1,E2,EMU,G,DP,EPSI,SIGX,SIGY,TAU)
      DIMENSION DP(1),DK(8),CTI(3,8),EPS(3),EPSI(1)
      C=COS(BETA/2.)
      S=SIN(BETA/2.)
      DK(1)=C*DP(1)+S*DP(5)
      DK(2)=C*DP(2)-S*DP(6)
      DK(3)=C*DP(3)-S*DP(7)
      DK(4)=C*DP(4)+S*DP(8)
      DK(5)=C*DP(5)-S*DP(1)
      DK(6)=C*DP(6)+S*DP(2)
      DK(7)=C*DP(7)+S*DP(3)
      DK(8)=C*DP(8)-S*DP(4)
      H=C*(R2-R1)
      A=2.*R1*S
      B=2.*R2*S
      X=0.
      Y=H/2.
      CTI(1,1)= Y/(B*H)
      CTI(1,2)=-CTI(1,1)
      CTI(1,3)=-1.0/A + Y/(A*H)
      CTI(1,4)=-CTI(1,3)
      CTI(1,5)= 0.
      CTI(1,6)= 0.
      CTI(1,7)= 0.
      CTI(1,8)= 0.
      CTI(2,1)= 0.
      CTI(2,2)= 0.
      CTI(2,3)= 0.
      CTI(2,4)= 0.
      CTI(2,5)= 1.0/(2.0*H) + X/(B*H)
      CTI(2,6)= 1.0/(2.0*H) - X/(B*H)
      CTI(2,7)=-1.0/(2.0*H) + X/(A*H)
      CTI(2,8)=-1.0/(2.0*H) - X/(A*H)
      CTI(3,1)= CTI(2,5)
      CTI(3,2)= CTI(2,6)
      CTI(3,3)= CTI(2,7)
      CTI(3,4)= CTI(2,8)
      CTI(3,5)= CTI(1,1)
      CTI(3,6)= CTI(1,2)
      CTI(3,7)= CTI(1,3)
      CTI(3,8)= CTI(1,4)
      DO 20 K=1,3
      EPS(K)=-EPSI(K)
      DO 20 J=1,8
      EPS(K)=EPS(K)+CTI(K,J)*DK(J)
   20 CONTINUE
      SIGX= EPS(1)*E1+EPS(2)*EMU
      SIGY= EPS(1)*EMU+EPS(2)*E2
      TAU = EPS(3)*G
      RETURN
      END
```